Role of linker histone H1 in epigenetic regulation of pluripotency genes and *Hox* genes

A Dissertation
Presented to
The Academic Faculty

By

Yunzhe Zhang

In Partial Fulfillment
Of the Requirements for the Degree
Doctor of Philosophy in Biology

Georgia Institute of Technology

May, 2014

Role of linker histone H1 in epigenetic regulation of pluripotency genes and *Hox* genes

Approved by:

Dr. Yuhong Fan, Advisor
School of Biology
Georgia Institute of Technology

Dr. Kirill Lobachev
School of Biology
Georgia Institute of Technology

Dr. Todd C. McDevitt
Department of Biomedical Engineering
Georgia Institute of Technology

Dr. Alfred H. Merrill
School of Biology
Georgia Institute of Technology

Dr. Francesca Storici
School of Biology
Georgia Institute of Technology

Date Approved: April 3, 2014

To my father, Weijun Zhang.

ACKNOWLEDGEMENTS

First, I would like to thank my thesis advisor, Dr. Yuhong Fan, for her guidance, encouragement and support. My thesis work would not have been possible without her time, ideas and funding support. I have not only learned experimental skills and critical thinking from her, but have always been encouraged by her enthusiasm to research.

I would like to thank all my committee members: Dr. Kirill Lobachev, Dr. Todd C. McDevitt, Dr. Alfred Merrill, and Dr. Francesca Storici, for their valuable suggestions and feedback for my Ph.D. studies.

I would like to thank our collaborators Marissa Cooke, Beth Krauth, and Dr. Todd C. McDevitt at Georgia Tech for their expertise and tremendous help with rotary suspension culture system and embryoid bodies differentiation and analysis.

I would like to thank all past and present Fan lab members for providing great help and support for my research. Especially, I want to thank Dr. Shiraj Panjwani for setting up the neural differentiation analysis, Dr. Zheng Liu for preliminary studies on *Hox* gene expression, Kaixiang Cao for chromatin immunoprecipitation assays, and several former undergraduate students, Rachel Fabiniak, Dawit Berhe, Chan Yoon Kim, Priya Patel, for their assistance. Special thanks go to Kaoxiang Cao, Chenyi Pan, Magdalena Medrzycki, and Po-Yi Ho for being my dear friends and offering immense help in my research and life all my graduate studies.

I am forever indebted to my mother, husband, son and my parents in law for their love, understand, trust and support. Their love always supports me throughout my life.

TABLE OF CONTENTS

LIST OF TABLES

LIST OF FIGURES

LIST OF ABBREVIATIONS

A_{214}: absorbence at 214 nm
AFP: alpha-fetoprotein
αMHC: alpha myosin heavy chain
bp: base pair
cDNA: complementary DNA
ChIP: chromatin immunoprecipitation
DMEM: Dulbecco's modified Eagle's medium
DNA: deoxyribonucleic acid
DNase I: deoxyribonuclease I
DNMT: DNA methyltransferase
DNMT1: DNA methyltransferase 1
DNMT3a: DNA methyltransferase 3 alpha
DNMT3b: DNA methyltransferase 3 beta
EB: embryoid body or ethidium bromide
E9.0: embryonic day 9.0
ESC: embryonic stem cell
ESI: electrospray ionization
FBS: fetal bovine serum
FRAP: fluorescence recovery after photobleaching
GAPDH: glyceraldehyde 3-phosphate dehydrogenase
GFAP: glial fibrillary acidic protein
GFP: green fluorescent protein
H1/nuc: The ratio of H1 variants to nucleosome
H3K27me3: histone H3 lysine 27 tri-methylation
H3K4me3: histone H3 lysine 4 tri-methylation
H3K9me3: histone H3 lysine 9 tri-methylation
HAT: histone acetyltransferase
HDAC: histone deacetylase
H&E: Hematoxylin and eosin
Hox: homeobox
HP1: heterochromatin protein 1
HPLC: High-performance liquid chromatography
HPRT: hypoxanthine-guanine phosphoribosyltransferase
HoxPG: Hox paralogous group
IACUC: the Institutional Animal Care and Use Committee
IgG: immunoglobulin G
IN: input
iPSC: induced pluripotent stem cell
Kb: kilo base pairs
KO: knockout
LIF: leukemia inhibitory factor
LINE: long interspersed elements

lncRNAs: long non-coding RNAs
LTR: long terminal repeat
MAR: matrix attachment region
MEF: mouse embryonic fibroblast
Nanog: nanog homeobox
Nes: Nestin
NSCs: neural stem cells
NuRD: nucleosome remodeling and deacetylation
Oct4: octamer-binding transcription factor 4
p53: tumor protein 53
PADIs: Peptidylarginine deiminases
PCR polymerase chain reaction
PLO+L: poly-L- ornithine and laminin
PcG: polycomb group
PRC1: polycomb repressive complex 1
PRC2: polycomb repressive complex 2
qChIP quantitative chromatin immunoprecipitation
qRT-PCR quantitative reverse transcription-PCR
RA: retinoic acid
rRNA: ribosomal RNA
RES: "rescue" cells
Rhox: reproductive homeobox
RNA: ribonucleic acid
RNase: ribonuclease
RP-HPLC: reversed phase HPLC
RT: reverse transcription
S.D.: standard deviation
S.E.M: standard error of the mean
SINE short interspersed elements
siRNA: small interference RNA
SirT1: sirtuin (silent mating type information regulation 2 homolog) 1
Sox2: SRY (sex determining region Y)-box 2
Su(var)3-9: suppressor of variegation 3-9
Suv39h: suppressor of variegation 3-9
SWI/SNF: Brg1/Brm-associated factor [BAF]
T: Brachyury
TH: Tyrosine hydroxylase
TKO: triple knockout
TrxG: Trithorax group
TSS: transcription start site
TUBB3: β-III tubulin
UTR: untranslated region
WT: wild-type

SUMMARY

Linker histone H1 plays a key role in facilitating folding of higher order chromatin structure. Previous studies have shown that deletion of three somatic H1 subtypes together leads to embryonic lethality and that H1c/H1d/H1e triple knockout (TKO) embryonic stem cells (ESCs) display bulk chromatin decompaction. Following this initial work, we investigated the role of H1 and chromatin compaction in stem cell pluripotency and differentiation, as well as the regulation of *Hox* genes expression. We find that H1 TKO ESCs are more resistant to spontaneous differentiation, impaired in embryoid body differentiation, and largely blocked in neural differentiation. We present evidence that H1 contributes to efficient repression of the expression of pluripotency factors, *Oct4* and *Nanog*, and participates in establishment and maintenance of DNA methylation and histone modification necessary for silencing pluripotency genes during stem cell differentiation and embryogenesis. In addition, we find reduced expression of a distinct set of *Hox* genes in embryos and ESCs, respectively. Furthermore, by characterizing $H1c^{-/-}$; $H1d^{-/-}$; and $H1e^{-/-}$ single-H1 null ESCs established in this study, we showed that individual H1 subtypes regulated specific *Hox* genes in ESCs. Finally, we demonstrate that the levels of H3K4me3 were significantly diminished at the affected *Hox* genes in H1 TKO- and single-H1 KO- ESCs, whereas H3K27me3 occupancy is modestly increased at specific *Hox* genes. Our results suggest that marked reduction of H1 levels and decondensation of bulk chromatin affect the expression of pluripotency genes and *Hox* genes in embryos and ESCs, which may be in part mediated through establishment and maintenance of epigenetic marks.

CHAPTER 1

INTRODUCTION

1.1 Linker Histone H1

In eukaryotic cells, DNA is packaged, through association with histones, into chromatin in the nucleus (Wolffe, 1998). The basic repeating unit of chromatin is the nucleosome, which consists of a histone octamer wrapped by 147 bp of DNA. The histone octamer is composed of 2 molecules of each core histones (H2A, H2B, H3 and H4) (Olins and Olins, 1974; Oudet et al., 1975; Wolffe, 1998). Linker DNA, connecting nucleosomes, has a variable length of (Felsenfeld and Groudine, 2003). Linker Histone H1 binds to the nucleosome at the entry/exit site of nucleosomal DNA and the linker DNA, mediating chromatin folding into higher order(Bednar et al., 1998; Ramakrishnan, 1997; Thoma et al., 1979).

Linker histone H1 has a tripartite domain structure with a short N-terminal domain, a central globular domain, and a long C-terminal domain. Both the globular and the C-terminal domains are involved in high affinity binding to chromatin (Brown et al., 2006; Hendzel et al., 2004; Stasevich et al., 2010; Syed et al., 2010). *In vivo* studies using H1-GFP fusion proteins show that the binding of H1 to chromatin is dynamic with a rapid exchange rate (Lever et al., 2000; Misteli et al., 2000). H1 is also subjected to multiple post-translational modifications, of which phosphorylation of H1 has been shown to increase the dissociation rate of H1 from chromatin (Dou and Gorovsky, 2002).

1.1.1 Linker Histone H1 family

The linker histone H1 family is highly divergent and heterogeneous. There are 11 subtypes in mammals, including 7 somatic H1s (H1a, H1b, H1c, H1d, H1e, $H1^0$ and H1x) and 4 germ cell specific H1s (H1t, H1ILS1, H1T2 and H1oo) (Happel and Doenecke, 2009). The H1 subtypes have different affinities for DNA binding and different abilities to promote chromatin condensation (Clausell et al., 2009). Each H1 subtype is encoded by a single copy gene. The H1 genes are developmentally regulated, and the composition of somatic H1s differs in different tissues. For example, while $H1^0$ and H1e are the major H1 subtypes in adult mouse liver, accounting for approximately 30% and 40% of total H1 respectively, these two H1 subtypes only constitute a respective ~2% and ~10% of total H1 in the mouse thymus (Fan et al., 2003). Given that H1 subtypes bind DNA with different affinities *in vitro* and vary in their abilities in chromatin condensation (Clausell et al., 2009), the dramatically different compositions of H1 in various tissues suggest distinct levels of chromatin condensation in these different cell types in adult tissues.

Even though H1 subtypes have different sequences and characteristics, they appear to have functional redundancy in cellular function and mouse development. Individual somatic H1 subtypes are dispensable for mouse development and mice deficient for one or two H1 subtypes do not show obvious phenotypes (Drabent et al., 2000; Fan et al., 2003; Lin et al., 2000; Rabini et al., 2000; Sirotkin et al., 1995). These H1 subtype single or double knockout (KO) mice do not have a reduction in the H1-to-nucleosome ratio due to the increase of other H1 subtypes to compensate for the lost H1s (Fan et al., 2003; Lin et al., 2004; Popova et al., 2013). Deletion of three H1 subtypes ($H1^0$, H1c, and H1e) causes growth retardation with smaller body size and a shorter life

span. Deletion of H1c, H1d, and H1e leads to embryonic lethality (Fan et al., 2003). These findings indicate that H1 is essential for mouse development and that the total level of histone H1 histones is important in embryogenesis and postnatal development.

1.1.2 Linker histone H1 and gene regulation

Previous studies in a variety of organisms demonstrate that histone H1 affects specific gene expression *in vivo* (Fan et al., 2005; Shen and Gorovsky, 1996; Vujatovic et al., 2012). Deletion of H1 in *Drosophila* affects a small number group of genes, including both active genes and inactive genes, as well as genes enriched in transposons (Lu et al., 2009; Vujatovic et al., 2012). H1 variant HIS-24, together with heterochromatin protein 1 like proteins HPL-1 and HPL-2, regulates transcription of immune-relevant genes in *C. elegans* (Studencka et al., 2012). In *Xenopus*, somatic H1 proteins are involved in the transcriptional silencing of genes required for mesodermal differentiation pathways (Steinbach et al., 1997). H1 is also involved in mediating the differential expression of the oocyte and somatic 5S rRNA genes during *Xenopus* development (Bouvet et al., 1994). In DT40 chicken B cell line, the deletion of H1 affects the transcriptions of multiple genes, of which most are underregulated (Hashimoto et al., 2010). Gene expression analysis show that specific genes are upregulated or downregulate in double knockout of H1a and H1t in mouse germ line cell and triples knockout of H1c, H1d, and H1e in mouse embryonic stem cells (ESCs) (Fan et al., 2005; Lin et al., 2004). Multiple mechanisms have been suggested to mediate the specific genes regulation, including the interaction between H1 and other proteins.

A few studies have indicated that H1 could directly interact with transcription factors, leading to repression of their target genes. For example, H1 represses p53 target genes by the formation of a p53-H1 repressive complex. The repression by P53-H1 complex can be removed when prothymosin alpha, a histone-binding nuclear protein, interacts with H1 on C-terminal domain where p53 binds, releasing p53 from the p53-H1 repressive complex (Zakharova et al., 2011). H1.5 interacts with FoxP3 via the leucine zipper domain to repress interleukin-2 expression in human T cells (Mackey-Cushman et al., 2011).

In addition, H1 has been shown to interact with histone modifying enzymes, suggesting a regulatory mechanism through affecting the levels of histone modifications. Lysine acetylation and methylation are most extensively studied histone modifications and play important roles in the regulation of genes. High levels of lysine acetylation are associated with gene activation (Wang et al., 2008). Histone acetyltransferases (HATs) catalyze the acetylation, while histone deacetylases (HDACs) erase the acetylation. H1 interacts with SirT1, a histone deacetylases, leading to deacetylation of histone and repression of the reporter gene (Vaquero et al., 2004). While histone acetylation is associated with gene activation, histone methylations have differential effects on gene expression depending on the sites of modification. For example, H3K4me3 and H3K36me3 are involved in gene activation, but H3K9me3 and H3K27me3 are associated with gene repression. H3K4me3 and H3K36me3 are often enriched at transcription start sites and gene bodies of active genes, respectively (Bernstein et al., 2005; Mikkelsen et al., 2007). H3K9me3 and H3K27me3 locate in the pericentric and facultative heterochromatin regions, respectively (Peters et al., 2001; Trojer and Reinberg, 2007).

Ploycomb repressive complex 2 (PRC2) catalyzes di- and tri- methylation of H3K27 (Cao et al., 2002; Margueron and Reinberg, 2011; Shen et al., 2008). The interaction between H1 and the components of PRC2 can stimulate its H3K27 methyltransferase activity (Martin et al., 2006). Recent studies show that *Drosophila* H1 interacts with H3K9 methyltransferases Su(var)3-9 *in vitro* and coordinates Su(var)3-9 to repress repetitive elements *in vivo* (Lu et al., 2013).

H1 may also regulate specific gene regulation through DNA methylation. Genomic DNA methylation plays an important role in gene silencing (Suzuki and Bird, 2008), and proper DNA methylation is required for development. H1 depletion leads to changes in DNA methylation at the regulatory regions of several imprinted genes in H1 TKO ESCs (Fan et al., 2005). H1 also silences transcription of *Rhox5* in mouse ESCs by regulating DNA methylation in *Rhox5* promoter region (Maclean et al., 2011). Three DNA methyltransferases (Dnmts) Dnmt1, Dnmt3a and Dnmt3b catalyze this epigenetic modification in mammals. H1 is found to interact with Dnmt1 and Dnmt3b in ESCs (Kashiwagi et al., 2011; Yang et al., 2013), indicating that H1 may regulate DNA methylation at specific regions by interaction with Dnmts.

1.2 Embryonic stem cells and pluripotency genes

1.2.1 Embryonic stem cells (ESCs)

Pluripotent embryonic stem cells , derived from inner cell mass of blastocysts (Evans and Kaufman, 1981; Thomson et al., 1998), can self-renew and differentiate to

diverse cell types in all three germ layers of endoderm, mesoderm, and ectoderm. Thus, ESC is a useful system for studying developmental biology, cell differentiation as well as offering a promising resource of regenerative medicine.

During differentiation, ESCs lose their pluripotency accompanying dramatic molecular changes. Compared with differentiated cells, ESCs exhibit global hyperactivity in transcription and hyperdynamic chromatin. In ESCs, repeat regions, including major and minor satellite, LINE and SINE, are active (Efroni et al., 2008), and lineage-specific genes are stochastically expressed at low levels (Bernstein et al., 2006; Efroni et al., 2008). The transcription of these regions is reduced during differentiation and becomes undetectable in differentiated cells except for the genes specific to that particular lineage (Efroni et al., 2008). In addition, global transcriptome analysis indicates that transcription both coding and non-coding regions are higher in ESCs compared with differentiated cells (Efroni et al., 2008).

Chromatin fibers in ESCs are highly dispersed in contrast to the more compacted forms of chromatin domain in differentiated cells (Ahmed et al., 2010; Fussner et al., 2010). More open chromatin structures are suggested to be associated with pluripotency of ESCs (Ahmed et al., 2010). Hyperdynamic plasticity is another characteristics of ESCs chromatin. Detected by fluorescent recovery after photobleach (FRAP), chromatin structure proteins, H2B, H3 and H1, have faster exchange rate in pluripotent stem cells than in differentiated cells (Misteli et al., 2000). In ESCs, a specific histone modification pattern, termed “bivalent domain”, has been identified in promoter regions of developmental genes and lineage-specific genes which are expressed at low level (Azuara et al., 2006; Bernstein et al., 2006; Efroni et al., 2008). The bivalent domain consists of

large regions of H3K27 methylation covering smaller regions of H3K4 methylation (Bernstein et al., 2006; Efroni et al., 2008). H3K4me3 alone, bivalent domain, and H3K27me3 alone are found to be present at the expressed genes, poised for expression genes, and silent genes, respectively (Mikkelsen et al., 2007). Developmental genes are repressed by polycomb complexes which catalyze H3K27me3, and global loss of H3K27me3 impaired proper differentiation of ESCs (Boyer et al., 2006; Pasini et al., 2007). These results suggest that the chromatin of ESCs is open, hyperdynamic and marked by specific histone modification patterns. These features are characteristic of ESCs and have been suggested to mark pluripotency.

1.2.2 Pluripotency genes

Pluripotency genes are required to maintain self-renew and pluripotency of ESCs. *Oct4*, also named as *Pou5f1*, is a prominent pluripotency gene. Its precise expression level determines the fate of ESCs during differentiation (Niwa et al., 2000). Oct4 is expressed throughout the preimplantation stages of mouse embryos but after embryonic day 9.0 (E9.0), it is only detectable in germ cells (Ovitt and Scholer, 1998). H3K9 methylation and DNA methylation in the *Oct4* promoter region are involved in repression of *Oct4* during differentiation (Feldman et al., 2006). *Oct4*, together with other two pluripotency factors, *Nanog* and *Sox2*, form a core pluripotency network, which controls regulation of developmentally regulated genes and ESCs differentiation (Boyer et al., 2005; Liang et al., 2008; Orkin and Hochedlinger, 2011).

Ample studies show that pluripotency network is associated with nucleosome remodeling complexes and histone-modifying proteins/complexes, regulating chromatin

structure (Endoh et al., 2008; Feldman et al., 2006; Lee et al., 2006;). Deletion of *Oct4* leads chromatin to form large blocks (Ahmed et al., 2010). As mentioned above, ESCs have unique chromatin structure and epigenetic marks, however, the function of chromatin in maintaining pluripotency and cell differentiation are undetermined.

Here, we utilize H1 triple knockout (TKO) ESCs, null for H1c, H1d and H1e, to study the impact of perturbation of chromatin structure on ESC differentiation and pluripotency gene expression. These H1 TKO ESCs have a decondensed chromatin, with reduced global nucleosome spacing and decreased local chromatin compaction as well as changes in certain histone modifications (Fan et al., 2005). These cells offer a good tool to study whether high order chromatin compaction is necessary for ESCs differentiation and pluripotency gene regulation and to identify the underlying regulatory mechanism.

1.3 *Hox* genes

In addition to pluripotency genes, *Hox* genes are another group of important developmental genes. *Hox* genes were first identified in *Drosophila* (Lewis, 1978). They encode evolutionarily conserved transcription factors containing homeodomain and control body segmentation. In mammals, there are 39 *Hox* genes organized to 4 clusters of 13 paralog groups, whose precise co-linear expression is required for embryonic development (Graham et al., 1989; Wagner et al., 2003). *Hox* genes clusters are coordinately regulated both temporally and spatially, serving as an especially attractive model to investigate the regulation of genes expression (Kmita and Duboule, 2003).

Hox genes play fundamental roles in regulating morphologies along the anterior-posterior axis during development. Mutations of whole *Hox* paralogous group (*HoxPG*) in mice have revealed the function of *Hox* genes in vertebrate development. *HoxPG3*, *HoxPG4* and *HoxPG5* are involved in establishing morphologies in cervical skeleton. *HoxPG5-9* are required for the formation of ribcage. *HoxPG10 and HoxPG11* are associated with the development of lumbar sacrum and tail (Mallo et al., 2010), and *HoxPG13* is related to posterior axial elongation (Economides et al., 2003; Young et al., 2009).

Hox genes are also critical for cell fate determination. *Hoxb1* induces the specification of neural stem cells (NSCs) toward a hindbrain-specific identity in ESC-derived NSCs, and is required for maintenance and expansion of posterior neural progenitor cells (Gouti and Gavalas, 2008). *Hoxa11* expression status affects progenitor cell differentiation during bone regeneration (Leucht et al., 2008).

Hox genes begin expression during gastrulation with a temporal pattern. More 3' genes are turned on in early gastrulation stage and more 5' genes express later in development (Wellik, 2007). The temporal collinearity of the activation of *Hox* genes is along their physical sequence of their genomic loci (Izpisua-Belmonte et al., 1991). Numerous studies have revealed that regulator elements, histone modification, chromatin decondencation and nuclear reorganization are involved in the precise regulation of *Hox* genes required for embryo development.

Different *cis*-regulator elements, flanking to *Hox1-4* genes, participate the regulation of *Hox1-4* in hindbrain and neural tube. Furthermore, the distance between elements and *Hox* genes, instead of the promoter sequence itself, affects the expression

patterns of *Hox* genes (Soshnikova and Duboule, 2009a). *Cis*-regulator elements are also involved in the regulation of *Hoxd* cluster. An interspecies conserved enhancer, located about 240 kb upstream of *Hoxd*, controls the transcription of *Hoxd* in development of digits (Spitz et al., 2003). Recently, a serial of new distal regulatory sites of *Hoxd*, which disperse the nearby gene desert, have been identified in presumptive digits (Montavon et al., 2011). The existence of these distal regulatory elements suggests a role chromatin structure in the activation of *Hox* genes.

A visible chromatin decondencation is found between early expressed gene *Hoxb1* and later expressed gene *Hoxb9* during the activation of *Hoxb* cluster induced by retinoic acid in mouse ESCs. *Hoxb1* loops out from chromosome territory earlier than *Hoxb9*, and relocalizes back toward chromosome territory when its expression switches off (Chambeyron and Bickmore, 2004). Decondencation and nuclear reorganization occur during mouse embryonic development; and in the activation of *Hoxd* in differentiation of ECSs and mouse embryonic tissues (Chambeyron et al., 2005; Morey et al., 2007).

Besides nuclear reorganization and chromatin decondensation, histone modifications have been found to coincide with the expression changes of *Hox* genes. In ESCs, the promoter regions of *Hox* genes are marked with both active histone mark, H3K4me3, and repressive histone mark, H3K37me3. These “bivalent domains” coincide with the pluripotency and lineage potential of ESCs (Boyer et al., 2006; Mikkelsen et al., 2007). In mouse embryos, H3K4me3 and H3K27me3 mark the active regions and inactive regions of *Hox* cluster respectively (Noordermeer et al., 2011). Furthermore, the

temporal activation of *Hox* genes is closely associated with the increase of active marks and decrease in repressive marks (Soshnikova and Duboule, 2009b).

Chromatin structure changes are likely to be important in regulating *Hox* genes. However, it is not clear how higher order chromatin structures regulate *Hox* genes. Deletion of linker histone H1c, H1d and H1e causes global chromatin structure change in ESCs and embryo death in gastrulation period (Fan et al., 2003; Fan et al., 2005), when precise transcription of *Hox* genes is required. The H1 TKO cells offer a good system to study whether and how H1 and higher order chromatin structure participate in the regulation of *Hox* genes.

1.4 Objectives

In this study, the main goal is to investigate the role of H1 in the regulation of pluripotency genes and developmental genes. To this end, we have studied the effects of H1 on the regulation of pluripotency genes, *Oct4 and Nanog*, during ESC differentiation. We have also inspected the role of H1 on the expression of cluster of important developmental genes, *Hox* genes, in embryos and ESCs. To elucidate the mechanisms by which H1 regulates these genes, we have examined the impact of H1 on epigenetic marks. These results identified novel functions of H1 in epigenetic gene regulation.

1.5 Reference

Ahmed, K., Dehghani, H., Rugg-Gunn, P., Fussner, E., Rossant, J., and Bazett-Jones, D.P. (2010). Global chromatin architecture reflects pluripotency and lineage commitment in the early mouse embryo. PloS one *5*, e10531.

Azuara, V., Perry, P., Sauer, S., Spivakov, M., Jorgensen, H.F., John, R.M., Gouti, M., Casanova, M., Warnes, G., Merkenschlager, M.*, et al.* (2006). Chromatin signatures of pluripotent cell lines. Nature cell biology *8*, 532-538.

Bednar, J., Horowitz, R.A., Grigoryev, S.A., Carruthers, L.M., Hansen, J.C., Koster, A.J., and Woodcock, C.L. (1998). Nucleosomes, linker DNA, and linker histone form a unique structural motif that directs the higher-order folding and compaction of chromatin. Proceedings of the National Academy of Sciences of the United States of America *95*, 14173-14178.

Bernstein, B.E., Kamal, M., Lindblad-Toh, K., Bekiranov, S., Bailey, D.K., Huebert, D.J., McMahon, S., Karlsson, E.K., Kulbokas, E.J., 3rd, Gingeras, T.R.*, et al.* (2005). Genomic maps and comparative analysis of histone modifications in human and mouse. Cell *120*, 169-181.

Bernstein, B.E., Mikkelsen, T.S., Xie, X., Kamal, M., Huebert, D.J., Cuff, J., Fry, B., Meissner, A., Wernig, M., Plath, K.*, et al.* (2006). A bivalent chromatin structure marks key developmental genes in embryonic stem cells. Cell *125*, 315-326.

Bouvet, P., Dimitrov, S., and Wolffe, A.P. (1994). Specific regulation of Xenopus chromosomal 5S rRNA gene transcription in vivo by histone H1. Genes & development *8*, 1147-1159.

Boyer, L.A., Lee, T.I., Cole, M.F., Johnstone, S.E., Levine, S.S., Zucker, J.P., Guenther, M.G., Kumar, R.M., Murray, H.L., Jenner, R.G.*, et al.* (2005). Core transcriptional regulatory circuitry in human embryonic stem cells. Cell *122*, 947-956.

Boyer, L.A., Plath, K., Zeitlinger, J., Brambrink, T., Medeiros, L.A., Lee, T.I., Levine, S.S., Wernig, M., Tajonar, A., Ray, M.K.*, et al.* (2006). Polycomb complexes repress developmental regulators in murine embryonic stem cells. Nature *441*, 349-353.

Brown, D.T., Izard, T., and Misteli, T. (2006). Mapping the interaction surface of linker histone H1(0) with the nucleosome of native chromatin in vivo. Nature structural & molecular biology *13*, 250-255.

Cao, R., Wang, L., Wang, H., Xia, L., Erdjument-Bromage, H., Tempst, P., Jones, R.S., and Zhang, Y. (2002). Role of histone H3 lysine 27 methylation in Polycomb-group silencing. Science *298*, 1039-1043.

Chambeyron, S., and Bickmore, W.A. (2004). Chromatin decondensation and nuclear reorganization of the HoxB locus upon induction of transcription. Genes & development *18*, 1119-1130.

Chambeyron, S., Da Silva, N.R., Lawson, K.A., and Bickmore, W.A. (2005). Nuclear re-organisation of the Hoxb complex during mouse embryonic development. Development *132*, 2215-2223.

Clausell, J., Happel, N., Hale, T.K., Doenecke, D., and Beato, M. (2009). Histone H1 subtypes differentially modulate chromatin condensation without preventing ATP-dependent remodeling by SWI/SNF or NURF. PloS one *4*, e0007243.

Dou, Y., and Gorovsky, M.A. (2002). Regulation of transcription by H1 phosphorylation in Tetrahymena is position independent and requires clustered sites. Proceedings of the National Academy of Sciences of the United States of America *99*, 6142-6146.

Drabent, B., Saftig, P., Bode, C., and Doenecke, D. (2000). Spermatogenesis proceeds normally in mice without linker histone H1t. Histochemistry and cell biology *113*, 433-442.

Economides, K.D., Zeltser, L., and Capecchi, M.R. (2003). Hoxb13 mutations cause overgrowth of caudal spinal cord and tail vertebrae. Developmental biology *256*, 317-330.

Efroni, S., Duttagupta, R., Cheng, J., Dehghani, H., Hoeppner, D.J., Dash, C., Bazett-Jones, D.P., Le Grice, S., McKay, R.D., Buetow, K.H.*, et al.* (2008). Global transcription in pluripotent embryonic stem cells. Cell stem cell *2*, 437-447.

Endoh, M., Endo, T.A., Endoh, T., Fujimura, Y., Ohara, O., Toyoda, T., Otte, A.P., Okano, M., Brockdorff, N., Vidal, M.*, et al.* (2008). Polycomb group proteins Ring1A/B are functionally linked to the core transcriptional regulatory circuitry to maintain ES cell identity. Development *135*, 1513-1524.

Evans, M.J., and Kaufman, M.H. (1981). Establishment in culture of pluripotential cells from mouse embryos. Nature *292*, 154-156.

Fan, Y., Nikitina, T., Morin-Kensicki, E.M., Zhao, J., Magnuson, T.R., Woodcock, C.L., and Skoultchi, A.I. (2003). H1 linker histones are essential for mouse development and affect nucleosome spacing in vivo. Molecular and cellular biology *23*, 4559-4572.

Fan, Y., Nikitina, T., Zhao, J., Fleury, T.J., Bhattacharyya, R., Bouhassira, E.E., Stein, A., Woodcock, C.L., and Skoultchi, A.I. (2005). Histone H1 depletion in mammals alters global chromatin structure but causes specific changes in gene regulation. Cell *123*, 1199-1212.

Feldman, N., Gerson, A., Fang, J., Li, E., Zhang, Y., Shinkai, Y., Cedar, H., and Bergman, Y. (2006). G9a-mediated irreversible epigenetic inactivation of Oct-3/4 during early embryogenesis. Nature cell biology *8*, 188-194.

Felsenfeld, G., and Groudine, M. (2003). Controlling the double helix. Nature *421*, 448-453.

Fussner, E., Ahmed, K., Dehghani, H., Strauss, M., and Bazett-Jones, D.P. (2010). Changes in chromatin fiber density as a marker for pluripotency. Cold Spring Harbor symposia on quantitative biology *75*, 245-249.

Gouti, M., and Gavalas, A. (2008). Hoxb1 controls cell fate specification and proliferative capacity of neural stem and progenitor cells. Stem cells *26*, 1985-1997.

Graham, A., Papalopulu, N., and Krumlauf, R. (1989). The murine and Drosophila homeobox gene complexes have common features of organization and expression. Cell *57*, 367-378.

Happel, N., and Doenecke, D. (2009). Histone H1 and its isoforms: contribution to chromatin structure and function. Gene *431*, 1-12.

Hashimoto, H., Takami, Y., Sonoda, E., Iwasaki, T., Iwano, H., Tachibana, M., Takeda, S., Nakayama, T., Kimura, H., and Shinkai, Y. (2010). Histone H1 null vertebrate cells exhibit altered nucleosome architecture. Nucleic acids research *38*, 3533-3545.

Hendzel, M.J., Lever, M.A., Crawford, E., and Th'ng, J.P. (2004). The C-terminal domain is the primary determinant of histone H1 binding to chromatin in vivo. The Journal of biological chemistry *279*, 20028-20034.

Izpisua-Belmonte, J.C., Falkenstein, H., Dolle, P., Renucci, A., and Duboule, D. (1991). Murine genes related to the Drosophila AbdB homeotic genes are sequentially expressed during development of the posterior part of the body. The EMBO journal *10*, 2279-2289.

Kashiwagi, K., Nimura, K., Ura, K., and Kaneda, Y. (2011). DNA methyltransferase 3b preferentially associates with condensed chromatin. Nucleic acids research *39*, 874-888.

Kmita, M., and Duboule, D. (2003). Organizing axes in time and space; 25 years of colinear tinkering. Science *301*, 331-333.

Lee, T.I., Jenner, R.G., Boyer, L.A., Guenther, M.G., Levine, S.S., Kumar, R.M., Chevalier, B., Johnstone, S.E., Cole, M.F., Isono, K.*, et al.* (2006). Control of developmental regulators by Polycomb in human embryonic stem cells. Cell *125*, 301-313.

Leucht, P., Kim, J.B., Amasha, R., James, A.W., Girod, S., and Helms, J.A. (2008). Embryonic origin and Hox status determine progenitor cell fate during adult bone regeneration. Development *135*, 2845-2854.

Lever, M.A., Th'ng, J.P., Sun, X., and Hendzel, M.J. (2000). Rapid exchange of histone H1.1 on chromatin in living human cells. Nature *408*, 873-876.

Lewis, E.B. (1978). A gene complex controlling segmentation in Drosophila. Nature *276*, 565-570.

Liang, J., Wan, M., Zhang, Y., Gu, P., Xin, H., Jung, S.Y., Qin, J., Wong, J., Cooney, A.J., Liu, D.*, et al.* (2008). Nanog and Oct4 associate with unique transcriptional repression complexes in embryonic stem cells. Nature cell biology *10*, 731-739.

Lin, Q., Inselman, A., Han, X., Xu, H., Zhang, W., Handel, M.A., and Skoultchi, A.I. (2004). Reductions in linker histone levels are tolerated in developing spermatocytes but cause changes in specific gene expression. The Journal of biological chemistry *279*, 23525-23535.

Lin, Q., Sirotkin, A., and Skoultchi, A.I. (2000). Normal spermatogenesis in mice lacking the testis-specific linker histone H1t. Molecular and cellular biology *20*, 2122-2128.

Lu, X., Wontakal, S.N., Emelyanov, A.V., Morcillo, P., Konev, A.Y., Fyodorov, D.V., and Skoultchi, A.I. (2009). Linker histone H1 is essential for Drosophila development, the establishment of pericentric heterochromatin, and a normal polytene chromosome structure. Genes & development *23*, 452-465.

Lu, X., Wontakal, S.N., Kavi, H., Kim, B.J., Guzzardo, P.M., Emelyanov, A.V., Xu, N., Hannon, G.J., Zavadil, J., Fyodorov, D.V.*, et al.* (2013). Drosophila H1 regulates the genetic activity of heterochromatin by recruitment of Su(var)3-9. Science *340*, 78-81.

Mackey-Cushman, S.L., Gao, J., Holmes, D.A., Nunoya, J.I., Wang, R., Unutmaz, D., and Su, L. (2011). FoxP3 interacts with linker histone H1.5 to modulate gene expression and program Treg cell activity. Genes and immunity *12*, 559-567.

Maclean, J.A., Bettegowda, A., Kim, B.J., Lou, C.H., Yang, S.M., Bhardwaj, A., Shanker, S., Hu, Z., Fan, Y., Eckardt, S.*, et al.* (2011). The rhox homeobox gene cluster is imprinted and selectively targeted for regulation by histone h1 and DNA methylation. Molecular and cellular biology *31*, 1275-1287.

Mallo, M., Wellik, D.M., and Deschamps, J. (2010). Hox genes and regional patterning of the vertebrate body plan. Developmental biology *344*, 7-15.

Margueron, R., and Reinberg, D. (2011). The Polycomb complex PRC2 and its mark in life. Nature *469*, 343-349.

Martin, C., Cao, R., and Zhang, Y. (2006). Substrate preferences of the EZH2 histone methyltransferase complex. The Journal of biological chemistry *281*, 8365-8370.

Mikkelsen, T.S., Ku, M., Jaffe, D.B., Issac, B., Lieberman, E., Giannoukos, G., Alvarez, P., Brockman, W., Kim, T.K., Koche, R.P.*, et al.* (2007). Genome-wide maps of chromatin state in pluripotent and lineage-committed cells. Nature *448*, 553-560.

Misteli, T., Gunjan, A., Hock, R., Bustin, M., and Brown, D.T. (2000). Dynamic binding of histone H1 to chromatin in living cells. Nature *408*, 877-881.

Montavon, T., Soshnikova, N., Mascrez, B., Joye, E., Thevenet, L., Splinter, E., de Laat, W., Spitz, F., and Duboule, D. (2011). A regulatory archipelago controls Hox genes transcription in digits. Cell *147*, 1132-1145.

Morey, C., Da Silva, N.R., Perry, P., and Bickmore, W.A. (2007). Nuclear reorganisation and chromatin decondensation are conserved, but distinct, mechanisms linked to Hox gene activation. Development *134*, 909-919.

Niwa, H., Miyazaki, J., and Smith, A.G. (2000). Quantitative expression of Oct-3/4 defines differentiation, dedifferentiation or self-renewal of ES cells. Nature genetics *24*, 372-376.

Noordermeer, D., Leleu, M., Splinter, E., Rougemont, J., De Laat, W., and Duboule, D. (2011). The dynamic architecture of Hox gene clusters. Science *334*, 222-225.

Olins, A.L., and Olins, D.E. (1974). Spheroid chromatin units (v bodies). Science *183*, 330-332.

Orkin, S.H., and Hochedlinger, K. (2011). Chromatin connections to pluripotency and cellular reprogramming. Cell *145*, 835-850.

Oudet, P., Gross-Bellard, M., and Chambon, P. (1975). Electron microscopic and biochemical evidence that chromatin structure is a repeating unit. Cell *4*, 281-300.

Ovitt, C.E., and Scholer, H.R. (1998). The molecular biology of Oct-4 in the early mouse embryo. Molecular human reproduction *4*, 1021-1031.

Pasini, D., Bracken, A.P., Hansen, J.B., Capillo, M., and Helin, K. (2007). The polycomb group protein Suz12 is required for embryonic stem cell differentiation. Molecular and cellular biology *27*, 3769-3779.

Peters, A.H., O'Carroll, D., Scherthan, H., Mechtler, K., Sauer, S., Schofer, C., Weipoltshammer, K., Pagani, M., Lachner, M., Kohlmaier, A.*, et al.* (2001). Loss of the Suv39h histone methyltransferases impairs mammalian heterochromatin and genome stability. Cell *107*, 323-337.

Popova, E.Y., Grigoryev, S.A., Fan, Y., Skoultchi, A.I., Zhang, S.S., and Barnstable, C.J. (2013). Developmentally regulated linker histone H1c promotes heterochromatin

condensation and mediates structural integrity of rod photoreceptors in mouse retina. The Journal of biological chemistry *288*, 17895-17907.

Rabini, S., Franke, K., Saftig, P., Bode, C., Doenecke, D., and Drabent, B. (2000). Spermatogenesis in mice is not affected by histone H1.1 deficiency. Experimental cell research *255*, 114-124.

Ramakrishnan, V. (1997). Histone H1 and chromatin higher-order structure. Critical reviews in eukaryotic gene expression *7*, 215-230.

Shen, X., and Gorovsky, M.A. (1996). Linker histone H1 regulates specific gene expression but not global transcription in vivo. Cell *86*, 475-483.

Shen, X., Liu, Y., Hsu, Y.J., Fujiwara, Y., Kim, J., Mao, X., Yuan, G.C., and Orkin, S.H. (2008). EZH1 mediates methylation on histone H3 lysine 27 and complements EZH2 in maintaining stem cell identity and executing pluripotency. Molecular cell *32*, 491-502.

Sirotkin, A.M., Edelmann, W., Cheng, G., Klein-Szanto, A., Kucherlapati, R., and Skoultchi, A.I. (1995). Mice develop normally without the H1(0) linker histone. Proceedings of the National Academy of Sciences of the United States of America *92*, 6434-6438.

Soshnikova, N., and Duboule, D. (2009a). Epigenetic regulation of vertebrate Hox genes: a dynamic equilibrium. Epigenetics : official journal of the DNA Methylation Society *4*, 537-540.

Soshnikova, N., and Duboule, D. (2009b). Epigenetic temporal control of mouse Hox genes in vivo. Science *324*, 1320-1323.

Spitz, F., Gonzalez, F., and Duboule, D. (2003). A global control region defines a chromosomal regulatory landscape containing the HoxD cluster. Cell *113*, 405-417.

Stasevich, T.J., Mueller, F., Brown, D.T., and McNally, J.G. (2010). Dissecting the binding mechanism of the linker histone in live cells: an integrated FRAP analysis. The EMBO journal *29*, 1225-1234.

Steinbach, O.C., Wolffe, A.P., and Rupp, R.A. (1997). Somatic linker histones cause loss of mesodermal competence in Xenopus. Nature *389*, 395-399.

Studencka, M., Konzer, A., Moneron, G., Wenzel, D., Opitz, L., Salinas-Riester, G., Bedet, C., Kruger, M., Hell, S.W., Wisniewski, J.R., *et al.* (2012). Novel roles of Caenorhabditis elegans heterochromatin protein HP1 and linker histone in the regulation of innate immune gene expression. Molecular and cellular biology *32*, 251-265.

Suzuki, M.M., and Bird, A. (2008). DNA methylation landscapes: provocative insights from epigenomics. Nature reviews Genetics *9*, 465-476.

Syed, S.H., Goutte-Gattat, D., Becker, N., Meyer, S., Shukla, M.S., Hayes, J.J., Everaers, R., Angelov, D., Bednar, J., and Dimitrov, S. (2010). Single-base resolution mapping of H1-nucleosome interactions and 3D organization of the nucleosome. Proceedings of the National Academy of Sciences of the United States of America *107*, 9620-9625.

Thoma, F., Koller, T., and Klug, A. (1979). Involvement of histone H1 in the organization of the nucleosome and of the salt-dependent superstructures of chromatin. The Journal of cell biology *83*, 403-427.

Thomson, J.A., Itskovitz-Eldor, J., Shapiro, S.S., Waknitz, M.A., Swiergiel, J.J., Marshall, V.S., and Jones, J.M. (1998). Embryonic stem cell lines derived from human blastocysts. Science *282*, 1145-1147.

Trojer, P., and Reinberg, D. (2007). Facultative heterochromatin: is there a distinctive molecular signature? Molecular cell *28*, 1-13.

Vaquero, A., Scher, M., Lee, D., Erdjument-Bromage, H., Tempst, P., and Reinberg, D. (2004). Human SirT1 interacts with histone H1 and promotes formation of facultative heterochromatin. Molecular cell *16*, 93-105.

Vujatovic, O., Zaragoza, K., Vaquero, A., Reina, O., Bernues, J., and Azorin, F. (2012). Drosophila melanogaster linker histone dH1 is required for transposon silencing and to preserve genome integrity. Nucleic acids research *40*, 5402-5414.

Wagner, G.P., Amemiya, C., and Ruddle, F. (2003). Hox cluster duplications and the opportunity for evolutionary novelties. Proceedings of the National Academy of Sciences of the United States of America *100*, 14603-14606.

Wang, Z., Zang, C., Rosenfeld, J.A., Schones, D.E., Barski, A., Cuddapah, S., Cui, K., Roh, T.Y., Peng, W., Zhang, M.Q., *et al.* (2008). Combinatorial patterns of histone acetylations and methylations in the human genome. Nature genetics *40*, 897-903.

Wellik, D.M. (2007). Hox patterning of the vertebrate axial skeleton. Developmental dynamics : an official publication of the American Association of Anatomists *236*, 2454-2463.

Wolffe, A.P. (1998). Chromatin: Structure and Function. CA: Academic Press, San Diego, CA.

Yang, S.M., Kim, B.J., Norwood Toro, L., and Skoultchi, A.I. (2013). H1 linker histone promotes epigenetic silencing by regulating both DNA methylation and histone H3 methylation. Proceedings of the National Academy of Sciences of the United States of America *110*, 1708-1713.

Young, R.A. (2011). Control of the embryonic stem cell state. Cell *144*, 940-954.

Young, T., Rowland, J.E., van de Ven, C., Bialecka, M., Novoa, A., Carapuco, M., van Nes, J., de Graaff, W., Duluc, I., Freund, J.N.*, et al.* (2009). Cdx and Hox genes differentially regulate posterior axial growth in mammalian embryos. Developmental cell *17*, 516-526.

Zakharova, N.I., Sokolov, V.V., Suvorova, A.A., Shiau, A.I., Wu, C.L., and Efstaf'eva, A.G. (2011). [Prothymosin alpha interacts with C-terminal domain of histone H1 and dissociates p53-histone H1 complex]. Molekuliarnaia biologiia *45*, 679-688.

CHAPTER 2

HISTONE H1 DEPLETION IMPAIRS EMBRYONIC STEM CELL DIFFERENTIATION

This chapter was published under the same name in the following article:

Yunzhe Zhang, Marissa Cooke, Shiraj Panjwani, Kaixiang Cao, Beth Krauth, Po-Yi Ho, Magdalena Medrzycki, Dawit T. Berhe, Chenyi Pan, Todd C. McDevitt, Yuhong Fan

Histone H1 Depletion Impairs Embryonic Stem Cell Differentiation

PLoS Genet. 2012;8(5):e1002691

2.1 Abstract

Pluripotent embryonic stem cells (ESCs) are known to possess a relatively open chromatin structure; yet, despite efforts to characterize the chromatin signatures of ESCs, the role of chromatin compaction in stem cell fate and function remains elusive. Linker histone H1 is important for higher-order chromatin folding and is essential for mammalian embryogenesis. To investigate the role of H1 and chromatin compaction in stem cell pluripotency and differentiation, we examine the differentiation of embryonic stem cells that are depleted of multiple H1 subtypes. H1c/H1d/H1e triple null ESCs are more resistant to spontaneous differentiation in adherent monolayer culture upon removal of leukemia inhibitory factor. Similarly, the majority of the triple-H1 null embryoid bodies (EBs) lack morphological structures representing the three germ layers and retain gene expression signatures characteristic of undifferentiated ESCs. Furthermore, upon neural differentiation of EBs, triple-H1 null cell cultures are deficient in neurite outgrowth and lack efficient activation of neural markers. Finally, we discover that triple-H1 null embryos and EBs fail to fully repress the expression of the pluripotency genes in comparison with wild-type controls and that H1 depletion impairs DNA methylation and changes of histone marks at promoter regions necessary for efficiently silencing pluripotency gene *Oct4* during stem cell differentiation and embryogenesis. In summary, we demonstrate that H1 plays a critical role in pluripotent stem cell differentiation, and our results suggest that H1 and chromatin compaction may mediate pluripotent stem cell differentiation through epigenetic repression of the pluripotency genes.

2.2 Introduction

Pluripotent embryonic stem cells (ESCs) can self-renew and differentiate into diverse cell types, including lineages from all three germ layers present in the adult organism, offering great promise in regenerative medicine in addition to serving as a useful system for developmental biology studies. The epigenome and transcriptional circuitry of pluripotent stem cells have been extensively investigated, and chromatin and epigenetic signatures have emerged as key components in defining and regulating stem cell pluripotency (Bernstein et al., 2006; Efroni et al., 2008; Meissner, 2010; Orkin and Hochedlinger, 2011). Recent reports have associated ESCs with a particularly open, hyperdynamic chromatin and hyperactive global transcription (Ahmed et al., 2010; Efroni et al., 2008; Meshorer et al., 2006), and open chromatin has been suggested as a marker for pluripotency (Fussner et al., 2010; Gaspar-Maia et al., 2011), However, it remains undetermined whether higher order chromatin compaction is required for pluripotent stem cell differentiation and how an open chromatin state impacts stem cell function.

In eukaryotic cells, histones are the major structural proteins that associate with DNA to form chromatin. The basic repeating unit of chromatin is the nucleosome core particle, which consists of an octamer of four core histones (H2A, H2B, H3 and H4) wrapped by 146 bp of DNA (Wolffe, 1998). Further compaction of chromatin into higher order structures, such as a 30 nm fiber, is facilitated by binding of H1 linker histones to DNA entry/exit points of nucleosomes and linker DNA between nucleosomes. Reducing the total amount of H1 *in vivo* leads to a relaxed chromatin structure(Fan et al., 2005; Shen et al., 1995; Woodcock et al., 2006).

The H1 histone family is the most divergent and heterogenous group of histones among the highly conserved family of histone proteins. In mammals, 11 non-allelic H1 subtypes have been identified, including five somatic H1 subtypes (H1a–e), the replacement subtype $H1^0$, four germ cell specific H1 subtypes (oocyte specific H1oo, and testis-specific H1t, H1t2, H1LS1) as well as a more recently identified and distantly related subtype H1x (Happel and Doenecke, 2009). Although the individual depletion of each of the three major somatic H1 subtypes, H1c, H1d and H1e, in mice does not lead to any detectable changes in total H1 levels or obvious phenotypes (Fan et al., 2001), deletion of H1c, H1d and H1e altogether leads to nearly a 50% reduction of total H1 levels and embryonic lethality with a broad phenotype (Fan et al., 2003), demonstrating that critical levels of total H1 histones are essential for mouse embryogenesis.

We have previously derived wild-type (WT) and H1c/H1d/H1e triple knockout (H1 TKO) embryonic stem cells from the outgrowth of the inner cell masses of blastocysts attained from intercrosses of H1 heterozygous mutants (Fan et al., 2005). We have measured that wild-type ESCs have an H1/nucleosome ratio of 0.46 (Fan et al., 2005), a much lower level compared with a ratio of 0.75~0.83 from various differentiated cell types in mouse tissues (Fan et al., 2003; Woodcock et al., 2006), suggesting that ESCs have a more open chromatin structure compared with differentiated cell types in adult tissues. H1 TKO ESCs have an even lower H1/nucleosome ratio that is close to 0.25, equivalent to 1 H1 per 4 nucleosomes. The compound H1 null ES cells display chromatin decondensation in bulk chromatin (Fan et al., 2005) and an increased nuclear size (Eskeland et al., 2010), offering an ideal system to test the necessity of chromatin compaction on ESC pluripotency and differentiation.

In the current study, we demonstrate, for the first time, that the differentiation capacity of ESCs that lack multiple H1 subtypes is severely impaired. We find that compound H1 null ESCs are more resistant to spontaneous differentiation, impaired in embryoid body differentiation, and largely blocked in neural differentiation. Finally, we present evidence that H1 contributes to efficient repression of the expression of pluripotency factors and participates in establishment and maintenance of epigenetic marks necessary for silencing pluripotency genes during stem cell differentiation and embryogenesis.

2.3 Materials and Methods

2.3.1 Embryonic stem cell culture

ESC lines derived from H1 TKO and wild-type littermates were expanded on mitotically inactivated mouse embryonic fibroblasts feeder layers and cultured feeder-free on tissue culture-treated dishes (Corning) pre-adsorbed with gelatin (Sigma, 0.1% solution in ddH_2O) prior to embryoid body differentiation studies. ESC culture media consisted of Dulbecco's modified Eagle's medium (DMEM) (Invitrogen) supplemented with 15% fetal bovine serum (FBS) (Hyclone), 100 U/ml penicillin, 100 µg/ml streptomycin and 0.25 µg/ml amphotericin (Mediatech), 2 mM L-glutamine (Mediatech), 1× MEM non-essential amino acids (Mediatech), 0.1 mM β-mercaptoethanol (Fisher Chemical), and 10^3 U/ml of leukemia inhibitory factor (LIF; ESGRO, Chemicon). Cultures were re-fed with fresh media every other day, and passaged every 2–3 days prior to reaching 70–80% confluence. For spontaneous differentiation studies, 2×10^5 cells were seeded in each well of 6-well plate at day 0 on gelatin coated plate without feeder layer, cultured with media without LIF, and harvested at indicated time points. Cell numbers were determined using a Multisizer 3 Coulter Counter (Beckman).

2.3.2 Karyotype analysis

Exponentially growing ESCs were cultured in the presence of Karyo-MAX colcemid (Gibco) for 60 minutes, washed with PBS, trypsinized, and collected. ESCs were subsequently treated with hypotonic solution (75 mM KCl) for 6 minutes at 37°C, fixed with fixation solution (3 volumes Methanol, 1 volume Acetic acid), concentrated

and dropped onto an angled, humidified microscope slide. The slide was dried and chromosomes were stained with Hoechst dye for 1 h in the dark. Images of metaphase spread were collected at a 60× objective on an Olympus Fluorescence Microscope.

2.3.3 Rotary suspension culture and embryoid body differentiation

Embryoid bodies were formed by inoculating a single-suspension of ESCs that have been passaged without feeder layers for two generations (referred to as "day 0" culture) at 2×10^5 cells/ml into 100 mm bacteriological grade polystyrene Petri dishes with 10 ml of differentiation media (DMEM, 15% FBS, 100 U/ml penicillin, 100 µg/ml streptomycin and 0.25 µg/ml amphotericin, 2 mM L-glutamine, 1× MEM non-essential amino acids, 0.1 mM β-mercaptoethanol). The EB cultures were immediately placed on rotary orbital shakers (Lab-Line Lab Rotator, Barnstead International) in a humidified incubator (37°C, 5% CO_2) and maintained at 40–45 rpm for the entire duration of suspension culture; rotary speed was calibrated daily to ensure accuracy throughout. Rotary orbital culture has been shown previously to significantly enhance the efficiency, yield and homogeneity of EB populations compared to static suspension culture methods (Carpenedo et al., 2007). Differentiation media was exchanged every two days by collecting EBs via gravity-induced sedimentation in 15 ml conical tubes before aspirating spent media, replenishing with fresh media and returning the cultures to the rotary orbital shakers.

2.3.4 RNA extraction and quantitative RT–PCR

Total RNA from ESCs and embryos was extracted with Trizol reagent (Invitrogen) and Allprep DNA/RNA Mini kit (Qiagen) respectively according to the manufacturer's instructions. RNA was reverse transcribed using a SuperScript III First-strand cDNA synthesis kit (Life Technologies). Real-time quantitative PCR (qPCR) were performed using iQ SYBR Green Supermix with MyIQ Single Color real-time PCR Detection System (Bio-Rad). The following primers were used: *Oct4*: forward 5′-GCTCA CCCTGGGCGTTCTC-3′, reverse 5′-GGCCGCAGCTTACACATGTTC-3′; *Nanog*: forward 5′-CCTCCAGCAGATGCAAGAACTC-3′, reverse 5′-CTTCAACCACTGGT TTTTCTGCC-3′; *Nkx2.5*: forward 5′-CAAGTGCTCTCCTGCTTTCC-3′, reverse 5′-GGCTTTGTCCAGCTCCACT-3′; alpha-MHC: forward 5′-GGTCCACATTCTTCA GGATTCTC-3′, reverse 5′-GCGTTCCTTCTCTGACTTTCG-3′; *Tyrosine hydroxylase*: forward 5′-GATTGCAGAGATTGCCTTCC-3′, reverse 5′-GGGTAGCATAGAGG CCCTTC-3′; *Nestin*: forward 5′-GCCTATAGTTCAACGCCCCC-3′, reverse 5′-AGAC AGGCAGGGCTAGCAAG-3′; *AFP*: forward 5′-AAACTCGCTGGAGTGTCTGC-3′, reverse 5′-AGGTTTGACGCCATTCTCTG-3′; *GFAP*: forward 5′-GCCACCAGT AACATGCAAGA-3′, reverse 5′-GGCGATAGTCGTTAGCTTCG; GAPDH: forward 5′-TTCACCACCATGGAGAAGGC-3′, reverse 5′-GGCATGGACTGTGGTCATGA-3′.

2.3.5 PCR SuperArray analysis

RNA was isolated from ESC and EB samples using QIAshredders (as needed) and RNeasy Mini kits (Qiagen) according to the manufacturer's instructions. RNA quantity and quality were assessed by taking absorbance measurements at 260 and 280 nm on a NanoDrop ND1000 Spectrophotometer (Nanodrop Technologies). First strand

cDNA synthesis was performed using the RT^2 First Strand Kit (SABiosciences) with 1 µg of input RNA per well followed by real-time PCR using the Mouse Embryonic Stem Cells PCR SuperArray and SYBR Green RT^2 qPCR Master Mix (SABiosciences), per manufacturer's recommended protocols. First strand synthesis and real-time PCR were performed using a BioRad MyCycler and BioRad MyIQ real time thermal cycler, respectively. Array results were first internally normalized to *GAPDH* levels and subsequently analyzed with Genesis software (Graz University of Technology) using $\log_2$ transformation, mean center gene analysis, and hierarchical clustering.

2.3.6 Neural differentiation of ESCs

ESCs cultures were trypsinized with 0.25% trypsin-EDTA solution, depleted with feeder cells, and resuspended in differentiation media at 5×10^4 cell/ml. Embryoid bodies were formed using hanging drop method by plating 20 µl drops (1000 cells per drop) on the inner side of the lid of 15 cm dishes. The bottom of the 15 cm dishes were filled with sterile water and incubated for 4 days. The neural differentiation protocol for ES cells was adapted from ES-Cult Neural differentiation protocols (StemCell Technologies, Vancouver, Canada). Briefly, four days old EBs were collected from the hanging drops and cultured for additional 2 days in 10 cm petri dishes in the presence of 1 µM *all-trans* retinoic acid. EBs were subsequently plated at 10 EBs per cm^2 in tissue culture plates, coated with poly-L-ornithin and laminin (5 µg/ml), in NeuroCult NSC proliferation medium (StemCell Technologies) supplemented with FGF-b 10 ng/ml. The plates were incubated and the media was change every 2–3 days.

2.3.7 Immunocytochemistry

Cells grown on glass cover slips were fixed with 4% paraformaldehyde for 20 min at room temperature before immunofluorescence staining. For immunocytochemistry, we used the following primary antibodies: GFAP (Abcam; rabbit IgG; 1:1000), TUBB3 (Millipore; mouse IgG1; 1:50); and secondary antibodies from Molecular Probes or Jackson Immuno Research Laboratories: Cy3-coupled donkey anti-rabbit, Alexa Fluor 488-coupled donkey anti-mouse antibodies. Nuclei were counter stained with Hoechst (1:1000). Images were collected at 20× and 60× on an Olympus Fluorescence Microscope.

2.3.8 Preparation and analysis of nuclei and histones of ESCs and EBs

mESC and EB nuclei and histones were prepared according to protocols described previously (Fan et al., 2005; Fan and Skoultchi, 2004; Medrzycki et al., 2012). Briefly, cultured ESCs or EBs were harvested and nuclei were extracted using 0.5% Nonidet P-40 in RSB (10 mM NaCl, 3 mM $MgCl_2$, 10 mM Tris-HCl, pH 7.5, protease inhibitors) and a Dounce homogenizer at 4°C. Released nuclei were pelleted and resuspended in RSB. Chromatin and histone proteins were subsequently extracted as described previously (Fan and Skoultchi, 2004; Medrzycki et al., 2012). 50–100 µg of total histone preparations were injected into a C18 reverse phase column (Vydac) on an ÄKTA UPC10 system (GE Healthcare). The effluent from the column was monitored at 214 nm (A_{214}), and the peaks areas were recorded and determined with ÄKTA UNICORN 5.11 software. Relative amounts of total H1s were determined by ratio of the total A_{214} of all H1 peaks to half of the A_{214} of H2B peak. The A_{214} values of the H1 and H2B peaks were adjusted to account

for the differences in the number of peptide bonds in each H1 subtype and H2B. Fractions corresponding to the H1d/H1e peak from HPLC analysis were collected and subjected to mass spectrometry analysis on a Qstar XL MS/MS system (Applied Biosystems) with electrospray ionization (ESI) as the ionization method. Analyst QS software (Applied Biosystems) was used for data acquirement and analysis.

2.3.9 Mouse embryo preparation

$H1c^{+/-}H1d^{+/-}H1e^{+/-}$ mice were set up for breeding in the afternoon, and embryos were staged as embryonic day 0.5 (E0.5) postcoitus at noon if a vaginal plug was found in the female in the next morning. The female was euthanized and embryos at E8.5 were dissected from the euthanized females according to procedures approved by Institutional Animal Care and Use Committee. DNA and RNA were extracted from embryos using Allprep DNA/RNA Micro kit (Qiagen) according to the manufacturer's instructions. Genotypes of embryos were determined by PCR assays described previously (Fan et al., 2001; Fan et al., 2003).

2.3.10 Quantitative chromatin immunoprecipitation (qChIP)

ChIP assays were performed as described previously (Fan et al., 2005) with modifications. Briefly, crosslinked chromatin was sheared to an average DNA fragment size of 200 to 400 bp by sonication. 20 µl of Dynabeads Protein G (Invitrogen) was incubated with 2 µg of antibody for 7 hours in 4°C. After washing three times with 1 ml PBS containing 0.5% BSA, the Dynabeads were then reacted with 40 µg of soluble chromatin overnight in 4°C. Dynabeads were washed five times with Washing Buffer (50

mM HEPES pH 7.6, 1 mM EDTA pH 8.0, 500 mM LiCl, 0.7% Sodium Deoxycholate, 1% NP-40) and one time with PBS. Protein/DNA complexes were subsequently eluted in 100 µl Elution Buffer (50 mM Tris-Cl pH 8.0, 10 mM EDTA pH 8.0, 1% SDS) at 65°C for 15 minutes, and incubated overnight at 65°C. DNA was purified with a Qiagen DNA Isolation column (Qiagen). The amount of each specific DNA fragment in immunoprecipitates was determined by real-time PCR. Triplicate PCR reactions using the iQ SYBR Green Supermix (BioRad) were analyzed in a MyIQ Real-Time PCR Detection System (BioRad). All samples were typically analyzed in triplicate in two independent experiments. The following primers were used: *Oct4*: forward 5′-TGGGCTGAAATACTGGGTTC-3′, reverse 5′- TTGAATGTTCGTGTGCCAAT-3′; *Nanog*: forward 5′-GGCATGGTGGTAGACAAGCC-3′, reverse 5′-TTAGTAAG TTGGTCCATGCTTTGG-3′. The percentage of input was calculated by dividing the amount of each specific DNA fragment in the immunoprecipitates by the amount of DNA present in the sample before immunoprecipitation (input DNA). The values from ChIP with control antibody (IgG) were typically less than 5% of the ChIP values with the antibodies against histone modifications.

2.3.11 Antibodies

The following antibodies were used for Western blotting and qChIP: anti-OCT4 (Santa Cruz sc8628), anti-GAPDH (Ambion AM4300), anti-β ACTIN (Sigma-Aldrich A5316), anti-FLAG (Sigma-Aldrich F3165), anti-H1 (Millipore 05-457), anti-$H1^0$ (Santa Cruz 56695), anti-H3K4me3 (Millipore 07-473), anti-H3K9me3 (Abcam 8898), anti-H3K27me3 (Millipore 07-449), anti-H3 (Abcam 1791) and IgG (Millipore 12-370).

2.3.12 Bisulfite modification, PCR amplification, and sequencing analysis

Genomic DNA was prepared from mESCs, EBs, and embryos. 0.1 to 1 μg of DNA was treated with the Bisulfite Conversion Kit (CpG Genome) according to the manufacturer's manual. 1 μl of treated DNA was used in each PCR reaction as previously described (Fan et al., 2005). The primers used to generate PCR products from the bisulfite-converted DNA are specific for the converted DNA sequence of the analyzed regions. The primer sequences were as follows: *Oct4* region1: forward 5′-GATATGGGTTGAAATATTGGGTTTAT-3′, reverse 5′-AATCCTCTCACCCCTA CCTTAAAT-3′; *Oct4* region 2: forward 5′-AAGGTTGAAAATGAAGGTTTTTTG-3′, reverse 5′-TCCAACCATAAAAAAAATAAACACC-3′; *Nanog*: forward 5′- TTTGTAG GTGGGATTAATTGTGAAT-3′, reverse 5′-AAAAAATTTTAAACAACAACCAAAA A-3′. The PCR products were subsequently cloned using the TOPO TA Cloning kit (Invitrogen), and clones containing the converted DNA inserts were picked and sequenced. DNA sequences were analyzed with BiQ analyzer (Bock et al., 2005).

2.3.13 Generation of H1d rescue (RES) cell lines

The H1d overexpression plasmid was constructed by cloning a 5 Kb fragment encompassing H1d coding region (with an insertion of FLAG tag at N-terminus) and proximal regulatory sequences into a vector containing a Blasticidin resistant gene. 20 μg of plasmid DNA was transfected into 2×10^7 H1 TKO ESCs as described before (Fan et al., 2001), and 96 cell clones resistant to blasticidin were picked and analyzed by Western blotting using an anti-FLAG antibody (Sigma-Aldrich). Two cell lines with the highest levels of H1d were selected as RES cell lines for further analysis.

2.4 Results

2.4.1 Loss of H1c/H1d/H1e inhibits spontaneous ESC differentiation

ESCs exhibit a relatively "open" chromatin structure compared with differentiated cells or lineage committed cells (Gaspar-Maia et al., 2011). H1c/H1d/H1e triple null ESCs we derived previously have a significant reduction in total H1 protein levels which leads to further decreased chromatin compaction (Fan et al., 2005), thus we postulated that loss of H1c, H1d, and H1e may interfere with ESC differentiation. We first compared the spontaneous differentiation tendency of two H1 TKO ESC lines with wild-type littermate ESC lines. Consistent with previous observations (Fan et al., 2005), H1 TKO ESCs cultured on mitotically inactivated mouse embryonic fibroblast (MEF) feeder cells with media containing leukemia inhibitory factor (LIF) have comparable growth rate to that of wild-type ESCs (data not shown) and normal karyotypes (Figure 2.1).

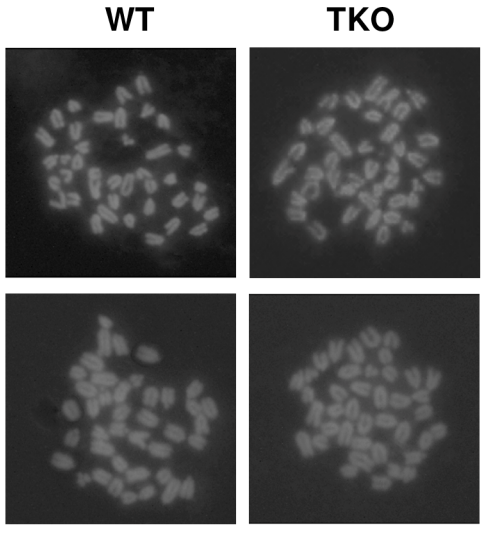

Figure 2.1 Chromosome spreads of WT and H1 TKO ESCs.

In addition, H1 TKO ESCs expressed comparable levels of pluripotency factor OCT4 (POU5F1) (Figure 2.2 A), and displayed a similar ESC colony morphology to that of WT ESCs under culture conditions which promote ESC self-renewal (Figure 2.2 B, left panel). However, when cultured in a feeder-free manner on gelatin-coated plates without MEFs, the H1 TKO cells displayed higher levels of OCT4, a more homogeneous, undifferentiated colony morphology, and a higher growth rate than WT ESCs under the same condition (Figure 2.2 A, 2.2B middle panel, and 2.2C). Furthermore, upon removal of LIF, the majority of H1 TKO ESCs continued to retain high expression levels of OCT4 (Figure 2.2 A) as well as a tightly packed colony morphology typical of undifferentiated ESCs (Figure 2.2 B, right panel) for a week. In contrast, wild-type ESCs differentiated readily, with approximate 90% of the cells appearing to differentiate by 2 days after LIF removal in feeder free culture, as judged by diminishing OCT4 expression and the loss of a compact colony morphology (Figure 2.2 A, 2.2B right panel). Removal of LIF reduced the growth of both WT and H1 TKO ESCs (Figure 2.2 C), consistent with LIF's known role in promoting self-renewal and proliferation of ESCs (Mereau et al., 1993). Collectively, these results suggest that ESCs lacking H1c, H1d, and H1e are more refractory to spontaneous ESC differentiation *in vitro*.

2.4.2 Loss of H1c, H1d, and H1e impairs EB differentiation

To assess whether loss of H1c, H1d and H1e impairs cellular differentiation of any of the three germ layers, we examined the ability of H1 TKO ESCs to form embryoid bodies (EB) using a rotary orbital suspension culture system to induce differentiation *in vitro*. We have previously shown that the rotary suspension culture method offers

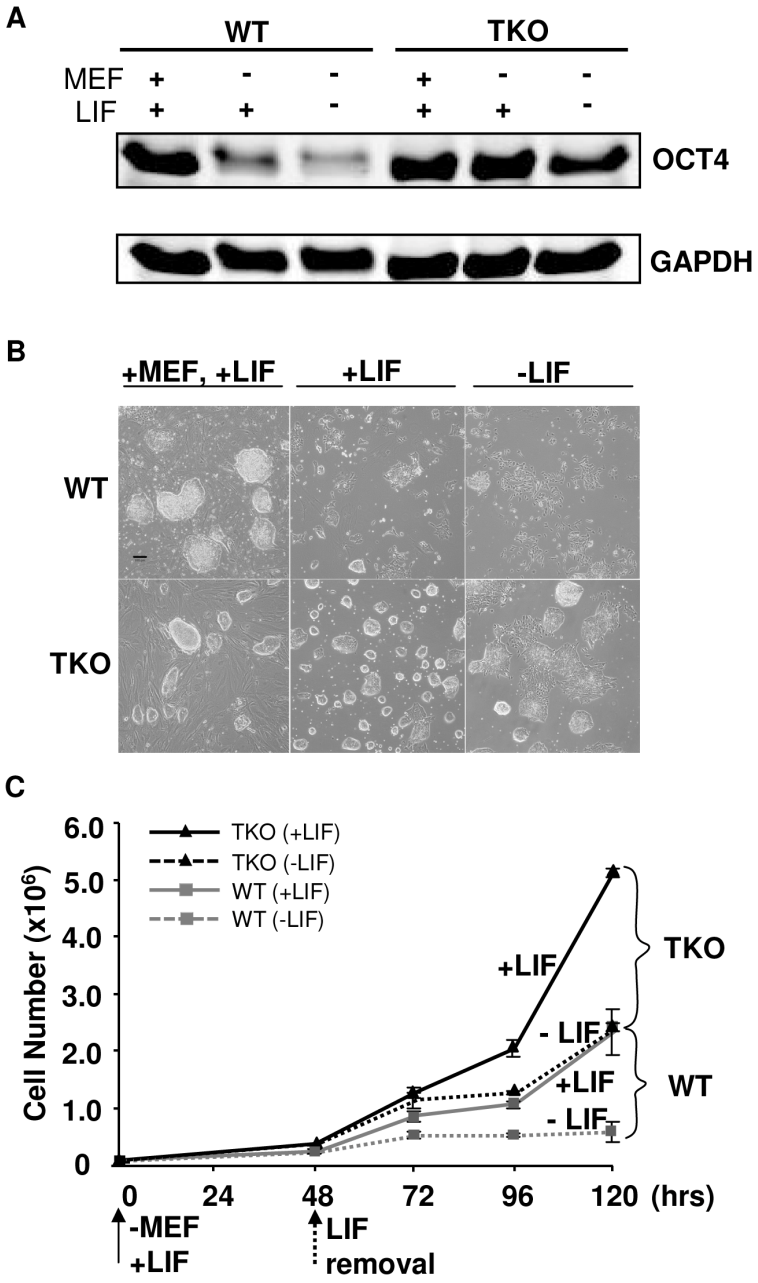

Figure 2.2 Loss of H1c/H1d/H1e inhibits spontaneous ESC differentiation.
(A) Western blot analysis of OCT4 level in WT and H1 TKO ESCs cultured under indicated conditions for 2 days. (B) Phase images of WT and H1 TKO ESCs cultured either on MEF with LIF (left panel), gelatin coated plate with LIF (middle panel), or gelatin coated plate without LIF (right panel) for 2 days. Scale bar: 100 μm. (C) Growth curves of WT and H1 TKO ESCs cultured on gelatin coated plate with or without LIF. Data are presented as average ± S.D.

improved efficiency and homogeneity of embryoid body production compared with the common practice of forming EB aggregates in static suspension culture (Carpenedo et al., 2007). During EB culture in serum-containing media, ESCs form aggregates and differentiate into cell types of all three primitive germ layers: endoderm, mesoderm and ectoderm, offering a temporal window to investigate specific defects in lineage differentiation. After 10 days of culture in rotary suspension, the wild-type EBs had a distinct outer endoderm-layer surrounding differentiated cell morphologies representing the three germ layers, including different epithelial cell types and mesenchymal cell populations (Figure 2.3 A). In contrast, although H1 TKO ESCs were able to form putative EBs, most H1 TKO EBs appeared blocked in the differentiation process in rotary suspension culture, forming undifferentiated masses of stem cells that lacked cavity formation and other types of differentiated structures even after prolonged culture in rotary suspension (up to 14 days) (Figure 2.3 A). Quantitative RT-PCR analyses also indicated that the expression of differentiation markers, such as the endoderm marker, alpha-fetoprotein (*AFP*), was drastically increased in WT EBs, but significantly curbed in H1 TKO EBs (Figure 2.2 B). The mRNA levels of other lineage specific markers, including mesoderm markers, such as the cardiac transcription factor *Nkx2.5*, and the sarcomeric muscle marker, alpha myosin heavy chain (*αMHC*), also progressively increased over time in WT EBs, but were not detected at similar levels in H1 TKO EBs (Figure 2.2 B).

To gain a more comprehensive view of the scope of genes affected by linker histone H1 depletion during differentiation, we performed quantitative PCR SuperArray analysis of wild-type and H1 TKO cells at the start (day 0) and the end point (day 10) of

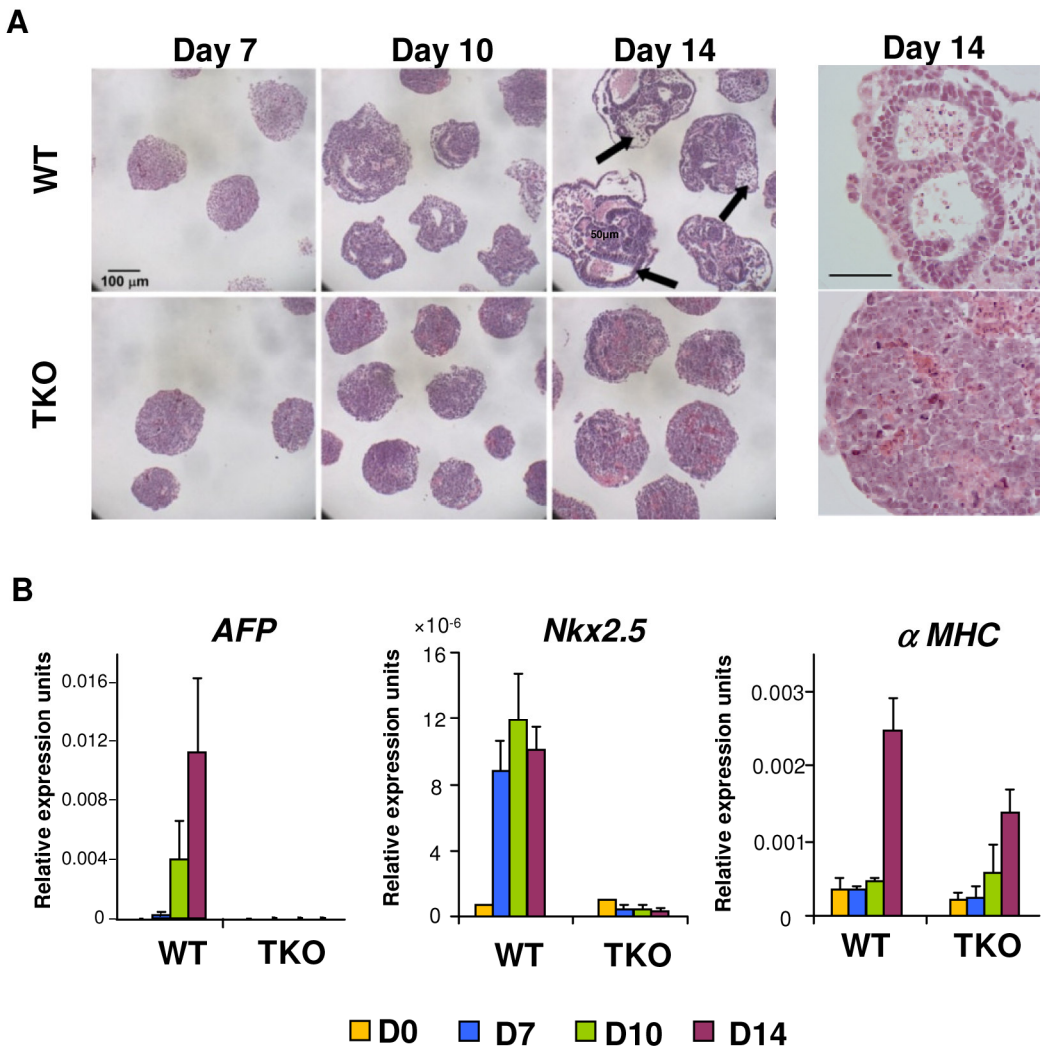

Figure 2.3 H1c/H1d/H1e triple knockout ESCs are impaired in EB differentiation. (A) Hematoxylin and eosin (H&E) staining of sections of WT EBs (top panels) and H1 TKO EBs (bottom panels) at 7 days, 10 days and 14 days in rotary suspension culture. High magnification images of H&E staining of sections of WT EB (top right) and H1 TKO EBs (bottom right) show that TKO EBs failed to cavitate. WT EBs showed more differentiated morphologies with cysts forming (black arrows). (B) Quantitative RT-PCR analysis of mRNA expression levels of *AFP* ,*Nkx2.5*, and *αMHC* in ESCs (day 0) and EBs throughout 14 days of rotary suspension culture. Data were normalized over the expression level of *GAPDH* and are presented as average ± S.D.

rotary suspension culture. The genes analyzed included pluripotency genes as well as important developmental genes for transcription factors and signaling molecules for all three germ layers. WT and TKO cultures at day 0 displayed very few differences in gene expression and their gene expression profiles clustered most similarly in hierarchical cluster analysis (Figure 2.4, Figure 2.5A, and Figure 2.6A). WT EBs differentiated as expected with significant increases of many differentiation markers and decreased expression of pluripotency associated genes (Figure 2.4, Figure 2.5B, and Figure 2.6B). In contrast, H1 TKO EBs exhibited very similar gene expression signatures to those of ESCs and had less expression changes during differentiation compared with that of WT EBs. (Figure 2.4, Figure 2.5C & D and Figure 2.6C), suggesting that the lack of H1c, H1d and H1e leads to diminished changes of transcriptional reprogramming during differentiation. The levels of ectoderm markers, such as *Nestin* (*Nes*), mesoderm markers, such as *Brachyury* (*T*) and *FLT1*, and endoderm markers, such as *AFP* and *Gata4*, were all markedly less or failed to be expressed in H1 TKO EBs (Figure 2.4 and Figure 2.5D), indicating that differentiation to all three germ layers was suppressed.

2.4.3 H1 is required for neural differentiation of embryonic stem cells

To further investigate if and when H1 impacts cell differentiation in a specific lineage, we induced differentiation of H1 TKO ESCs under a neural differentiation regimen established using *all-trans* retinoic acid (RA), which is known to induce neural differentiation in ESCs (Bain et al., 1995; Kim et al., 2009). EBs were prepared using the hanging-drop method, and day 4 EBs were collected and treated with RA for additional two days followed by further differentiation with neural differentiation media on poly-L-

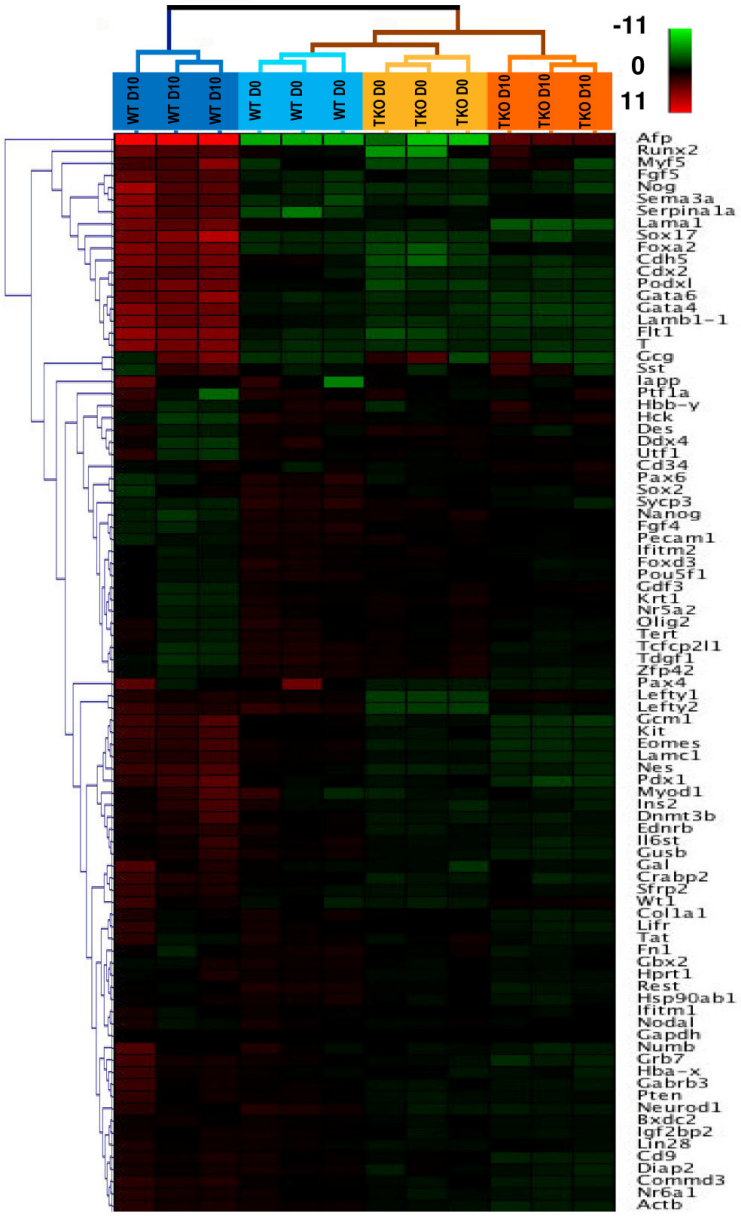

Figure 2.4 Hierarchical clustering analysis of qRT-PCR SuperArray gene expression profiling of ESCs (day 0) and EBs (day 10) formed from WT and H1 TKO ESCs.
Red, green or black represent higher, lower, or no change in relative expression.

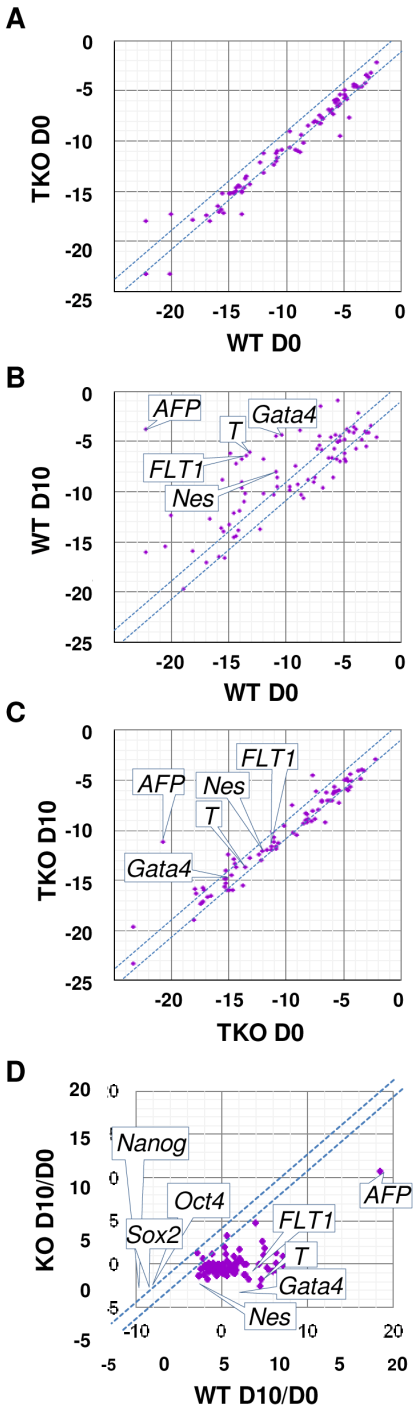

Figure 2.5 Scatter Plot analysis of gene expression of ESCs and EBs formed in rotary suspension culture.

(A) H1 TKO vs. WT ESCs (day 0); (B) WT EBs (day 10) vs. WT ESCs (day 0); (C) H1 TKO EBs (day 10) vs. H1 TKO ESCs (day 0). (D) the degree of changes in gene expression in WT and H1 TKO; X- and y- axes are delta CTs using *GAPDH* to normalize. Genes with more than 2-fold differences lie outside of the blue lines.

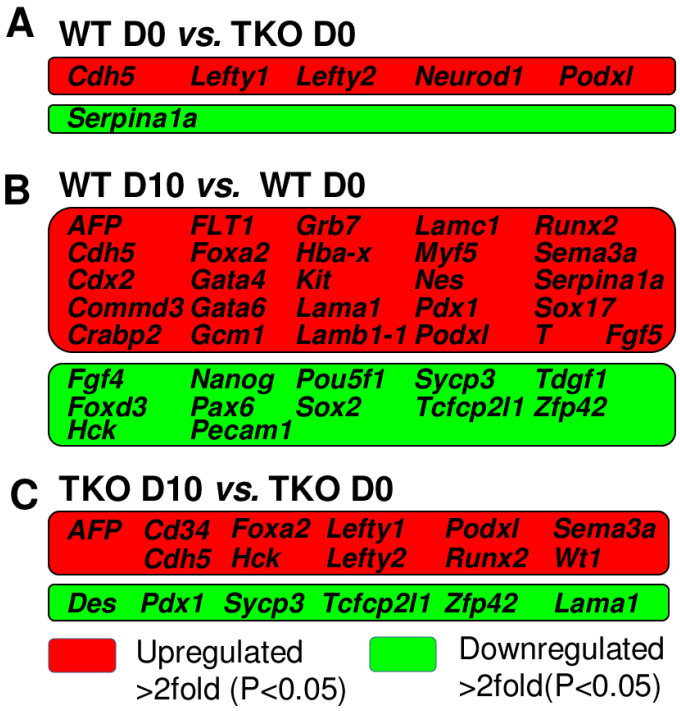

Figure 2.6 List of genes that displayed more than two-fold differences (P<0.05) in expression shown in Figure 2.5A (A), B (B), and C (C), respectively.

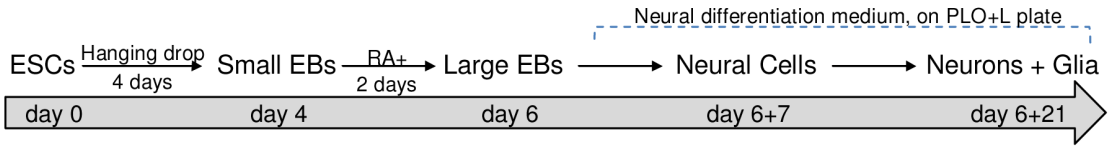

Figure 2.7 Neural differentiation scheme for ESCs.

ornithine and laminin (PLO+L) coated tissue culture plates (Figure 2.7). By day 6+7 of this *in vitro* neural differentiation scheme, neural cells were clearly established and neurite outgrowth from EBs was seen with neuronal cell proliferation. Neurites are enriched in cylindrical bundles of microtubules, made primarily of β-III tubulin (TUBB3) protein, extending from the body of all neurons, finally differentiating into an axon or a dendrite (da Silva and Dotti, 2002). However, at this time point, neural differentiation of WT and TKO ES cells exhibited several striking differences.

While neurite-formation was efficient in WT culture with bundles of neurites cylindrically extending from EB to adjacent EB, H1 TKO EBs had much less neurite outgrowth (Figure 2.8A, 2.8B). Approximately 50% of WT EBs plated for neural differentiation formed neurites compared to only about 10% of H1 TKO EBs forming neurites (Figure 2.8B, left panel). Furthermore, those 10% TKO EBs that were capable of forming neurites only produced on average 8 neurites per EB, whereas each WT EB had on average 18 neurites (Figure 2.8B, right panel). During *in vitro* neural differentiation, neurons aggregated into mounds of cells forming neuronal clusters (Figure 2.8A; black arrows), connected by bundles of neurites (Figure 2.8A; white arrows), forming a network pattern. While WT cultures showed formation of a neural network with neural clusters inter-connected by bundles of neurites, H1 TKO cultures failed to develop such an extensive intercellular network (Figure 2.8A, 2.8B), evidenced by smaller neuronal clusters with negligible inter-connecting neurites. This was further confirmed with immunofluorescence detection of TUBB3 protein expression, and minimal TUBB3 staining was seen in H1 TKO cultures (Figure 2.8C). It appeared that both neurite formation and outgrowth were limited in H1 knock-out mutants, affecting the ability of

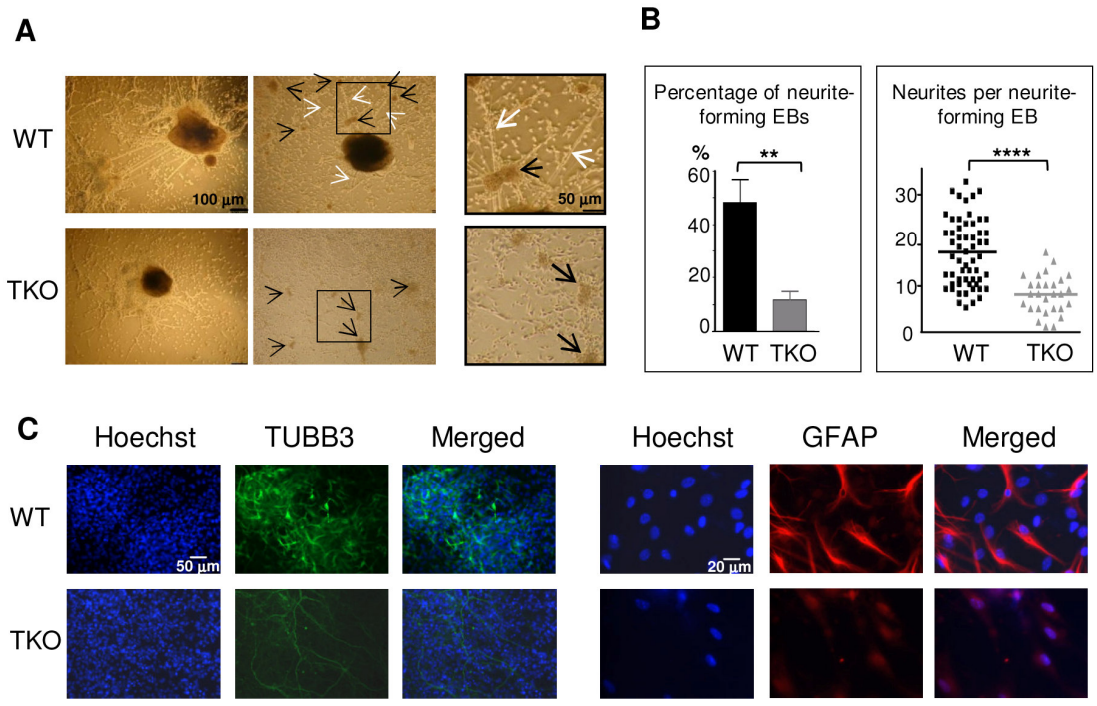

Figure 2.8 Characterization of WT and H1 TKO cultures on day 6+7 under neural differentiation protocol.

(A). Phase contrast images shows that H1 TKO mutants were unable to adequately form neurites and neural networks. Right panels: zoom-in images of the areas encircled with black rectangles. Scale bar: 100 µm (left panels) and 50 µm (right panels). (B). Left panel: Percentage of neurite-forming EBs. Numbers were averaged from 6 experiments. 80 EBs were counted per experiment. Right panel: Numbers of neurites per neurite-forming EB. Number of neurites was counted from EBs that produced neurites. 58 and 28 neurite-forming EBs from respective WT and TKO were selected and counted for neurite numbers. **: $P<0.01$; ****: $P<0.0001$.(C). Immunostaining for expression of TUBB3 and GFAP. Nuclei were stained with Hoechst 33342. Scale bars: 50 µm (left panels) and 20 µm (right panels). Results are representative of three independent experiments.

neurons to form neural networks. We also noted that TKO cultures yielded markedly less glial cells as revealed by much fewer GFAP positive astrocytes in comparison with WT cultures (Figure 2.8C). Since glial cells are essential for the normal growth and development of neurons, the near-lack of glial cells in TKO cultures may contribute to the poor development of TUBB3 positive neuronal cells from TKO EBs.

To examine whether the aforementioned defects of the H1 TKO cultures represent a temporary delay or a blockage in neural differentiation, we cultured the cells for an additional 14 days under neural differentiation conditions. As expected, the neural marker (*Nestin*) and the astrocyte marker (*GFAP*) were efficiently and progressively induced in WT cell cultures, and the neuronal gene *Tyrosine hydroxylase (TH)* peaked at day 6+7 when neuronal proliferation occurred (Figure 2.9). In contrast, the expression levels of neural genes were significantly curtailed in H1 TKO cultures, suggesting the lack of progression in neural differentiation of H1 TKO culture (Figure 2.9). Furthermore, we observed that pluripotency genes *Oct4* and *Nanog* were expressed at higher levels in TKO than WT throughout the differentiation process (Figure 2.9). These data suggest that H1 TKO cells are largely blocked in neural differentiation.

2.4.4 Levels of H1 increase progressively during differentiation

To address the mechanisms by which H1 modulates differentiation, we first examined the expression profile of linker histone H1 subtypes during EB formation and differentiation of wild-type ESCs. Histones from wild-type, H1 TKO ESCs and EBs were isolated at various time points during differentiation, and the levels of individual H1 subtype proteins as well as the H1 to nucleosome ratio were quantified from HPLC and

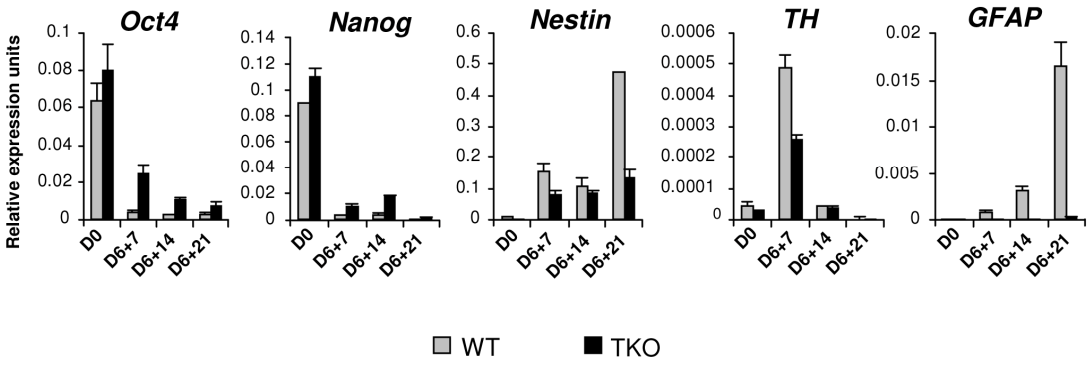

Figure 2.9 H1 TKO ESCs were unable to adequately repress the pluripotency genes and to efficiently induce the expression of neural genes under neural differentiation protocol.
Expression levels of pluripotency genes (*Oct4* and *Nanog*), neural marker (*Nestin*), neuronal marker (*Tyrosine hydroxylase (TH)*), astrocyte marker (*GFAP*) from WT and H1 TKO cultures at indicated days in differentiation cultures were determined by qRT-PCR. Data were normalized over the expression level of *GAPDH* and are presented as average ± S.D.

mass spectrometry analysis as described previously (Fan et al., 2003; Fan and Skoultchi, 2004; Medrzycki et al., 2012). In ESCs (day 0), $H1^0$ was nearly undetectable in WT cells but was increased in H1 TKO cultures as we observed previously (Figure 2.10A and (Fan et al., 2005)). Upon EB differentiation, the levels of H1c, H1d and H1e and $H1^0$ in WT cultures were all progressively increased over time, with the total H1 to nucleosome ratio elevated nearly 40% from 0.45 for ESCs to 0.62 for day 10 EBs (Figure 2.10B & C). Consistent with HPLC analysis, Western blotting showed that levels of total H1 and $H1^0$ were increased (Figure 2.11). The cumulative increase in the protein levels of H1c, H1d and H1e was responsible for 87% of the increase in the total H1 levels during differention (data not shown). Despite less abundant than H1d, H1c and H1e were significantly increased ($P<0.001$), and H1e levels in differentiated EBs were over 2-fold of that in

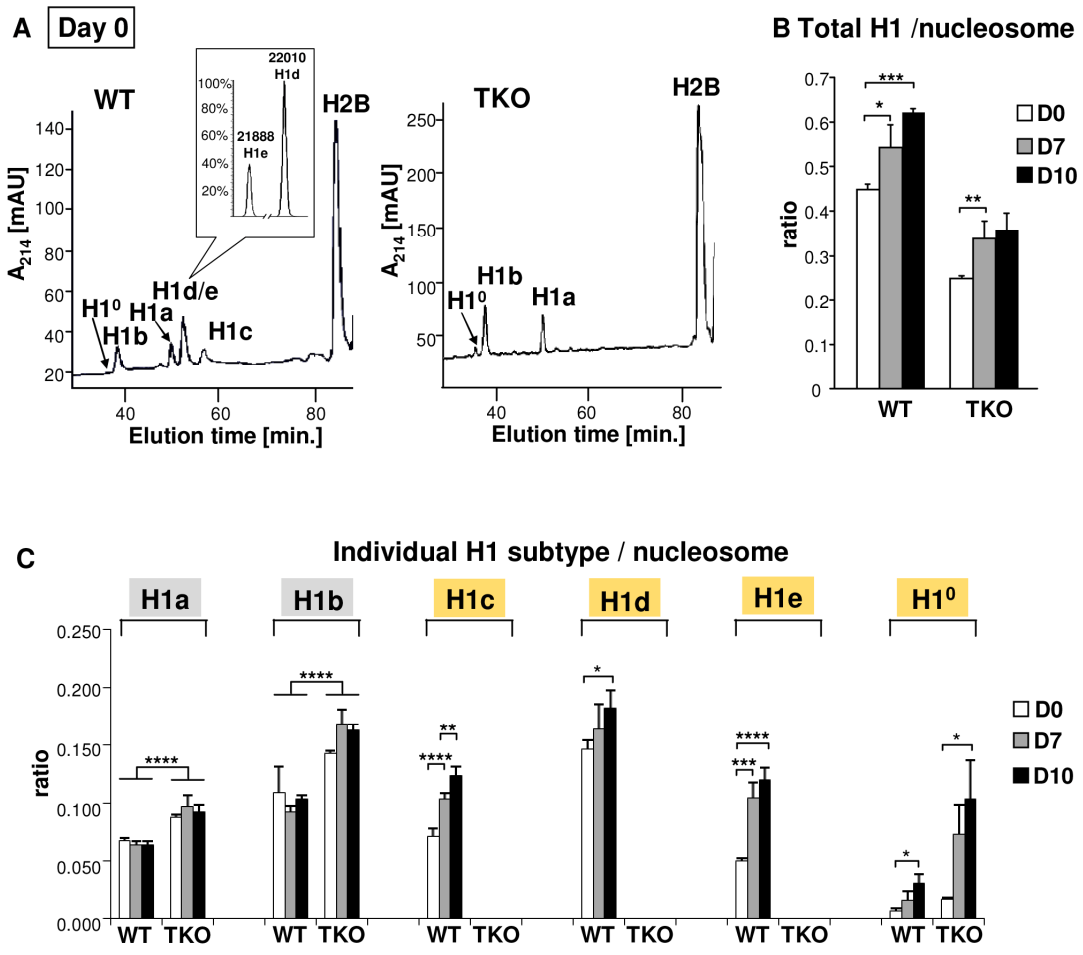

Figure 2.10 Expression profiles of linker histones in WT and H1 TKO cultures during EB differentiation.

(A) Reverse-phase HPLC and Mass Spectrometry (inset) analysis of histones from WT and H1 TKO ESCs. X axis: elution time; Y axis: absorbency at A214. mAU, milli-absorbency units. Inset shows the relative signal intensity of H1d and H1e mass spectral peaks in the H1d/H1e fraction collected from HPLC eluates of WT histones. (B,C) H1/nucleosome ratio of the total H1 (B) and individual H1 subtype (C) during EB formation and differentiation. Day 0, day 7 and day 10 of EB cultures were collected and HPLC analyses as shown in (A) were performed. The ratio of total H1 (or individual H1 subtype) to nucleosome was calculated as described in Materials and Methods. Values are means ± S.D., n = 4. *: P<0.05; **: P<0.01; ***: P<0.001; ****: P<0.0001.

undifferentiated ESCs (Figure 2.10C). The protein levels of H1a and H1b remained constant during differentiation, indicating that H1a and H1b were not responsible for the increase of total H1 during ESC differentiation. Albeit higher than that in TKO ESCs (0.25), the ratio of total H1 to nucleosome in day 10 TKO EBs (0.36) remained lower than the ratio in WT ESCs (0.45) (Figure 2.10B). The increase in the total H1 level in TKO EBs compared with ESCs was largely due to the increase in the level of $H1^0$ (Figure 2.10B & C, and Figure 2.11), indicating $H1^0$ being the major H1 subtype upregulated in the face of deficiency of H1c, H1d, and H1e, in both ESCs and EBs. These results show that the levels of H1c, H1d, H1e and $H1^0$ are elevated significantly during embryonic stem cell differentiation, and that the H1 TKO EB has a total H1 level lower than the WT ESC.

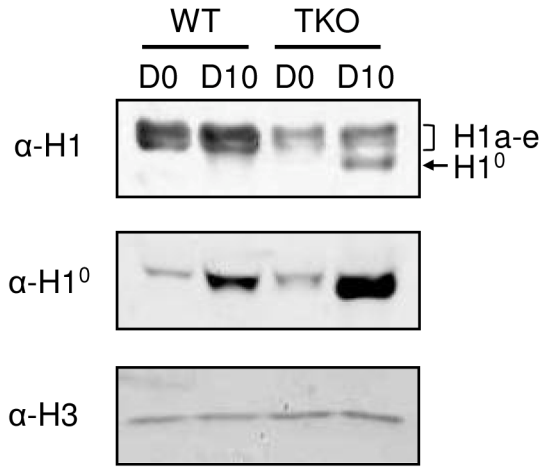

Figure 2.11 Analysis of total H1 and $H1^0$ levels during EB differentiation.
2 µg histone proteins were analyzed with immunoblotting with antibodies indicated. The bottom panel of Western blotting with anti-H3 antibody demonstrates equal loading of proteins in each lane.

2.4.5 H1c/H1d/H1e is necessary for efficient transcriptional repression of pluripotency genes *Oct4* and *Nanog* during embryogenesis and ESC differentiation

The results from the aforementioned experiments suggest that H1c/H1d/H1e triple null ESCs are less effective than WT ESCs in repressing the expression of pluripotency genes, such as *Oct4* and *Nanog*, during spontaneous differentiation, rotary suspension differentiation, and neural differentiation *in vitro* (Figure 2.2A, Figure 2.4, and Figure 2.9). Therefore, we next investigated if H1 contributes to stable repression of pluripotency gene expression *in vivo* during embryogenesis. *Oct4* is expressed in undifferentiated cells in the preimplantation embryo, and is progressively down-regulated in differentiating embryonal cells during gastrulation, becoming restricted to germ cell

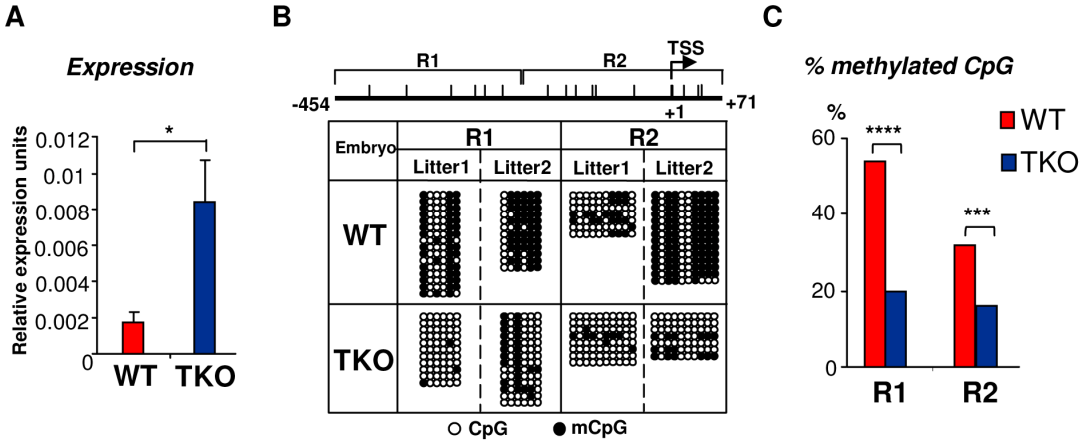

Figure 2.12 Elevated *Oct4* expression and hypomethylation of CpG sites at *Oct4* promoters in H1 TKO embryos compared with littermates at E8.5.
(A) qRT-PCR analysis of mRNA expression levels of *Oct4*. Values are means ± SEM, n = 5 for each genotype. Expression levels were normalized over *GAPDH*. *: P<0.05. (B) Bisulfite sequencing analysis of DNA methylation status at *Oct4* promoter regions. Results of two wild-type and two knockout E8.5 embryos are shown. The positions of CpG sites analyzed are depicted schematically as vertical ticks on the line. TSS: transcription start site. (C) Percentage of methylated CpG sites at *Oct4* promoter regions in WT and H1 TKO embryos. Statistical analysis was performed using Fisher's exact test. ***: P<0.001; ****: P<0.0001.

precursors after E8.5 (Ovitt and Scholer, 1998), whereas *Nanog* expression is largely downregulated after E4.5 (Chambers et al., 2003). We analyzed expression of *Oct4* and *Nanog* from E8.5 embryos, when many of the surviving TKO embryos appeared comparable to WT littermates. E8.5 embryos were harvested from intercrosses of H1c/H1d/H1e triple heterozygotes and the expression levels of *Oct4* and *Nanog* in TKO and WT embryos were analyzed from three litters using quantitative RT-PCR. On average, expression levels of *Oct4* and *Nanog* in TKO embryos were more than 4-fold of that from WT littermate controls (Figure 2.12A, Fighre 2.13A), indicating that depletion of H1 impairs repression of the expression of pluripotency factors in E8.5 embryos *in vivo*.

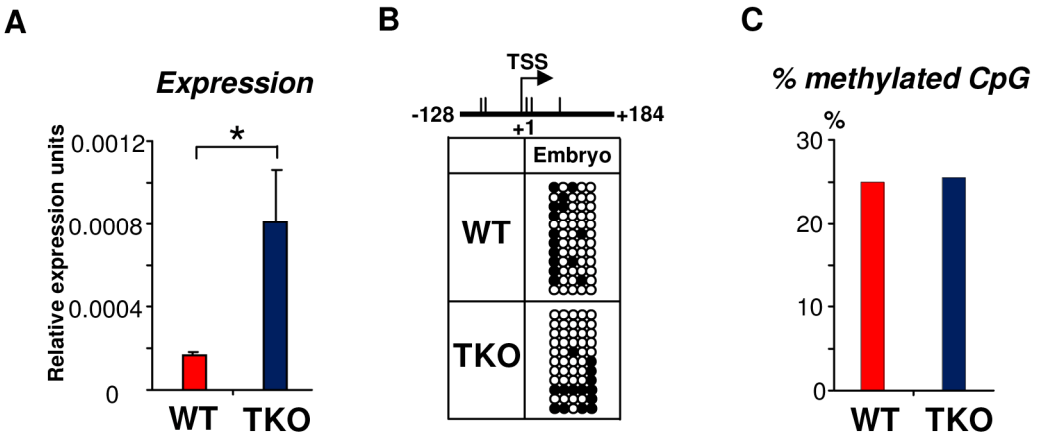

Figure 2.13 Increased expression of *Nanog* by H1 depletion in embryos.
(A) qRT-PCR analysis of E8.5 embryos indicating the higher levels of *Nanog* expression in H1 TKO embryos compared with WT. Values are means ± SEM, n = 5 for each genotype. Expression levels were normalized over *GAPDH*. *: P<0.05. (B) DNA methylation status of promoter regions of *Nanog* in E8.5 embryos analyzed by bisulfite sequencing. (C) Percentage of CpG methylation calculated from results in (B).

DNA methylation of cytosine nucleotide at CpG sites within gene promoter regions contributes to stable gene silencing, and thus is a key determinant in regulating the expression of pluripotency genes (Farthing et al., 2008), so we asked if the DNA methylation status at the *Oct4* and *Nanog* promoters is affected in H1 TKO embryos. Results from bisulfite sequencing analysis demonstrated that the extent of CpG methylation at the *Oct4* promoter region was markedly reduced in triple-H1 null embryos in comparison with corresponding wild-type littermates (Figure 2.12B &C), whereas the level of DNA methylation (percent methylation of analyzed CpGs) at *Nanog* promoter did not display differences between WT and H1 TKO embryos (Figure 2.13B & C). This suggests that H1 participates in establishing and/or maintaining CpG methylation at *Oct4* promoter during embryogenesis.

To further investigate the mechanisms by which H1 regulates pluripotency genes during ESC differentiation, we analyzed the epigenetic profiles of the *Oct4* and *Nanog* genes during EB differentiation in rotary suspension culture. We demonstrated previously that this method produces a large quantity of homogeneous EBs that progressively differentiate (Carpenedo et al., 2007), thus the sequential epigenetic events can be readily followed. Expression of *Oct4* and *Nanog* was reduced during continuous suspension culture for WT cultures, but remained high in TKO EB cultures (Figure 2.14A, Figure 2.15A,). DNA methylation analysis by bisulfite sequencing indicated that WT EBs had an increase in the sporadic DNA methylation at specific CpG sites throughout the *Oct4* proximal promoter region at day 10 ($P = 0.002$ and 0.036 for the respective R1 and R2 regions) (Figure 2.14B & C), whereas TKO EBs remained completely unmethylated at

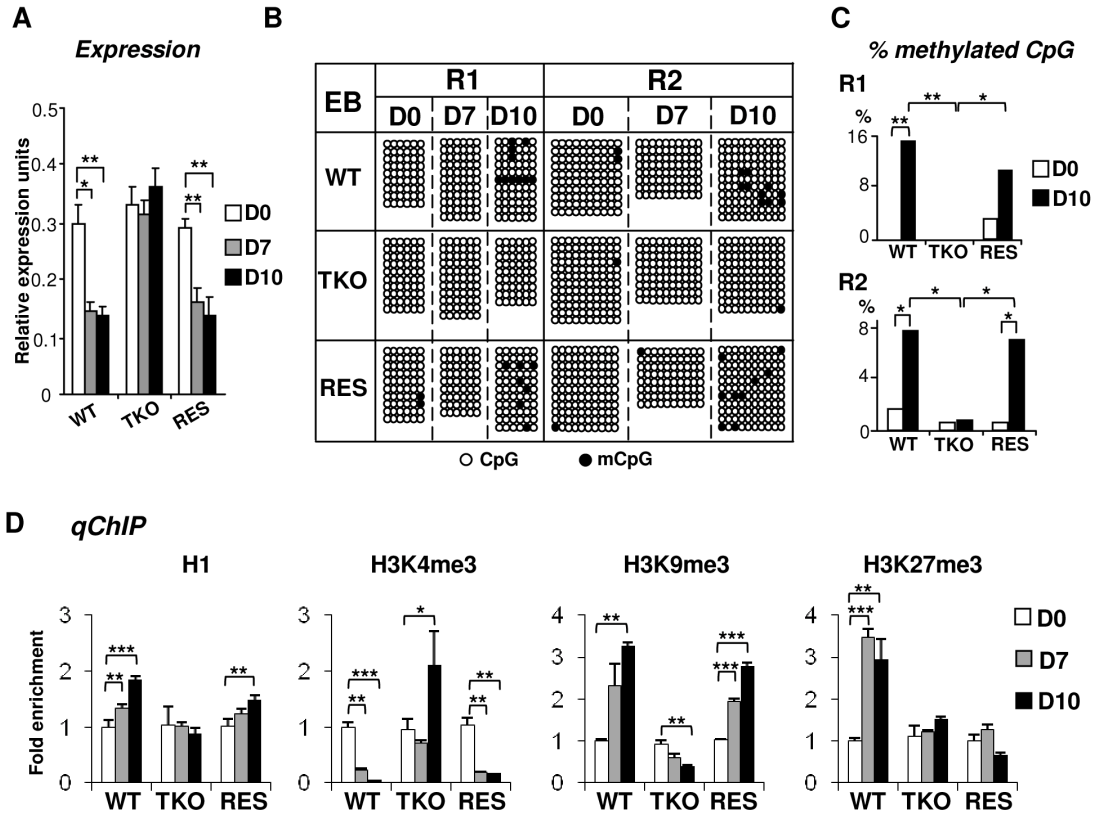

Figure 2.14 Analysis of expression and epigenetic marks at *Oct4* pluripotency gene during EB differentiation in rotary suspension culture.
Analyses of expression (A), DNA methylation (B), % of mCpG (C); and occupancy of H1 and three histone marks (D) of *Oct4* in WT, H1 TKO and RES cells during EB differentiation. Relative expression levels were normalized over *GAPDH*. Relative fold enrichment is calculated by normalizing the qChIP values (as described in Material and Methods) of ESCs (day 0) or EBs at each time point by that of WT ESCs (WT D0). Values are presented as mean ± S.D. *: P<0.05; **: P<0.01; ***: P<0.001.

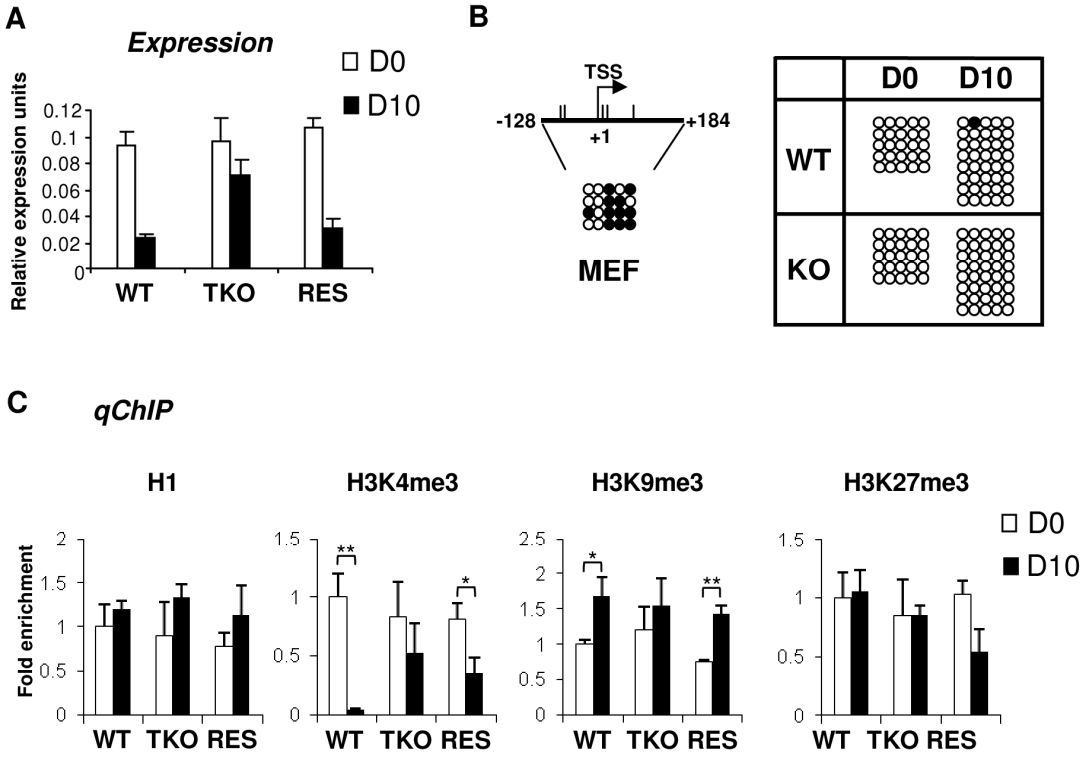

Figure 2.15 Analysis of expression and epigenetic marks at *Nanog* promoter.
(A) qRT-PCR analysis of *Nanog* expression in ESCs and day 10 EBs. Expression levels were normalized over *GAPDH*. (B) DNA methylation status of *Nanog* promoter in mouse embryonic fibroblasts (MEFs) (left) or in ESCs (day 0) and day 10 EBs (right). (C) qChIP analysis of H1, H3K4me3, H3K9me3 and H3K27me3 levels at *Nanog* promoters in ESCs (day 0) and day 10 EBs. Data were normalized as described in Figure 2.15 D . *: P<0.05; **: P<0.01.

these sites. On the other hand, *Nanog* promoter region remained unmethylated throughout the differentiation in both WT and H1 TKO cultures (Figure 2.15B).

To further investigate the effect of H1 levels in affecting expression and DNA methylation of pluripotency genes in EB differentiation, we generated "rescue" cell lines (referred to as "RES") by stably overexpressing exogenous H1d in the H1 TKO cells (Figure 2.16A). RES cells had a H1/nucleosome ratio of 0.31 (Figure 2.16B), displayed a normal karyotype (Figure 2.16C), and were able to differentiate into EBs with cystic structures which were observed in WT, but not in TKO, EBs (Figure 2.16D). RES EBs had elevated expression of differentiation markers, such as *AFP* and *Nkx2.5* (Figure 2.16E) and reduced expression of *Oct4* and *Nanog* pluripotency genes upon differentiation (Figure 2.14A and Figure 2.15A), suggesting that the expression of exogenous H1d alleviates the differentiation defects and restores the repression of pluripotency factors in H1 TKO EBs. In addition, the percent of methylated CpG was increased in RES EBs to a level comparable to that of WT EBs at the same time points, suggesting that reintroduction of H1d into the H1 TKO ESCs is able to reestablish DNA methylation and the stable repression of the *Oct4* gene in differentiating EBs (Figure 2.14B & C).

We next analyzed the status of H1, H3K4me3, H3K9me3 and H3K27me3 at the promoters of pluripotency genes *Oct4* and *Nanog* by quantitative chromatin immunoprecipitation (qChIP). Whereas H1 occupancy at *Oct4* promoter increased in WT and RES cultures during differentiation, it remained unchanged in H1 TKO EBs (Figure 2.14D). It is interesting to note that the occupancy of the replacement subtype, $H1^0$, at

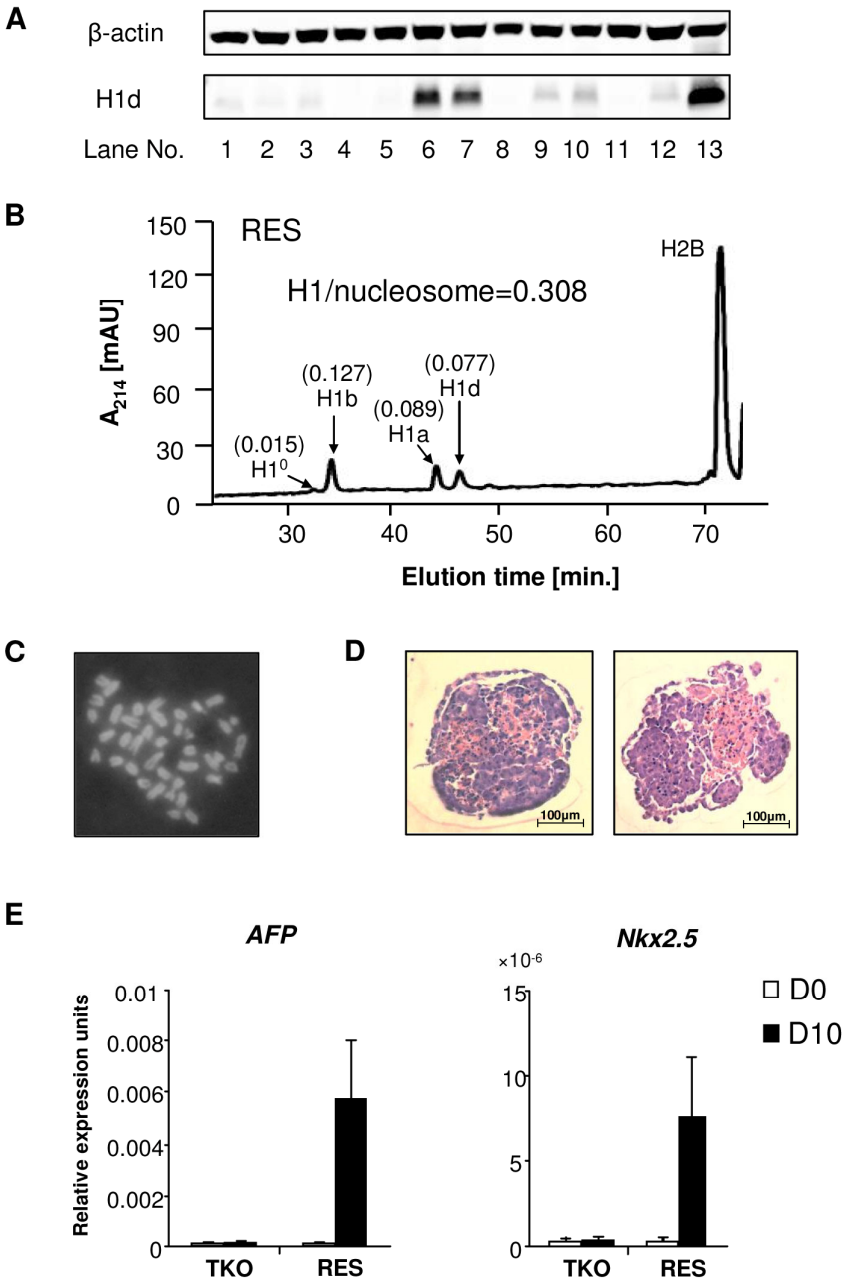

Figure 2.16 Generation and characterization of RES ESC lines.
(A) Representative Western blotting analysis of "rescue" clones. Immunoblotting with anti-β-ACTIN antibody indicates equal loading of whole cell lysates. (B) Reverse phase HPLC analysis of a RES cell line with high levels of H1d expression. (C) Chromosome spread of the RES cell shown in B). (D) Hematoxylin and eosin staining of sections of day 10 EBs generated from RES cells in rotary suspension culture. Scale bar: 100 µm. (E) qRT-PCR analysis of differentiation markers in RES cells during EB differentiation. Expression levels were normalized over *GAPDH*.

Oct4 promoter was markedly increased in both WT and RES cultures but only mildly elevated in H1 TKO cultures (Figure 2.17), suggesting that efficient binding of $H1^0$ at *Oct4* promoter may be facilitated by sufficient amount of other somatic H1s. Furthermore, wild-type and RES EBs displayed decreasing levels of the active histone mark H3K4me3 accompanied with a significant increase in the levels of the repressive histone mark H3K9me3, at promoter regions of pluripotency genes *Oct4* and *Nanog* upon EB differentiation (Figure 2.14D and Figure 2.15C). In contrast, H1 TKO EBs did not display similar or significant changes in the levels of these histone marks at the same promoter regions (Figure 2.14D and Figure 2.15C). Levels of H3K27me3, another repressive histone mark, were significantly increased in WT cultures during differentiation at *Oct4* promoter, while such increases were not detected at H1 TKO or RES EBs (Figure 2.14D).

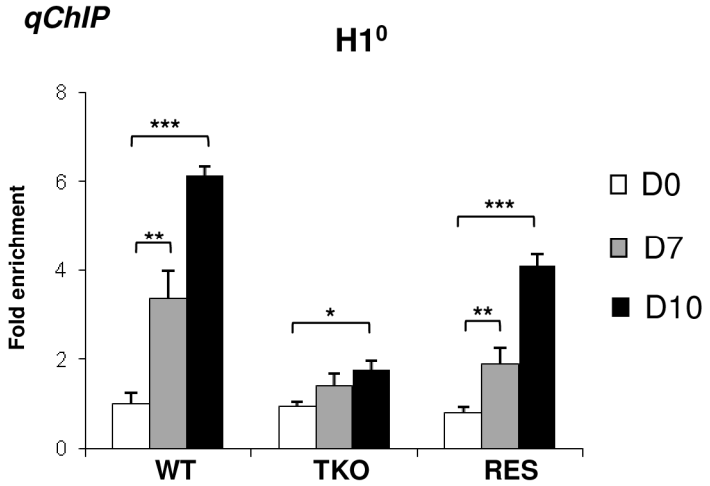

Figure 2.17 qChIP Analysis of $H1^0$ occupancy at *Oct4* promoter during EB differentiation.
Data were normalized as described in Figure 2.15 D. *: P<0.05; **: P<0.01; ***: P<0.001.

These analyses suggest that the increase of H1 levels and the changes in histone modifications, such as H3K4me3, H3K9me3 and H3K27me3, precede DNA methylation establishment in mediating *Oct4* gene silencing during EB differentiation. Overall, the results indicate that lack of H1c, H1d and H1e impairs the establishment or maintenance of epigenetic changes in DNA methylation and histone modifications that are necessary for stable repression of pluripotent transcription factor *Oct4* in differentiated cells (Figure 2.18).

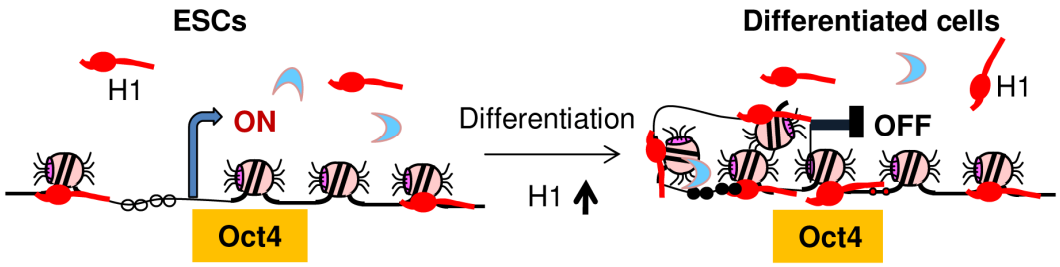

Figure 2.18 Model for H1 in repression of *Oct4* during ESC differentiation.
ESCs have low H1 content with an relatively "open" chromatin. During differentiation, total H1 content increases, which facilitates local chromatin compaction at *Oct4* gene and contributes to establishment and/or maintenance of epigenetic changes necessary for stable silencing of *Oct4* pluripotency gene.

2.5 Discussion

Embryonic stem cells, derived from the inner cell mass of the blastocyst stage mammalian embryos (Evans and Kaufman, 1981; Thomson et al., 1998), can self-renew nearly indefinitely in culture and give rise to all cell types of the three germ layers, ectoderm, mesoderm and endoderm, during differentiation. ESCs possess distinctive transcriptional regulatory circuits and chromatin signatures that are critical for maintaining pluripotency and self-renewal (Boyer et al., 2005; Kashyap et al., 2009). Recent studies suggest that ESCs exhibit a relatively "open" chromatin state, and during differentiation, heterochromatin formation increases (Dialynas et al., 2007; Efroni et al., 2008; Gaspar-Maia et al., 2011). However, whether this "open" chromatin state is necessary for pluripotency and whether the compaction of chromatin is required for ESC differentiation remain to be addressed.

Linker histone H1 is the major chromatin architectural protein in mediating higher order chromatin folding. H1 TKO ESCs have an H1/nucleosome ratio of 0.25, equivalent to 1 H1 per 4 nucleosomes, a nearly 50% reduction in total H1 levels in comparison with WT ESCs (Fan et al., 2005). The H1 level is especially low in H1 TKO ESCs when compared with an H1/nucleosome ratio of 0.75~0.8 in differentiated cell types from various adult tissues (Fan et al., 2003; Woodcock et al., 2006). H1 TKO ESCs have globally decondensed chromatin (Fan et al., 2005), offering an approachable means to examine the effect of chromatin decondensation on ESC pluripotency and differentiation. H1 TKO ESCs maintain ESC colony morphology, express pluripotency factors (Figure 2.2A), propagate and self-renew normally as wild-type ESCs, suggesting that a more

"open" chromatin structure than normal WT ESCs does not interfere with the "basal" state of ESCs, and may even promote the maintenance of this primitive state. This prediction is consistent with the fact that H1 TKO ESCs are easier to maintain and have sustainable OCT4 pluripotency factor expression and robust growth even under conditions normally promoting spontaneous differentiation, such as culturing ESCs in the absence of LIF and feeder cells for a prolonged period. ESCs are found to have hyperdynamic chromatin with loosely bound major chromatin architectural proteins, such as H1 and HP1 (Meshorer and Misteli, 2006). A more "open" chromatin in H1 TKO ESCs may suggest a more dynamic chromatin structure due to the lack of structural constraints. However, it is not clear at present whether the remaining H1 proteins in H1 TKO ESCs undergo a change in post-translational modifications, such as phosphorylation, which would change the binding affinity of these remaining H1 subtypes to chromatin (Dou et al., 2002; Hendzel et al., 2004). We also note the considerable amount of H1s remaining in these TKO ESCs, thus further reducing H1 amount by knockout or siRNA could help determine if a minimal level of H1 is required to permit self-renewal of ESCs.

While a significant reduction in H1 levels does not interfere with ESC self-renewal, it appears to clearly impair ESC differentiation. This is manifested in static culture conditions that promote spontaneous ESC differentiation, in a rotary suspension culture system which induces highly reproducible and robust EB formation and differentiation (Carpenedo et al., 2007; Sargent et al., 2009), as well as in a well defined neural differentiation regimen. H1 TKO EBs formed in rotary culture have a reduced level of activation of many developmental genes and markers from all three germ layers, suggesting that the effects of H1 depletion on differentiation and cell fate decision

broadly impact early developmental gene expression. This may explain why only 50% of H1 TKO embryos are present at E7.5 (Fan et al., 2003). Furthermore, H1 TKO ESCs are defective in forming neuronal cells, glial cells, and lack formation of neural network, which are essential for nervous system development *in vivo*. Total levels of H1 increases progressively in EB formation and differentiation, suggesting an increasingly more condensed chromatin state during EB differentiation in WT cultures. H1 TKO EBs have an H1 to nucleosome ratio lower than WT ESCs. The fact that H1 TKO ESCs cells are unable to execute normal differentiation programs suggests that an especially low H1 level (and the resulting more open chromatin structure (Fan et al., 2005)) impairs ESC pluripotency and differentiation. Thus, elevated levels of the total H1 amount as well as a more compact chromatin are not mere consequences of differentiation processes, but a necessity to enable it to proceed normally.

H1c, H1d, H1e and $H1^0$ are four H1 subtypes that increase significantly during ESC differentiation. H1x, although whose mRNA expression has been reported to increase during differentiation of human ESCs and embryocarcinoma cells (Shahhoseini et al., 2010; Terme et al., 2011), is not detected in HPLC profiles of both WT and TKO ESCs throughout differentiation despite a 2-fold increase in mRNA levels in TKO ESCs compared with WT ((Fan et al., 2005) and data not shown). Thus, this more distantly related H1 subtype (H1x) is present at a negligible level compared with the 6 somatic H1 subtypes (H1a-e and $H1^0$) in ESCs and EBs. In contrast, H1a and H1b are abundantly present in ESCs, together accounting for one third of total H1 content in WT ESCs. Although both H1a and H1b increase approximately 50% in TKO ESCs upon depletion of H1c, H1d and H1e, the levels of H1a and H1b do not increase during EB

differentiation of WT or TKO cultures. Thus, H1c, H1d, H1e, and $H1^0$, but not H1a and H1b, are likely to be the major contributors for the effects of H1 on ESC differentiation and repression of pluripotency genes during ESC differentiation. In particular, $H1^0$, a subtype highly expressed in differentiated cells and tissues (Happel and Doenecke, 2009), progressively increases in bulk chromatin and at the *Oct4* promoter during EB differentiation and largely accounts for the increase in total H1 levels in TKO EBs during differentiation (Figure2.10, Figure 2.11, and Figure 2.17). Thus it would be very interesting to investigate if further deletion of $H1^0$ in the face of H1 TKO will result in a complete inhibition of ESC differentiation. Nevertheless, none of these four H1 subtypes alone appears to be required for mouse ESC differentiation, because knockout mice with deletion of one of these four H1 subtypes develop normally (Fan et al., 2001; Sirotkin et al., 1995), suggesting that the differentiation defects we observed here are more likely caused by a marked reduction of total H1 content in H1 TKO cells. Furthermore, we show that a partial rescue of H1 content by reintroduction of H1d into TKO cells mitigates the impairment of differentiation. Together, we surmise that a potential threshold of H1 levels, but not necessarily a specific H1 subtype, is required for proper ESC differentiation.

The effects of H1 depletion on gene expression in EBs are significant and wide-spread, drastically affecting many genes (Figure 2.4, Figure 2.5), in sharp contrast to the limited number of genes with altered expression in H1 TKO ESCs (Fan et al., 2005). It is conceivable that H1 depletion in ESCs and a marked decondensation of the chromatin pose little effects on the "basal" state of ESCs, but more so on impairing the capability of ESCs to transit to differentiated cells which exhibit more compact chromatin.

Nevertheless, the influence of H1 on many developmental genes in EBs could be a secondary effect resulting from the lack of effecient repression of pluripotency gene expression, such as *Oct4* and *Nanog*, which associate with repressor complexes to silence developmental genes (Liang et al., 2008). The effects might also be caused by misregulation of multiple key developmental genes required for normal differentiation to proceed. It is interesting to note that 50% of H1 TKO embryos are able to progress to mid-gestation, suggesting that early differentiation in three germ layers *in vivo* is possible for some TKO embryos (Fan et al., 2003). Consistently, H1 TKO ES cells are capable of forming EBs (Figure 2.3), albeit mostly impaired in differentiation, and teratomas that contain a small fraction of cells differentiated into the three germ layers (data not shown). The impairment of ESC differentiation *in vitro* yet survival of some knockout embryos to mid-gestation stage is reminiscent of several other knockouts of ubiquitously expressed proteins that bind and modify chromatin (Gaspar-Maia et al., 2011; Lei et al., 1996; Pasini et al., 2007; Pasini et al., 2004), which probably reflects more heterogenous cell populations and conditions *in vivo*.

Importantly, we discovered that, compared with WT ESCs, the H1 TKO cells fail to effectively silence the expression of pluripotency genes *Oct4* and *Nanog*, which are critical for pluripotency (Niwa et al., 2000; Silva et al., 2009). We believe that this effect of H1 on repression of *Oct4* is direct because 1) *Oct4* expression is higher in H1 TKO compared with WT both *in vivo* in embryos and *in vitro* using three differentiation schemes for ESCs and EBs, although the degree of effects varies according to different differentiation schemes employed; 2) reconstitution of H1d into H1 TKO ESCs restores the effective repression of expression and dynamic changes in histone modifications and

DNA methylation levels during differentiation; 3) the level of H1 is cumulatively increased at the *Oct4* promoter during differentiation of WT, but not of H1 TKO, cultures. We suggest that the H1 occupancy at *Oct4* promoter in ESCs could be the basal/minimal level for detection by qChIP assay, as H1 has been found to be relatively depleted from active promoters compared with other regions (Bresnick et al., 1992; Krishnakumar et al., 2008). Interestingly, qChIP analysis showed that the association of $H1^0$ at *Oct4* promoters was significantly higher in RES cells than TKO cells (Figure 2.17), suggesting that the presence of sufficient H1 proteins may facilitate $H1^0$ binding. We surmise that the progressive increase of H1c, H1d and H1e during differentiation and the increased H1 occupancy at *Oct4* promoter lead to a transition to a more condensed local chromatin structure necessary for stable silencing of *Oct4* during differentiation (Figure 2.18). These results together with the observation that OCT4 is present at the promoters of several H1 subtypes in human ESCs (Boyer et al., 2005; Terme et al., 2011) suggest a potential feedback loop between OCT4 and H1 in stem cell fate determination.

Interestingly, we found that CpG methylation of *Oct4* promoter in H1 TKO embryos is significantly reduced compared with wild-type littermates. Although less pronounced in EB differentiation, the effects of H1 depletion on DNA methylation at *Oct4* promoter are also apparent in day 10 EBs. This observation reinforces the link between H1 and DNA methylation, which was initially discovered at imprinting control regions (ICRs) of *H19* and *Gtl2* loci (Fan et al., 2005) and later at regulatory regions of the immunoglobin heavy chain locus and homeobox *Rhox* gene cluster (Giambra et al., 2008; Maclean et al., 2011). Future studies on how DNA methylation changes at these regions in H1 TKO ESCs during differentiation will provide additional insights on

dynamic profiles of DNA methylation upon differentiation in the face of minimal level of H1 and/or open chromatin structure.

H1 TKO EBs do not exhibit the opposite changes in the levels of the active histone mark (H3K4me3) and the repressive histone mark (H3K9me3) at promoters of *Oct4* and *Nanog* that normally occur in wild-type EBs during differentiation. Interestingly, we did observe significant changes in the levels of histone modifications in wild-type EBs at day 7 in rotary culture, before an increase in DNA methylation levels occurred at *Oct4* promoter. This result reinforces the notion that DNA methylation is a slower mark to establish compared with histone marks (Feldman et al., 2006). It is noteworthy that the levels of DNA methylation at the *Nanog* promoter do not display a difference in WT and H1 TKO embryos at day 8.5 and are not altered during EB differentiation, suggesting that DNA methylation is unlikely to be responsible for gene expression changes of *Nanog* during this period of time.

Our results suggest a role of H1 and chromatin compaction in epigenetic regulation of the pluripotency gene *Oct4*, likely mediated through DNA methylation and histone modifications. To our knowledge, this represents a novel mechanistic link by which bulk chromatin compaction is directly linked to pluripotency, by participating in repression of the pluripotency genes. In ESCs, DNMT3b has been shown to interact with H1 (Kashiwagi et al., 2011). *In vitro* studies demonstrated that H1 interacts with HP1 (Daujat et al., 2005; Nielsen et al., 2001) which can in turn bind to SUV39H which methylates H3K9. Moreover, H1 has been shown *in vitro* to stimulate the activity of PRC2 toward methylation of H3K27me3 when H1 is incorporated into nucleosomes (Martin et al., 2006), and we have also observed interactions between H1 and PRC2

components in ESCs (Cao, Ho, Lasater, and Fan, unpublished observation). Therefore, we envision that during ESC differentiation, H1 levels increase, which may facilitate the recruitment of DNMTs, SUV39H and PRC2 to *Oct4* promoter, promoting the establishment and/or maintenance of repressive epigenetic modifications and silencing the expression of this pluripotency gene (Figure 2.18).

In summary, we have demonstrated that loss of linker histone subtypes H1c, H1d, and H1e impairs embryonic stem cell differentiation. Furthermore, our results indicate that H1 contributes to silencing of pluripotency factors and participates in mediating changes in DNA methylation and histone marks necessary for silencing of pluripotency genes during differentiation. Thus, modulating the levels of H1 linker histones and chromatin compaction may potentially serve as a new strategy for regulating stem cell pluripotency.

2.6 Reference

Ahmed, K., Dehghani, H., Rugg-Gunn, P., Fussner, E., Rossant, J., and Bazett-Jones, D.P. (2010). Global chromatin architecture reflects pluripotency and lineage commitment in the early mouse embryo. PloS one *5*, e10531.

Bain, G., Kitchens, D., Yao, M., Huettner, J.E., and Gottlieb, D.I. (1995). Embryonic stem cells express neuronal properties in vitro. Developmental biology *168*, 342-357.

Bernstein, B.E., Mikkelsen, T.S., Xie, X., Kamal, M., Huebert, D.J., Cuff, J., Fry, B., Meissner, A., Wernig, M., Plath, K.*, et al.* (2006). A bivalent chromatin structure marks key developmental genes in embryonic stem cells. Cell *125*, 315-326.

Bock, C., Reither, S., Mikeska, T., Paulsen, M., Walter, J., and Lengauer, T. (2005). BiQ Analyzer: visualization and quality control for DNA methylation data from bisulfite sequencing. Bioinformatics *21*, 4067-4068.

Boyer, L.A., Lee, T.I., Cole, M.F., Johnstone, S.E., Levine, S.S., Zucker, J.P., Guenther, M.G., Kumar, R.M., Murray, H.L., Jenner, R.G.*, et al.* (2005). Core transcriptional regulatory circuitry in human embryonic stem cells. Cell *122*, 947-956.

Bresnick, E.H., Bustin, M., Marsaud, V., Richard-Foy, H., and Hager, G.L. (1992). The transcriptionally-active MMTV promoter is depleted of histone H1. Nucleic acids research *20*, 273-278.

Carpenedo, R.L., Sargent, C.Y., and McDevitt, T.C. (2007). Rotary suspension culture enhances the efficiency, yield, and homogeneity of embryoid body differentiation. Stem cells *25*, 2224-2234.

Chambers, I., Colby, D., Robertson, M., Nichols, J., Lee, S., Tweedie, S., and Smith, A. (2003). Functional expression cloning of Nanog, a pluripotency sustaining factor in embryonic stem cells. Cell *113*, 643-655.

da Silva, J.S., and Dotti, C.G. (2002). Breaking the neuronal sphere: regulation of the actin cytoskeleton in neuritogenesis. Nature reviews Neuroscience *3*, 694-704.

Daujat, S., Zeissler, U., Waldmann, T., Happel, N., and Schneider, R. (2005). HP1 binds specifically to Lys26-methylated histone H1.4, whereas simultaneous Ser27

phosphorylation blocks HP1 binding. The Journal of biological chemistry *280*, 38090-38095.

Dialynas, G.K., Terjung, S., Brown, J.P., Aucott, R.L., Baron-Luhr, B., Singh, P.B., and Georgatos, S.D. (2007). Plasticity of HP1 proteins in mammalian cells. Journal of cell science *120*, 3415-3424.

Dou, Y., Bowen, J., Liu, Y., and Gorovsky, M.A. (2002). Phosphorylation and an ATP-dependent process increase the dynamic exchange of H1 in chromatin. The Journal of cell biology *158*, 1161-1170.

Efroni, S., Duttagupta, R., Cheng, J., Dehghani, H., Hoeppner, D.J., Dash, C., Bazett-Jones, D.P., Le Grice, S., McKay, R.D., Buetow, K.H., *et al.* (2008). Global transcription in pluripotent embryonic stem cells. Cell stem cell *2*, 437-447.

Eskeland, R., Leeb, M., Grimes, G.R., Kress, C., Boyle, S., Sproul, D., Gilbert, N., Fan, Y., Skoultchi, A.I., Wutz, A., *et al.* (2010). Ring1B compacts chromatin structure and represses gene expression independent of histone ubiquitination. Molecular cell *38*, 452-464.

Evans, M.J., and Kaufman, M.H. (1981). Establishment in culture of pluripotential cells from mouse embryos. Nature *292*, 154-156.

Fan, Y., Braut, S.A., Lin, Q., Singer, R.H., and Skoultchi, A.I. (2001). Determination of transgenic loci by expression FISH. Genomics *71*, 66-69.

Fan, Y., Nikitina, T., Morin-Kensicki, E.M., Zhao, J., Magnuson, T.R., Woodcock, C.L., and Skoultchi, A.I. (2003). H1 linker histones are essential for mouse development and affect nucleosome spacing in vivo. Molecular and cellular biology *23*, 4559-4572.

Fan, Y., Nikitina, T., Zhao, J., Fleury, T.J., Bhattacharyya, R., Bouhassira, E.E., Stein, A., Woodcock, C.L., and Skoultchi, A.I. (2005). Histone H1 depletion in mammals alters global chromatin structure but causes specific changes in gene regulation. Cell *123*, 1199-1212.

Fan, Y., and Skoultchi, A.I. (2004). Genetic analysis of H1 linker histone subtypes and their functions in mice. Methods in enzymology *377*, 85-107.

Farthing, C.R., Ficz, G., Ng, R.K., Chan, C.F., Andrews, S., Dean, W., Hemberger, M., and Reik, W. (2008). Global mapping of DNA methylation in mouse promoters reveals epigenetic reprogramming of pluripotency genes. PLoS genetics *4*, e1000116.

Feldman, N., Gerson, A., Fang, J., Li, E., Zhang, Y., Shinkai, Y., Cedar, H., and Bergman, Y. (2006). G9a-mediated irreversible epigenetic inactivation of Oct-3/4 during early embryogenesis. Nature cell biology *8*, 188-194.

Fussner, E., Ahmed, K., Dehghani, H., Strauss, M., and Bazett-Jones, D.P. (2010). Changes in chromatin fiber density as a marker for pluripotency. Cold Spring Harbor symposia on quantitative biology *75*, 245-249.

Gaspar-Maia, A., Alajem, A., Meshorer, E., and Ramalho-Santos, M. (2011). Open chromatin in pluripotency and reprogramming. Nature reviews Molecular cell biology *12*, 36-47.

Giambra, V., Volpi, S., Emelyanov, A.V., Pflugh, D., Bothwell, A.L., Norio, P., Fan, Y., Ju, Z., Skoultchi, A.I., Hardy, R.R.*, et al.* (2008). Pax5 and linker histone H1 coordinate DNA methylation and histone modifications in the 3' regulatory region of the immunoglobulin heavy chain locus. Molecular and cellular biology *28*, 6123-6133.

Happel, N., and Doenecke, D. (2009). Histone H1 and its isoforms: contribution to chromatin structure and function. Gene *431*, 1-12.

Hendzel, M.J., Lever, M.A., Crawford, E., and Th'ng, J.P. (2004). The C-terminal domain is the primary determinant of histone H1 binding to chromatin in vivo. The Journal of biological chemistry *279*, 20028-20034.

Kashiwagi, K., Nimura, K., Ura, K., and Kaneda, Y. (2011). DNA methyltransferase 3b preferentially associates with condensed chromatin. Nucleic acids research *39*, 874-888.

Kashyap, V., Rezende, N.C., Scotland, K.B., Shaffer, S.M., Persson, J.L., Gudas, L.J., and Mongan, N.P. (2009). Regulation of stem cell pluripotency and differentiation involves a mutual regulatory circuit of the NANOG, OCT4, and SOX2 pluripotency transcription factors with polycomb repressive complexes and stem cell microRNAs. Stem cells and development *18*, 1093-1108.

Kim, M., Habiba, A., Doherty, J.M., Mills, J.C., Mercer, R.W., and Huettner, J.E. (2009). Regulation of mouse embryonic stem cell neural differentiation by retinoic acid. Developmental biology *328*, 456-471.

Krishnakumar, R., Gamble, M.J., Frizzell, K.M., Berrocal, J.G., Kininis, M., and Kraus, W.L. (2008). Reciprocal binding of PARP-1 and histone H1 at promoters specifies transcriptional outcomes. Science *319*, 819-821.

Lei, H., Oh, S.P., Okano, M., Juttermann, R., Goss, K.A., Jaenisch, R., and Li, E. (1996). De novo DNA cytosine methyltransferase activities in mouse embryonic stem cells. Development *122*, 3195-3205.

Liang, J., Wan, M., Zhang, Y., Gu, P., Xin, H., Jung, S.Y., Qin, J., Wong, J., Cooney, A.J., Liu, D.*, et al.* (2008). Nanog and Oct4 associate with unique transcriptional repression complexes in embryonic stem cells. Nature cell biology *10*, 731-739.

Maclean, J.A., Bettegowda, A., Kim, B.J., Lou, C.H., Yang, S.M., Bhardwaj, A., Shanker, S., Hu, Z., Fan, Y., Eckardt, S.*, et al.* (2011). The rhox homeobox gene cluster is imprinted and selectively targeted for regulation by histone h1 and DNA methylation. Molecular and cellular biology *31*, 1275-1287.

Martin, C., Cao, R., and Zhang, Y. (2006). Substrate preferences of the EZH2 histone methyltransferase complex. The Journal of biological chemistry *281*, 8365-8370.

Medrzycki, M., Zhang, Y., Cao, K., and Fan, Y. (2012). Expression analysis of mammalian linker-histone subtypes. Journal of visualized experiments : JoVE.

Meissner, A. (2010). Epigenetic modifications in pluripotent and differentiated cells. Nature biotechnology *28*, 1079-1088.

Mereau, A., Grey, L., Piquet-Pellorce, C., and Heath, J.K. (1993). Characterization of a binding protein for leukemia inhibitory factor localized in extracellular matrix. The Journal of cell biology *122*, 713-719.

Meshorer, E., and Misteli, T. (2006). Chromatin in pluripotent embryonic stem cells and differentiation. Nature reviews Molecular cell biology *7*, 540-546.

Meshorer, E., Yellajoshula, D., George, E., Scambler, P.J., Brown, D.T., and Misteli, T. (2006). Hyperdynamic plasticity of chromatin proteins in pluripotent embryonic stem cells. Developmental cell *10*, 105-116.

Nielsen, A.L., Oulad-Abdelghani, M., Ortiz, J.A., Remboutsika, E., Chambon, P., and Losson, R. (2001). Heterochromatin formation in mammalian cells: interaction between histones and HP1 proteins. Molecular cell *7*, 729-739.

Niwa, H., Miyazaki, J., and Smith, A.G. (2000). Quantitative expression of Oct-3/4 defines differentiation, dedifferentiation or self-renewal of ES cells. Nature genetics *24*, 372-376.

Orkin, S.H., and Hochedlinger, K. (2011). Chromatin connections to pluripotency and cellular reprogramming. Cell *145*, 835-850.

Ovitt, C.E., and Scholer, H.R. (1998). The molecular biology of Oct-4 in the early mouse embryo. Molecular human reproduction *4*, 1021-1031.

Pasini, D., Bracken, A.P., Hansen, J.B., Capillo, M., and Helin, K. (2007). The polycomb group protein Suz12 is required for embryonic stem cell differentiation. Molecular and cellular biology *27*, 3769-3779.

Pasini, D., Bracken, A.P., Jensen, M.R., Lazzerini Denchi, E., and Helin, K. (2004). Suz12 is essential for mouse development and for EZH2 histone methyltransferase activity. The EMBO journal *23*, 4061-4071.

Sargent, C.Y., Berguig, G.Y., and McDevitt, T.C. (2009). Cardiomyogenic differentiation of embryoid bodies is promoted by rotary orbital suspension culture. Tissue engineering Part A *15*, 331-342.

Shahhoseini, M., Favaedi, R., Baharvand, H., Sharma, V., and Stunnenberg, H.G. (2010). Evidence for a dynamic role of the linker histone variant H1x during retinoic acid-induced differentiation of NT2 cells. FEBS letters *584*, 4661-4664.

Shen, X., Liu, Y., Hsu, Y.J., Fujiwara, Y., Kim, J., Mao, X., Yuan, G.C., and Orkin, S.H. (2008). EZH1 mediates methylation on histone H3 lysine 27 and complements EZH2 in maintaining stem cell identity and executing pluripotency. Molecular cell *32*, 491-502.

Shen, X., Yu, L., Weir, J.W., and Gorovsky, M.A. (1995). Linker histones are not essential and affect chromatin condensation in vivo. Cell *82*, 47-56.

Silva, J., Nichols, J., Theunissen, T.W., Guo, G., van Oosten, A.L., Barrandon, O., Wray, J., Yamanaka, S., Chambers, I., and Smith, A. (2009). Nanog is the gateway to the pluripotent ground state. Cell *138*, 722-737.

Sirotkin, A.M., Edelmann, W., Cheng, G., Klein-Szanto, A., Kucherlapati, R., and Skoultchi, A.I. (1995). Mice develop normally without the H1(0) linker histone. Proceedings of the National Academy of Sciences of the United States of America *92*, 6434-6438.

Terme, J.M., Sese, B., Millan-Arino, L., Mayor, R., Izpisua Belmonte, J.C., Barrero, M.J., and Jordan, A. (2011). Histone H1 variants are differentially expressed and incorporated into chromatin during differentiation and reprogramming to pluripotency. The Journal of biological chemistry *286*, 35347-35357.

Thomson, J.A., Itskovitz-Eldor, J., Shapiro, S.S., Waknitz, M.A., Swiergiel, J.J., Marshall, V.S., and Jones, J.M. (1998). Embryonic stem cell lines derived from human blastocysts. Science *282*, 1145-1147.

Wolffe, A.P. (1998). Chromatin: Structure and Function.

Woodcock, C.L., Skoultchi, A.I., and Fan, Y. (2006). Role of linker histone in chromatin structure and function: H1 stoichiometry and nucleosome repeat length. Chromosome research : an international journal on the molecular, supramolecular and evolutionary aspects of chromosome biology *14*, 17-25.

CHAPTER 3

REDUCTION OF *HOX* GENE EXPRESSION BY HISTONE H1 DEPLETION

This chapter was published under the same name in the following article:

Yunzhe Zhang, Zheng Liu, Magdalena Medrzycki, Kaixiang Cao, Yuhong Fan

Reduction of *Hox* Gene Expression by Histone H1 Depletion

PLoS One. 2012;7(6):e38829.

3.1 Abstract

The evolutionarily conserved homeotic (*Hox*) genes are organized in clusters and expressed collinearly to specify body patterning during embryonic development. Chromatin reorganization and decompaction are intimately connected with *Hox* gene activation. Linker histone H1 plays a key role in facilitating folding of higher order chromatin structure. Previous studies have shown that deletion of three somatic H1 subtypes together leads to embryonic lethality and that H1c/H1d/H1e triple knockout (TKO) embryonic stem cells (ESCs) display bulk chromatin decompaction. To investigate the potential role of H1 and higher order chromatin folding in the regulation of *Hox* gene expression, we systematically analyzed the expression of all 39 *Hox* genes in triple H1 null mouse embryos and ESCs by quantitative RT-PCR. Surprisingly, we find that H1 depletion causes significant reduction in the expression of a broad range of *Hox* genes in embryos and ESCs. To examine if any of the three H1 subtypes (H1c, H1d and H1e) is responsible for decreased expression of *Hox* gene in triple-H1 null ESCs, we derived and characterized $H1c^{-/-}$, $H1d^{-/-}$, and $H1e^{-/-}$ single-H1 null ESCs. We show that deletion of individual H1 subtypes results in down-regulation of specific *Hox* genes in ESCs. Finally we demonstrate that, in triple-H1- and single-H1- null ESCs, the levels of H3K4 trimethylation (H3K4me3) and H3K27 trimethylation (H3K27me3) were affected at specific *Hox* genes with decreased expression. Our data demonstrate that marked reduction in total H1 levels causes significant reduction in both expression and the level of active histone mark H3K4me3 at many *Hox* genes and that individual H1 subtypes

may also contribute to the regulation of specific *Hox* gene expression. We suggest possible mechanisms for such an unexpected role of histone H1 in *Hox* gene regulation.

3.2 Introduction

The *Hox* genes, encoding a family of evolutionarily conserved transcription factors that contain a DNA binding homeodomain, play fundamental roles in specifying anterior-posterior body patterning during development and are critical for cell fate determination (Gouti and Gavalas, 2008; Leucht et al., 2008; Mallo et al., 2010). The expression levels of *Hox* genes are tightly controlled throughout embryonic development, and aberrant expression and mutation of *Hox* genes can lead to body malformations and multiple types of malignancies (Goodman, 2002; Shah and Sukumar, 2010).

Hox genes are organized into genomic clusters and their physical order within the cluster corresponds to their expression order along the anterior-posterior axis. In mammals, there are 39 *Hox* genes arranged in four genomic clusters of thirteen paralog groups (A-D) (Graham et al., 1989), which are thought to derive from tandem duplication of ancestral genes (Ruddle et al., 1994; Wagner et al., 2003). Progressive transition of histone modifications and local chromatin decondensation have been found to associate with sequential expression of *Hoxb* and *Hoxd* loci during embryonic development and/or stem cell differentiation (Chambeyron and Bickmore, 2004; Chambeyron et al., 2005; Eskeland et al., 2010; Morey et al., 2007; Soshnikova and Duboule, 2009). *Hox* gene clusters are spatially compartmentalized and the transition in their 3D structure corresponds with the changes of H3K4me3 and H3K27me3 (Noordermeer et al., 2011). The temporal collinearity of the order of *Hox* gene activation along their physical sequence at genomic loci (Izpisua-Belmonte et al., 1991), stepwise transition of chromatin status and spatial configuration (Noordermeer et al., 2011; Soshnikova and

Duboule, 2009), and the necessity of the cluster organization for full repression of the entire cluster suggest an important role of chromatin structure in regulation of *Hox* genes (Chambeyron and Bickmore, 2004; Chambeyron et al., 2005; Eskeland et al., 2010; Morey et al., 2007; Soshnikova and Duboule, 2009). However, it remains to be determined whether the change of chromatin structure is a contributing factor or a consequence of *Hox* gene activation.

Linker histone H1 is the major chromatin structural protein involved in folding of chromatin into high order structure. H1 binds to the nucleosome and the linker DNA between nucleosomes to promote compaction of nucleosome arrays (Bednar et al., 1998; Thoma et al., 1979). Multiple H1 subtypes exist in mammals, providing additional levels of modulation on chromatin structure and function. Among the 11 mammalian H1 subtypes identified, 5 somatic H1 subtypes (H1a-e) are present in abundance in all dividing and non-dividing cells, whereas the replacement H1 ($H1^0$) and the 4 germ cell specific H1s are expressed in differentiating cells and germ cells, respectively (Happel and Doenecke, 2009). Depletion of three somatic H1 subtypes (H1c, H1d, and H1e) together results in embryonic lethality at midgestation, demonstrating the necessity of H1 for mammalian development (Fan et al., 2003). We have previously shown that H1c, H1d, and H1e triple knockout (H1 TKO) embryos and embryonic stem cells (ESCs) have marked reduction of total H1 levels and that H1 TKO ESCs display changes in bulk chromatin, including chromatin decondensation, a decreased nucleosome repeat length, as well as reduced levels of histone modifications H3K27me3 and H4K12Ac (Fan et al., 2003; Fan et al., 2005). Thus H1 TKO embryos and ESCs offer a unique opportunity to examine how the changes in chromatin structure influence *Hox* gene expression.

In the present study, we firstly analyzed the expression changes of all *Hox* genes in H1 TKO embryos and ESCs, and found reduced expression of a distinct set of *Hox* genes in embryos and ESCs, respectively. Furthermore, by characterizing H1c$^{-/-}$; H1d$^{-/-}$; and H1e$^{-/-}$ single-H1 null ESCs established in this study, we showed that individual H1 subtypes regulate specific *Hox* genes in ESCs. Finally we demonstrated that the levels of H3K4me3 were significantly diminished at the affected *Hox* genes in H1 TKO- and single-H1 KO- ESCs, whereas H3K27me3 occupancy was modestly increased at specific *Hox* genes. These results suggest that the marked reduction of H1 levels and decondensation of bulk chromatin cause repression of many *Hox* genes in embryos and ESCs, which may be in part mediated through individual H1 subtypes as well as changes in H3K4me3 and H3K27me3.

3.3 Materials and Methods

3.3.1 Establishment of Mouse Single-H1 KO ESCs and Formation of Embryoid Bodies

Mouse ESCs deficient in histone H1c, or H1d, or H1e were derived from outgrowth of the respective H1c$^{-/-}$, H1d$^{-/-}$, and H1e$^{-/-}$ blastocysts (E3.5) as described previously (Fan et al., 2005). Two ESC lines were established for each single KO. Genotyping analysis of WT and KO alleles of H1c, H1d, and H1e loci was carried out as reported (Fan et al., 2003). Animal breeding and experimental procedures were approved by Georgia Tech Institutional Animal Care and Use Committee. Embryoid bodies were formed by seeding 1×10^6 ESCs in a 10-cm ultra-low attachment culture dish (Corning) and cultured for 10 days in media containing Dulbecco's modified Eagle's medium (DMEM) (Life Technologies) with 15% fetal bovine serum (Gemini), 0.1 mM MEM Non-essential amino acids (Life Technologies), 55 μM 2-mercaptoethanol (Life Technologies) and 100 U/ml penicillin/100 μg/ml streptomycin (Life Technologies).

3.3.2 RNA Extraction and Quantitative Reverse Transcription PCR (qRT-PCR)

Total RNAs from ESCs were extracted with Trizol reagent (Life Technologies) according to the manufacturers' instructions. Total RNAs from embryos were prepared using Allprep DNA/RNA Micro kit (Qiagen). Reverse transcription was carried out using a SuperScript III First-Strand cDNA Synthesis kit (Life Technologies). cDNAs were subsequently analyzed with real-time quantitative PCR (qPCR) using iQ SYBR Green

upermix (Bio-Rad) with a MyIQ Single Color real-time PCR Detection System (Bio-Rad). *Hox* gene specific primers used for qRT-PCR are listed in Table 3.1.

3.3.3 Statistical Analysis

Statistical analyses and P-values were calculated by the Student T two-tailed test. A P-value of less than 0.05 was considered to be statistically significant.

3.3.4 Preparation and HPLC/MS Analysis of Histones

Total histones were extracted from ES cells as described previously (Fan and Skoultchi, 2004; Medrzycki et al., 2012). Briefly, the cells were washed with PBS and harvested. The cell pellet was resuspended in Sucrose Buffer (0.3 M Sucrose, 15 mM NaCl, 10 mM HEPES [pH 7.9], 2 mM EDTA, 0.5 mM PMSF, protease inhibitor) with 0.5% NP-40 and homogenized with a dounce homogenizer (Wheaton). 0.2 N H_2SO_4 was used to extract histones from chromatin pellet. HPLC and mass spectrometry analysis of histone proteins were carried out as described previously (Fan and Skoultchi, 2004; Medrzycki et al., 2012; Zhang et al., 2012). Approximately 50 µg histone proteins were injected to a C18 reverse phase column (Vydac) on an Äktapurifier UPC 900 instrument (GE Healthcare). The effluent was monitored at 214 nm (A_{214}), and the profiles were recorded and analyzed with UNICORN 5.11 software (GE Healthcare). The values of all peaks were adjusted according to the peptide bonds present in respective proteins. Percentage of total H1 for individual H1 subtypes was determined by the ratio of A_{214} values of individual H1 subtype to that of all H1 peaks. H1 to nucleosome ratio was

determined by the ratio of A_{214} values of individual H1 subtype to that of half of the H2B peak.

3.3.5 Karyotyping

Exponentially growing ESCs were treated with colcemid (Life Technologies) at 37°C for 60 minutes, trypsinized, and harvested. Cells were subsequently resuspended with pre-warmed hypotonic solution (75 mM KCl) and incubated at 37°C for 6 minutes, and fixed as described previously (Zhang et al., 2012). Fixed cells were concentrated and dropped onto an angled, humidified microscope slide, dried and stained with Hoechst dye for 60 minutes in the dark. Images were collected at a 60x objective on an Olympus Fluorescence Microscope.

3.3.6 Quantitative Chromatin Immunoprecipitation (qChIP)

qChIP assays were performed as described previously (Fan et al., 2005) with modifications. The following antibodies were used: anti-H3K4me3 (Millipore 07–473), anti-H3K9me3 (Abcam 8898), anti-H3K27me3 (Millipore 07–449), anti-H3K36me3 (abcam 9050), anti-JARID1A (abcam 65769), anti-JARID1B (abcam 50958), anti-MLL1 (Bethyl Lab A300–086A) and rabbit IgG (Millipore 12–370). Briefly, crosslinked chromatin was sheared by sonication. Pre-blocked Protein G Dynabeads (Life Technologies) were incubated with the antibody and 40 µg of soluble chromatin overnight in 4°C, and subsequently washed with Washing Buffer (50 mM HEPES pH 7.6, 1 mM EDTA pH 8.0, 500 mM LiCl, 0.7% Sodium Deoxycholate, 1% NP-40). Immunoprecipated protein-DNA complexes were eluted and reverse-crosslinked at 65°C,

and DNA was purified with a Qiagen DNA Isolation column (Qiagen). The amount of each specific immunoprecipitated DNA fragment was determined by real-time PCR. All samples were analyzed in triplicate in two independent experiments. The percentage of input was calculated by dividing the amount of each specific DNA fragment in the immunoprecipitates by the amount of DNA present in input DNA. qChIP primers are listed in Table 3.2.

Table 3.1 Primers for qRT-PCR analysis

Name	Forward	Reverse
Homeobox A1	tggccacgtataataactcc	aagtggaactccttctccag
Homeobox A2	agtatccctggatgaaggag	aagctgagtgttggtgtacg
Homeobox A3	aacaaatctttccctggatg	cataggtagcggttgaagtg
Homeobox A4	cctggatgaagaagatccac	tctgaaaccagatcttgacc
Homeobox A6	agcagcagtacaaacctgac	agtggaattccttctcaagc
Homeobox A7	tcctacgaccaaaacatcc	aattccttctccagttccag
Homeobox A9	ttgtccctgactgactatgc	aactccttctccagttccag
Homeobox A10	cccttcagaaaacagtaaagc	ttcacttgtctgtccgtgag
Homeobox A11	gacccgagagcagcag	gacgcttctctttgttgatg
Homeobox A13	aaatgtactgccccaaagag	gatatcctcctccgtttgtc
Homeobox B1	acctcctctctgaggacaag	aaatgaaatcccttctccag
Homeobox B2	aagaaatccaccaagaaacc	aagtggaactccttctccag
Homeobox B3	atgaaagagtcgaggcaaac	aagtggaactccttctccag
Homeobox B4	aaagagcccgtcgtctac	ggtagcgattgtagtgaaactc
Homeobox B5	cagatattcccctggatgag	aaccagattttgatctgacg
Homeobox B6	aagagcgtgttcggagag	tgaaattccttctccagctc
Homeobox B8	cagctctttccctggatg	cacttcattctccgattctg
Homeobox B9	taatcaaagagctggctacg	ccctggtgaggtacatattg
Homeobox B13	atgtgttgccaaggtgaac	aacttgttggctgcatactc
Homeobox C4	aagcaacccatagtctaccc	gtcaggtagcggttgtaatg
Homeobox C6	tcaatcgctcaggattttag	aattccttctccagttccag
Homeobox C8	aggacaaggccacttaaatc	tggaaccaaatcttcacttg
Homeobox C9	cgcagctacccggactac	aactccttctccagttccag
Homeobox C10	gtccagacacctcggataac	aatggtcttgctaatctccag
Homeobox C11	aggaggagaacacgaatcc	ttttcacttgtcggtctgtc
Homeobox C12	actccagttcgtccctactc	tgaactcgttgaccagaaac
Homeobox C13	gtcaggtgtactgctccaag	ccttctctagctccttcagc
Homeobox D3	ctacccttggatgaagaagg	aagaggagcaggaagatgag
Homeobox D9	gaaggaggaggagaagcag	tggaaccagattttgacttg
Homeobox D10	gaagtgcaggagaaggaaag	tgaaaccaaatcttgacctg
Homeobox D11	cagtccctgcgccaag	cgagagagttggagtcttttc
Homeobox D12	cttcaaggaagacaccaaag	tgaggttcagcctgttagac
Homeobox D13	gaacagccaggtgtactgtg	gagctgcagtttggtgtaag

Table 3.2 Primers for qChIP analysis

Name	Forward	Reverse
Homeobox A1	gggaatccaacagacaccac	tcctcccagtcaatcctctg
Homeobox A1-2	ggcaccctacaccactcact	gaaaccctcccaaaacaggt
Homeobox A3	aattacctccctgcatctcaaa	ttatcagagcagacccacaatg
Homeobox B4	atttccttatccgggaatcg	gtttccgaaagccctcctac
Homeobox B4-2	gtgggcaattcccagaaa	gctggaagccgctctctc
Homeobox B5	taacgaccacgatccacaaa	agagctgccactgccataat
Homeobox B5 -2	cctccaaaatcacccaaatg	gctgagatccatcccattgt
Homeobox B8	gctccgttccaaacacctac	cctccttcaaaggaagcaaa
Homeobox B8 -2	taagcaaggactccctcgtc	gaattacggcgtgaataggc
Homeobox B13	ccctctcttttttccaccaca	ttgcgcctcttgtccttagt
Homeobox B13 -2	gaggggggtcggaatctagtc	cgcctccaaagtagccataa
Homeobox C13	agctggagcagatcatgtca	gcgctgtcctcatagacgta
Homeobox C13 -2	tgctgaccctgctcactgta	aattctgagcttccctccag
Homeobox D11	tgaacgactttgacgagtgc	ggttggaggagtaggggaaa
Homeobox D11 -2	cctagctcagtggccagagt	agcatccgagagagttggag
Homeobox D13	agctcgaggagccaaagag	gacccaggagttgactttgc
Homeobox D13 -2	gaaaagggtgccttacacca	tgtccttcacccttcgattc
Tcf4	cggatgtgaatggattacaatg	attgttcttcggtcttgttggt

3.4 Results

3.4.1 Loss of H1c, H1d and H1e Leads to Decreased Expression of *Hox* Genes in Embryos and Embryonic Stem Cells

To gain a comprehensive view of the effects histone H1 depletion and changes in bulk chromatin on the regulation of *Hox* gene clusters, we designed a full set of quantitative reverse-transcription PCR assays (qRT-PCR) to measure the expression levels of all 39 murine *Hox* genes across the 4 *Hox* gene clusters in H1 TKO embryos. H1c/H1d/H1e triple heterozygotes were intercrossed to obtain H1 TKO and wild-type (WT) littermate embryos. Most of the H1 TKO embryos display growth retardation and various defects at E9.5 (Fan et al., 2003). To minimize the secondary effects caused by broad defects of H1 TKO embryos, we chose to analyze *Hox* gene expression at E8.5 when H1 TKO embryos with comparable size to WT embryos can be recovered. We selected two littermate pairs of WT and H1 TKO embryos at E8.5, and examined the expression patterns of all 39 *Hox* genes using the highly sensitive qRT-PCR assays. As expected, most *Hox* genes were expressed in E8.5 embryos, except the most posterior genes within each cluster (Figure 3.1 and Figure 3.2). However, surprisingly, many *Hox* genes were expressed at reduced levels in H1 TKO embryos, including *Hoxa2*, *Hoxa3*, *Hoxa5, Hoxa6, Hoxa9*, *Hoxc4*, *Hoxc5*, *Hoxc6*, *Hoxc8*, *Hoxc9*, *Hoxc10, Hoxd3,* and *Hoxd8* (Figure 3.1). This effect is especially prominent in *Hoxa* and *Hoxc* clusters, in which nearly all of the expressed genes were reduced 3-fold or more (Figure 3.1). Interestingly, we did not find increased expression among any of the *Hox* genes

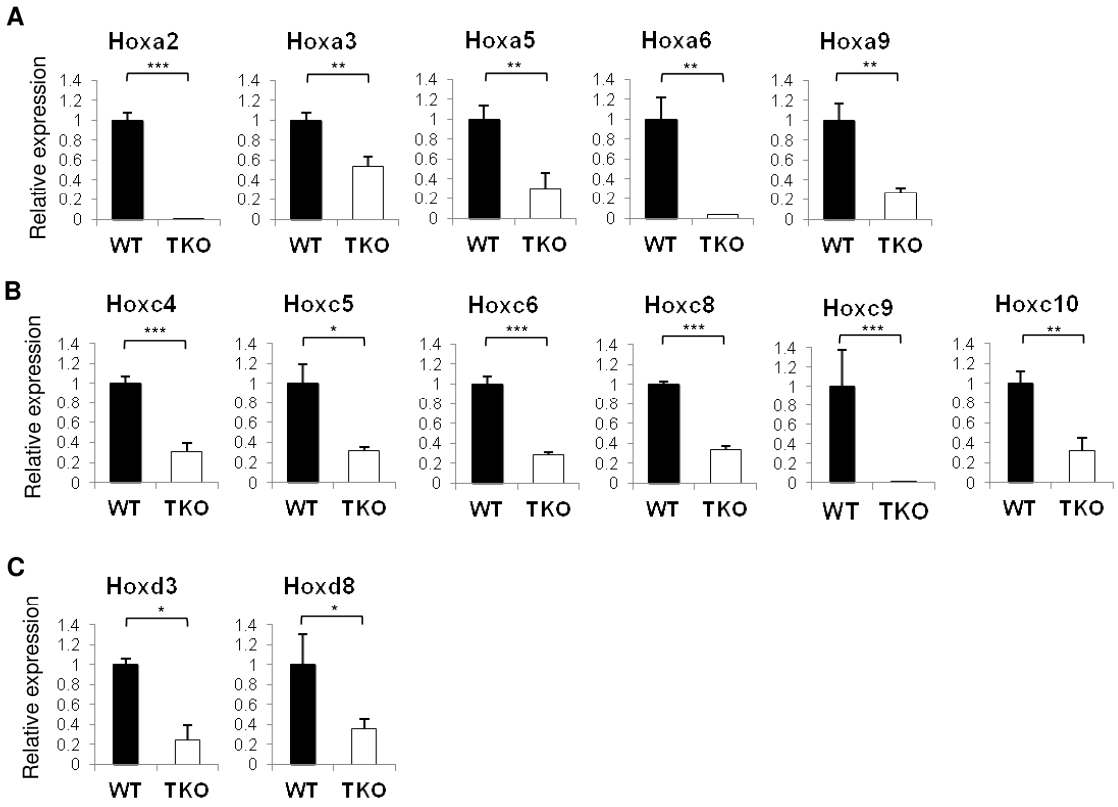

Figure 3.1. Reduction of *Hox* gene expression in H1 TKO embryos.
Relative expression of *Hox* genes with altered mRNA levels in H1 TKO embryos compared with WT. Down-regulated *Hox* genes are located in *HoxA* (A), *HoxC* (B), and *HoxD* (C) clusters. Expression levels of *Hox* genes were analyzed by qRT-PCR and normalized over *GAPDH* and represented as a fold change between H1 TKO and WT embryos at E8.5. *: P<0.05, **: P<0.01, ***: P<0.001. Error bars: S.D.

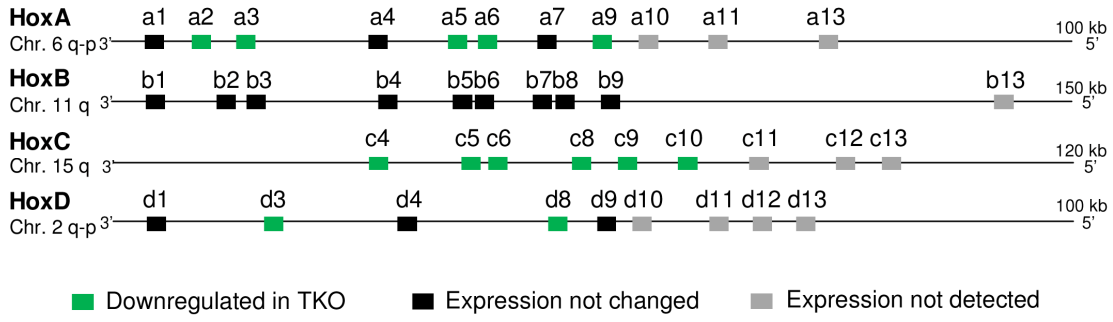

Figure 3.2. The schematic representation of *Hox* gene clusters with expression patterns in H1 TKO embryos compared with WT.

(Figure 3.2), and none of the *Hoxb* genes were affected in H1 TKO embryos in comparison with WT embryo.

The reduction of expression of many *Hox* genes may cause the growth retardation often observed in H1 TKO embryos at E9.5. However, it remained a formal possibility that the decreased expression of *Hox* genes in H1 TKO embryos was a result of the slight growth retardation presented in the KO embryos, although the H1 TKO embryos used for this analysis were indistinguishable from their WT and heterozygous littermate controls in size and developmental stage. In order to analyze the effects of H1 on a homogeneous cell population, we gauged the effects of H1 depletion on *Hox* gene expression in H1 TKO ESCs. *Hox* genes are repressed by polycomb repressive complexes (PRCs) in ESCs (Azuara et al., 2006; Boyer et al., 2006; Endoh et al., 2008; Jorgensen et al., 2006; Lee et al., 2006; Stock et al., 2007). Loss of components of either PRC1 or PRC2 in ESCs leads to upregulation of *Hox* genes, presumably due to respective loss of chromatin compaction

and H3K27 trimethylase activity (Boyer et al., 2006; Chamberlain et al., 2008; Eskeland et al., 2010). We have shown previously that H1 TKO ESCs have decondensed local chromatin and reduced levels of H3K27m3 in bulk chromatin (Fan et al., 2005). We surmise that these changes may lead to elevated levels of expression of specific *Hox* genes. Examination of previous expression data from microarray assays showed that the microarray used for hybridization only contained 11 *Hox* genes, most of which were undetectable in ESCs by the array (Fan et al., 2005).

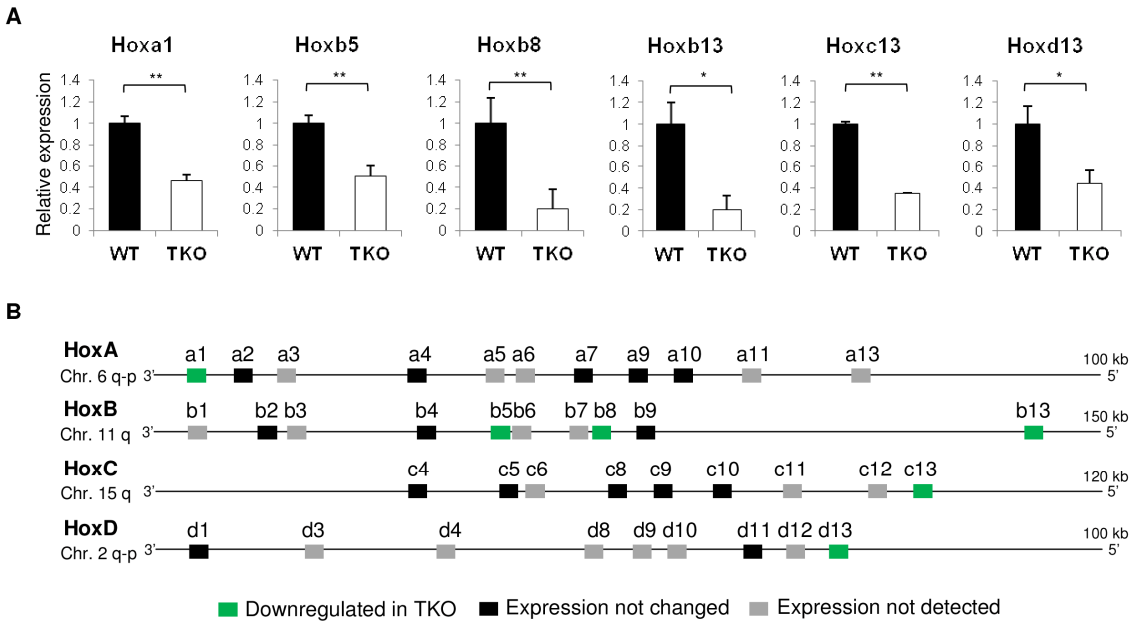

Figure 3.3. Decreased expression of *Hox* genes in H1 TKO ESCs.
(A) Expression analysis of *Hox* genes in WT and H1 TKO ESCs. Y axis and data normalization are as described in the legend to Figure 2.1. *: P<0.05, **: P<0.01, ***: P<0.001. Error bars: S.D. (B) Expression patterns of *Hox* genes in H1 TKO in comparison with WT ESCs.

We thus applied the qRT-PCR assays to compare the expression levels of all 39 *Hox* genes in WT and TKO ESCs. Consistent with the finding that pluripotent ESCs possess a hyperactive transcriptome (Efroni et al., 2008), we detected expression of 21 *Hox* genes, albeit at low levels, in either or both of WT and H1 TKO ESCs. These genes include *Hoxa1, Hoxa2, Hoxa4, Hoxa7, Hoxa9, Hoxa10, Hoxb2, Hoxb4, Hoxb5, Hoxb8, Hoxb9, Hoxb13, Hoxc4, Hoxc5, Hoxc8, Hoxc9, Hoxc10, Hoxc13, Hoxd1, Hoxd11, and Hoxd13* (Figure 3.3). Unexpectedly, no increased expression in any of the *Hox* genes was found in H1 TKO ESCs. Instead, the expression levels of 6 *Hox* genes, *Hoxa1, Hoxb5, Hoxb8, Hoxb13, Hoxc13*, and *Hoxd13,* were reduced, with an average of 2–3 fold less in H1 TKO ESCs compared with WT (Figure 3.3 A). Other *Hox* genes did not show consistent changes in expression by loss of H1c, H1d and H1e in ESCs (Figure 3.3 B).

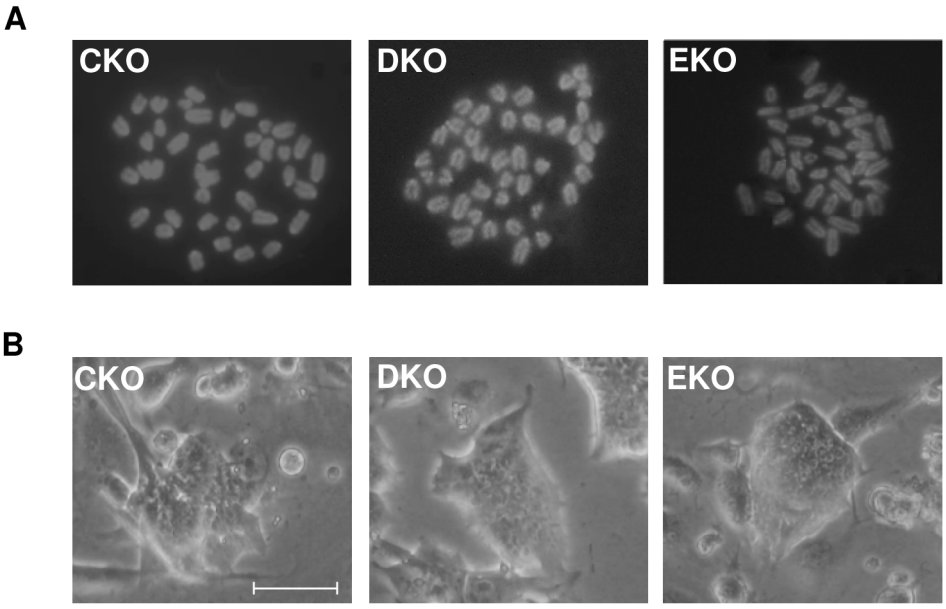

Figure 3.4 Characterization of the single-H1 KO ESCs.
Karyotypes (A) and phase images (B) of the single-H1 KO ESCs. Scale bar: 50 μm.

3.4.2 Specific Regulation of *Hox* Genes in ESCs by Individual H1 Subtypes

To assess the effects of each of the three deleted somatic H1 subtypes in H1 TKO (H1c, H1d and H1e) on *Hox* gene expression in ESCs, we established ESCs that are null for only one of these three H1 subtypes. $H1c^{-/-}$; $H1d^{-/-}$; and $H1e^{-/-}$ mice develop normally and are fertile (Fan et al., 2001). Male and female mice homozygous for each single-H1 deletion were bred, $H1c^{-/-}$; $H1d^{-/-}$; and $H1e^{-/-}$ blastocysts were harvested from pregnant female mice at 3.5 day post coitum and their respective single-H1 knockout (KO) ESCs were derived from outgrowth of blastocysts. As shown in metaphase

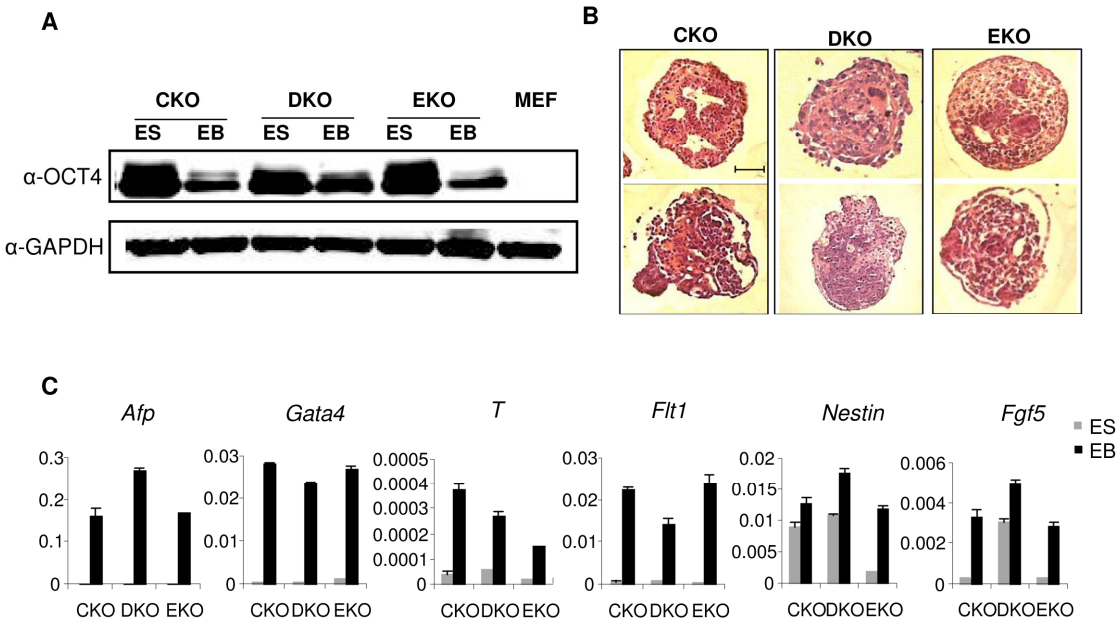

Figure 3.5 Characterization of the single-H1 KO EBs.
(A) hematoxylin and eosin staining images of single-H1 KO EBs. Scale bar: 50 μm. (B) Western blotting analysis of OCT4 in single-H1 KO ESCs and EBs. *GAPDH* expression levels indicate equal loading of cell lysates. (C) qRT-PCR analysis of differentiation markers in single-H1 KO ESCs and EBs.

chromosome spreads, the single-H1 KO ESCs had normal karyotypes with 40 chromosomes (Figure 3.4 A) and showed colony morphology typical of undifferentiated ESCs when cultured under conditions promoting self-renewal of ESCs (Figure 3.4 B). They expressed high levels of pluripotency factor OCT4, which is absent in differentiated cells, such as mouse embryonic fibroblasts (MEF) (Figure 3.5 A). These single-H1 KO ESCs also had comparable growth rate to WT ESCs (data not shown). Upon differentiation, the single-H1 KO ESCs were able to form embryoid bodies (EB) with characteristic cystic structures and differentiated cell morphologies (Figure 3.5 B). As expected, these EBs displayed decreased levels of OCT4 (Figure 3.5 A), and increased expression of many differentiation markers, such as *AFP*, *Gata4, T (Brachyury),* and *FLT1*, compared with ESCs (Figure 3.5 C). In addition, teratoma formation analysis indicated that the single-H1 KO ESCs formed typical teratomas containing cells differentiated into all three germ layers after injection into immunodeficient mice (data not shown). These data indicate that any one of these three somatic H1 subtypes is dispensable for self-renewal and differentiation of ESCs.

We next analyzed the total H1 levels and composition of H1 subtypes in these single-H1 KO ESCs. HPLC and mass spectrometry analyses of histone extracts from these cells confirmed the lack of the deleted H1 subtype in the respective $H1c^{-/-}$, $H1d^{-/-}$, and $H1e^{-/-}$ ESCs (Figure 3.6). As described previously and shown here (Fan and Skoultchi, 2004; Medrzycki et al., 2012), quantification of the peaks of each H1 subtype and H2B allows calculation of the H1 to nucleosome ratio (H1/nuc). Such analysis showed that, except for H1e in H1d-KO ESCs, the absolute levels of the remaining H1 subtypes were largely unchanged in single-H1 null ESCs (Figure 3.7 A Left), indicating

that there was little increase or compensation in the levels of the remaining H1s for the lost H1. As expected, undifferentiated ESCs express negligible amount of $H1^0$ (Figure 3.6 and Figure 3.7), an H1 subtype enriched in differentiating and non-dividing cells (Panyim and Chalkley, 1969; Pehrson and Cole, 1980). Although relative proportions of H1 subtypes were altered by single-H1 deletion (Figure 3.7 B), the total H1/nuc ratios of $H1c^{-/-}$, $H1d^{-/-}$, and $H1e^{-/-}$ ESCs were comparable with respective values of 0.38, 0.35,

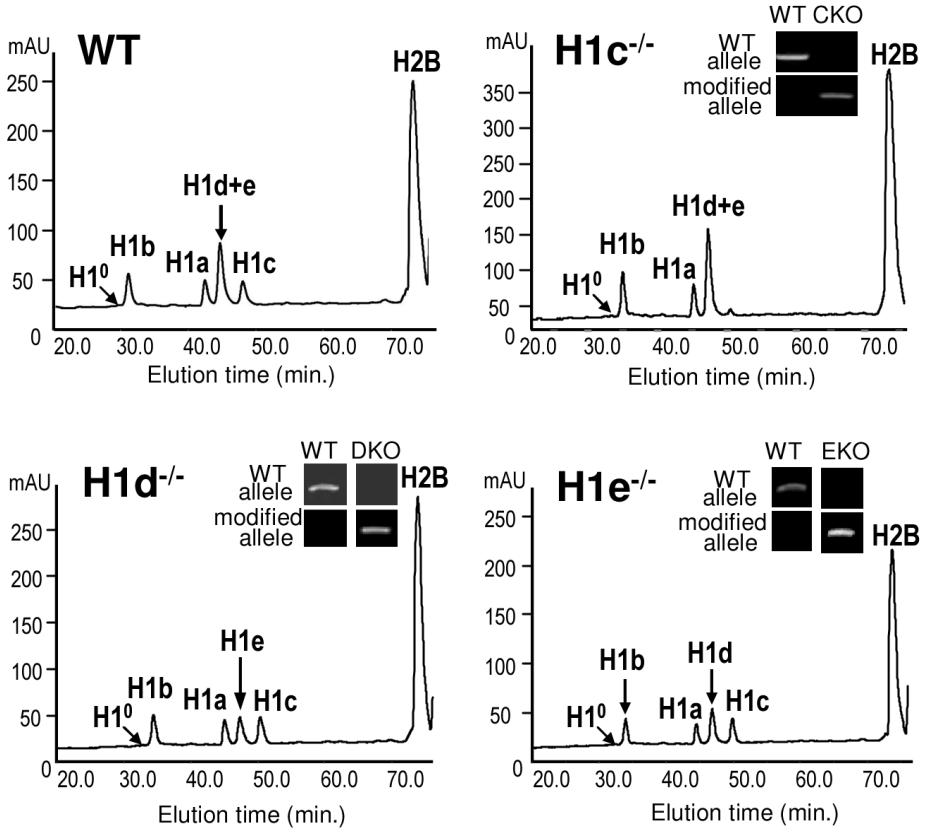

Figure 3.6 Generation and reverse-phase HPLC analysis of single-H1 KO ESCs. RP-HPLC analysis of total histones from WT and the single-H1 KO ESCs. The identity of the histone subtypes is indicated above each peak. mAU, milli-absorbency at 214 nm. Genotype analyses of single-H1 KO ESCs are shown in insets in respective HPLC profiles.

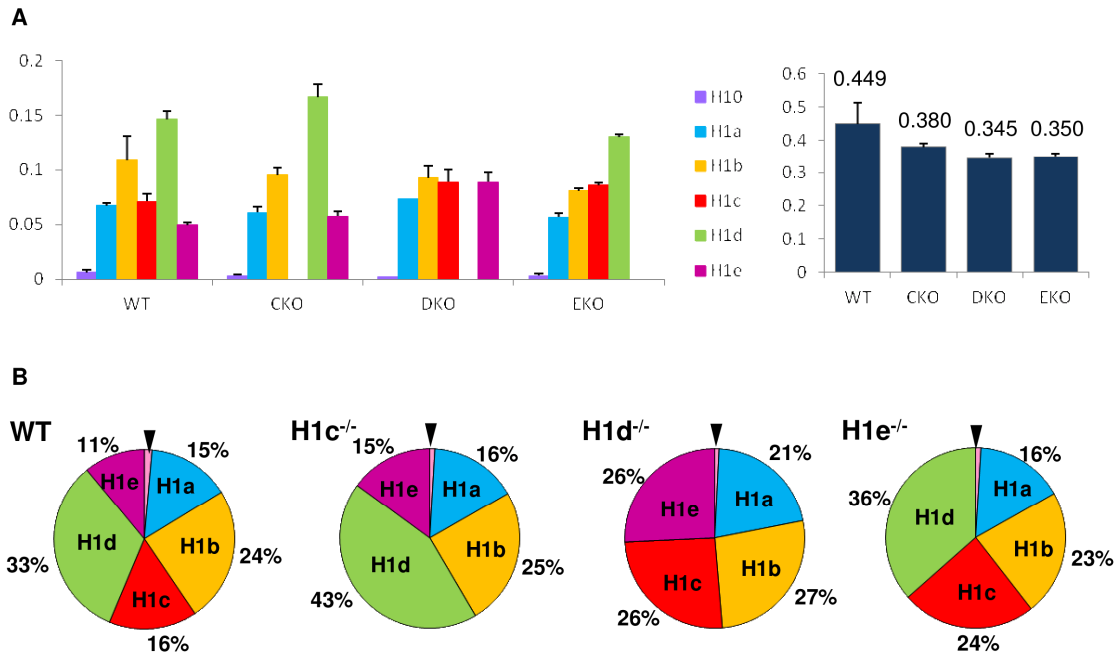

Figure 3.7 Expression profiles of linker histones in H1 single KO ESCs.
The ratios of individual H1 (Left) and total H1 (Right) to nucleosome for WT and single-H1 KO ESCs. Ratios were determined from the RP-HPLC and mass spectrometry analyses as described in methods. ***: P<0.001 (B) The percentage of each H1 subtype among total H1 histones for WT and single-H1 KO ESCs. % total H1 for $H1^0$ (marked with arrowhead) is equal to or less than 1%.

and 0.35 (Figure 3.7 A Right). These ratios were about 25% lower than that of WT ESCs (0.45), but about 50% higher than that of H1 TKO ESCs (0.25) (Fan et al., 2005). These single-H1 KO ESCs provide ideal cell resources to ascertain if the effects present in H1 TKO ESCs were caused by any one of the lost H1 subtypes or by the marked reduction in total H1 levels in H1 TKO ESCs.

We focused our expression analysis in H1 single KO ESCs on the 6 *Hox* genes that displayed reduced expression in H1 TKO ESCs. *Hoxb8* exhibited decreased expression in all three single-H1 KO ESCs, whereas *Hoxa1* and *Hoxc13* had reduced expression in $H1c^{-/-}$ and $H1d^{-/-}$, but not in $H1e^{-/-}$ ESCs compared with WT (Figure 3.8), indicating that these *Hox* genes are differentially regulated by H1c, H1d and H1e. Interestingly, the expression levels of these *Hox* genes in single-H1 KO ESCs were similar to that in H1 TKO (Figure 3.8), suggesting that these genes may be especially sensitive to alterations of local chromatin structure or H1 to nucleosome stoichiometry. The other three *Hox* genes did not show consistent expression changes in any of the single-H1 null ESCs, indicating that their expression reduction in H1 TKO ESCs is likely due to the marked reduction of the total H1 levels in TKO cells.

3.4.3 Dynamic Changes of H3K4me3 and H3K27me3 at Affected *Hox* Genes in H1 TKO ESCs

Trithorax group (TrxG) and polycomb group (PcG) proteins are known to regulate the expression of *Hox* genes (Ringrose and Paro, 2004; Schuettengruber et al., 2007). TrxG mediates H3K4 tri-methylation (H3K4me3), corresponding to transcriptional activation (Bernstein et al., 2005; Dou et al., 2006), whereas PcG directs

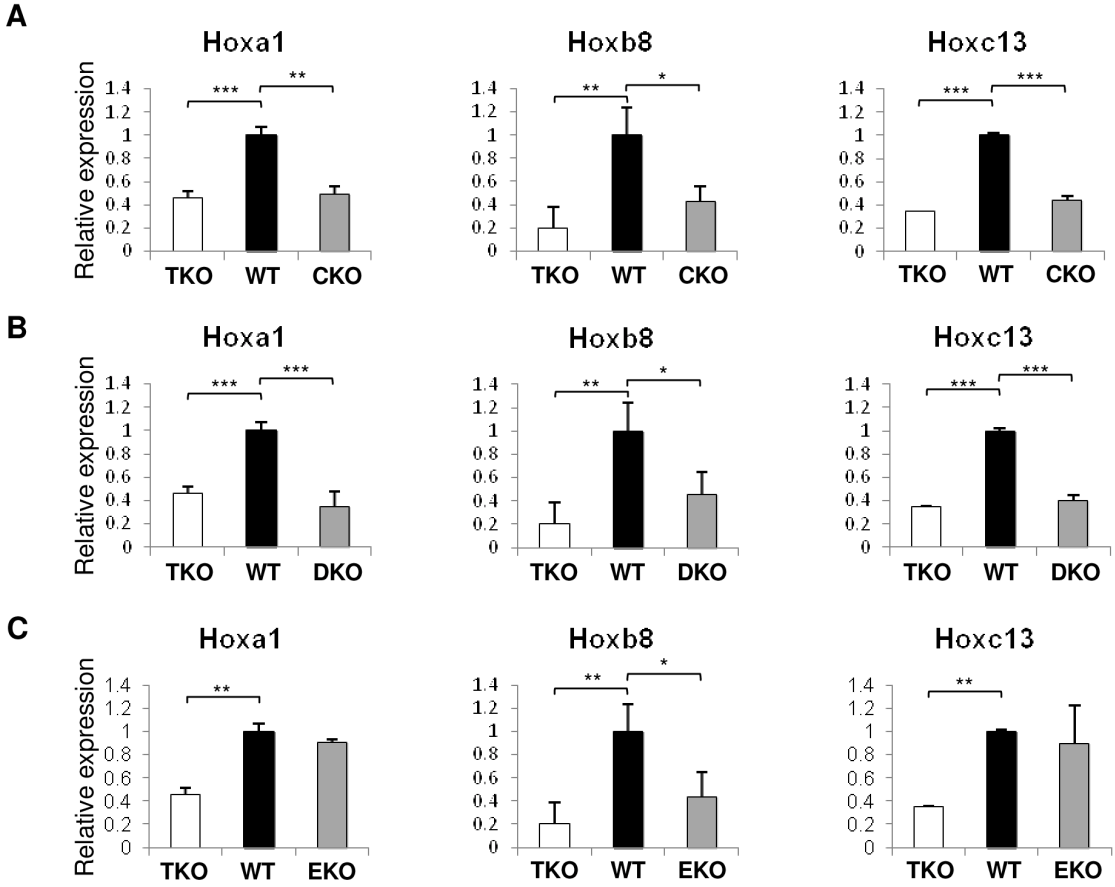

Figure 3.8 The expression profiles of *Hox* genes in single-H1 KO ESCs.
Relative expression of *Hoxa1, Hoxb8, and Hoxc13* in H1c–/– (A), H1d–/– (B), and H1e–/– (C) ESCs were shown. *: P<0.05, **: P<0.01, ***: P<0.001.

H3K27 tri-methylation (H3K27me3), correlating with transcriptional repression (Boyer et al., 2006; Bracken et al., 2006; Cao et al., 2002). In ESCs, many developmental genes display both H3K4me3 and H3K27me3 marks, a "bivalent" chromatin signature for genes poised for expression and important for maintenance of ESC pluripotency (Azuara et al., 2006; Bernstein et al., 2006).

To investigate whether H1 depletion has an impact on bivalent chromatin marks on the 6 *Hox* genes (*Hoxa1, Hoxb5, Hoxb8, Hoxb13, Hoxc13 and Hoxd13*) affected in H1 TKO ESCs, we performed quantitative chromatin immunoprecipitation (qChIP) analysis on the promoter regions of these genes as well as two *Hox* genes (*Hoxb4* and *Hoxd11*) whose expression levels were not altered by triple-H1 deletion. As expected, most *Hox* genes analyzed displayed the bivalent marks in WT ESCs, with higher levels of H3K4me3 and H3K27me3 compared with *Hoxa3* and *Tcf4* (Figure 3.9 A&C), which have been shown to harbor minimum levels of respective histone marks (Bernstein et al., 2006). The levels of H3K4me3 were decreased significantly at all six *Hox* genes affected in H1 TKO ESCs (Figure 3.9 A), but not at *Hoxb4* or *Hoxd11* loci, suggesting that H1 depletion did not lead to a general reduction of H3K4me3 throughout the *Hox* gene clusters. The changes in H3K4me3 level at the promoters of the six *Hox* genes correlated with the reduction of gene expression in H1 TKO ESCs, indicating that the effects of H1 depletion on *Hox* genes may be mediated through regulating the establishment and/or maintenance of specific H3K4me3 patterns. Increased levels of H3K27me3 were observed at 4 of the 6 *Hox* genes affected in H1 TKO ESCs (*Hoxa1, Hoxb5, Hoxb13, and Hoxd13*) (Figure 3.9 C), suggesting that an increase in the H3K27me3 level may also contribute to the reduced expression of these genes. In contrast, H3K36me3, which is

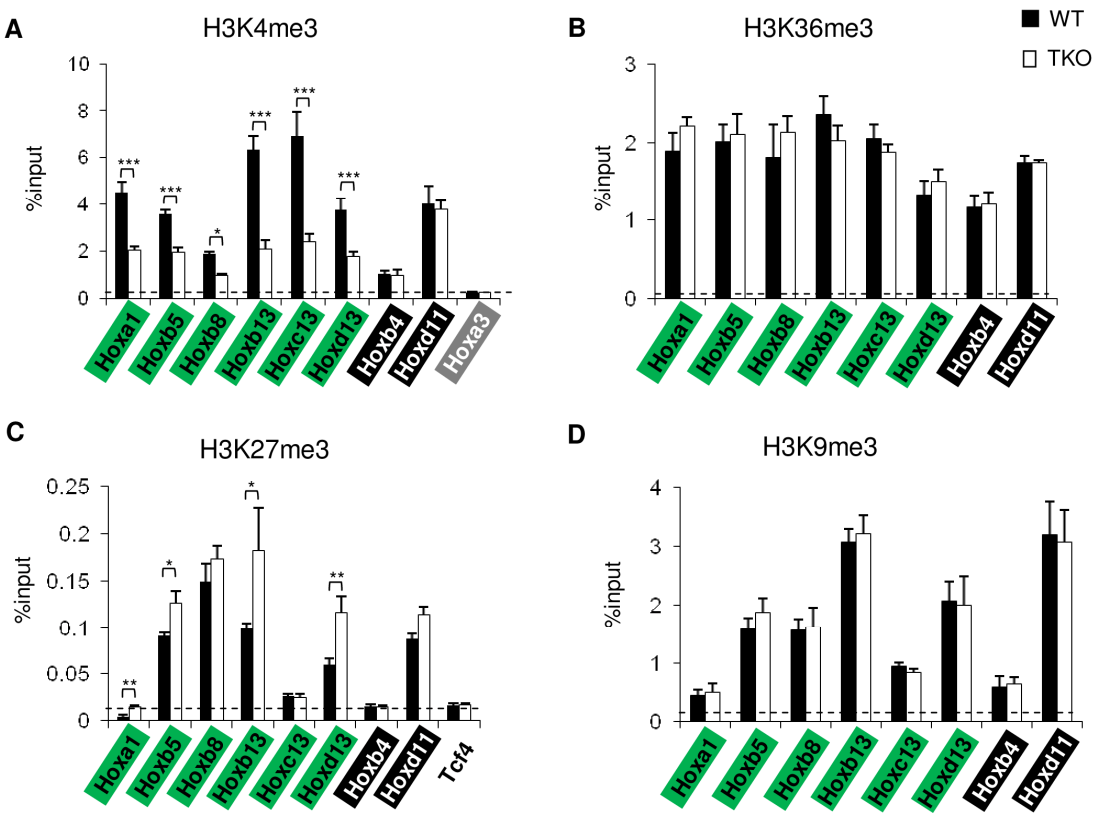

Figure 3.9 qChIP analysis of histone marks at *Hox* genes in WT and H1 TKO ESCs. The levels of H3K4me3 (A), H3K36me3 (B), H3K27me3 (C), and H3K9me3 (D) were analyzed by qChIP. Promoter regions of the indicated Hox genes were assayed, except for (B), for which gene body regions were analyzed. Dashed lines denote the highest signal level of control IgG qChIP. *: P<0.05, **: P<0.01, ***: P<0.001.

enriched at gene bodies of active genes (Mikkelsen et al., 2007), and H3K9me3, which marks heterochromatin and associated with gene repression (Lachner et al., 2001), remained unchanged at all sites after triple H1 depletion (Figure 3.9 B&D), indicating that the effects of marked H1 reduction on H3K4me3 and H3K27me3 (to a less extent) are rather specific. qChIP analysis in single-KO ESCs indicated that H3K4me3 was decreased significantly at the promoters of the *Hox* genes with reduced expression in the respective H1 KO ESCs, but not at unaffected genes, such as *Hoxd11* (Figure 3.10). The level of H3K4me3 was not affected by single-H1 deletion at those genes which displayed reduced expression only in H1 TKO ESCs, such as *Hoxb5* (Figure 3.10). The increase of H3K27me3 occupancy was more restricted, detected only at *Hoxa1* promoter in H1c- and H1d- KO ESCs with 2–3 fold over WT (Figure 3.11). Taken together, our results demonstrate that H1 depletion leads to dynamic changes of the H3K4me3 and H3K27me3 marks, which may regulate *Hox* gene expression.

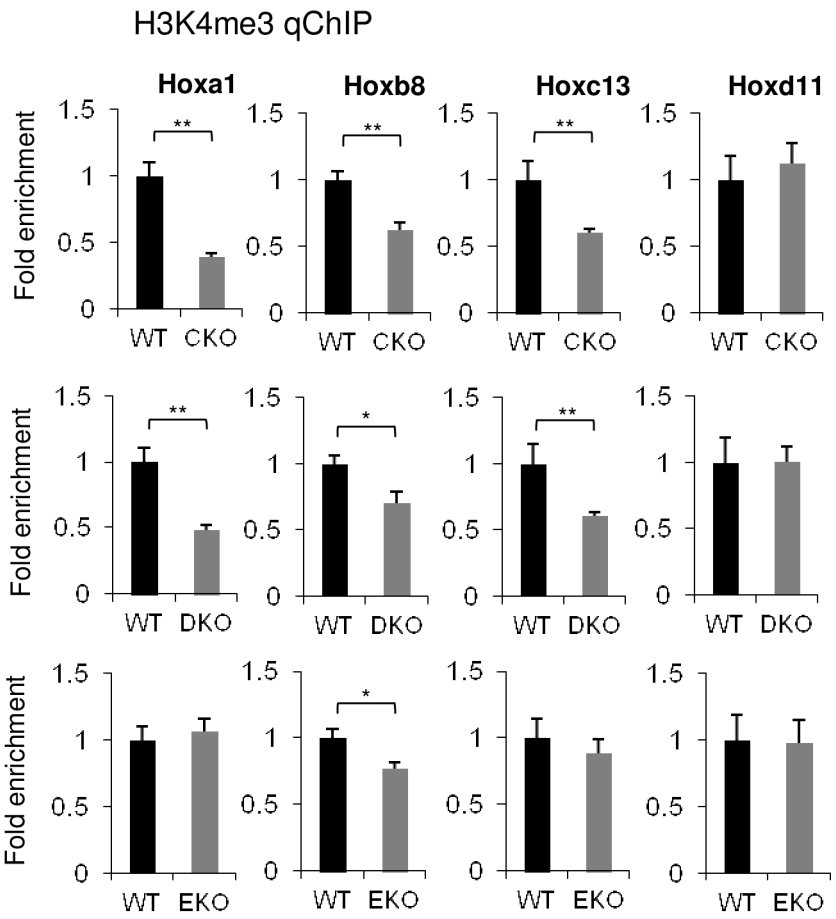

Figure 3.10 qChIP analysis of H3K4me3 in single -H1 KO ESCs.
qChIP signals of H3K4me3 at indicated *Hox* genes in single-H1 KO ESCs were normalized to input controls and represented as fold changes over that of WT ESCs. *: P<0.05, **: P<0.01.

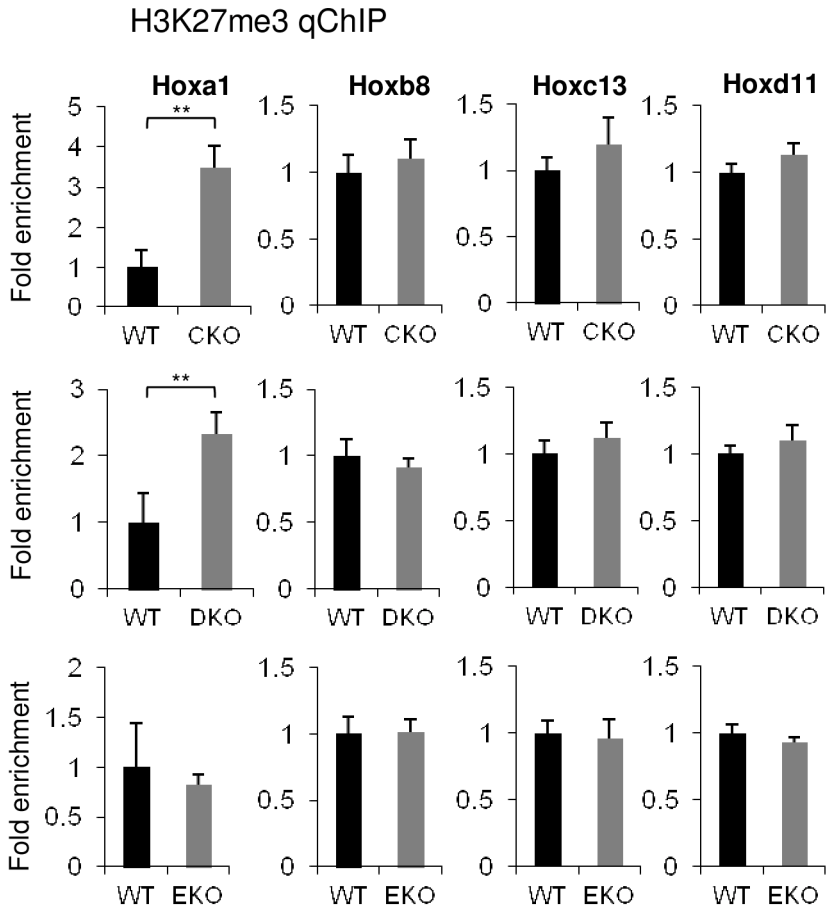

Figure 3.11 qChIP analysis of H3K27me3 in single -H1 KO ESCs.
qChIP signals of H3K27me3 at indicated *Hox* genes in single-H1 KO ESCs were normalized to input controls and represented as fold changes over that of WT ESCs. *: P<0.05, **: P<0.01.

3.5 Discussion

Hox genes encode a large family of transcription factors crucial for body patterning and positioning along the anterior-posterior axis during animal development (Alexander et al., 2009; Mallo et al., 2010). Multiple mechanisms have been shown to regulate the spatial and temporal collinearity of *Hox* genes, such as the antagonism between PcG and TrxG proteins (Ringrose and Paro, 2004; Schuettengruber et al., 2007), local chromatin condensation and reorganization (Chambeyron and Bickmore, 2004; Chambeyron et al., 2005; Eskeland et al., 2010), spatial configuration or compartmentalization (Noordermeer et al., 2011), targeting of miRNAs and long non-coding RNAs (lncRNAs) (Rinn et al., 2007; Yekta et al., 2004). Chromatin conformation and compaction appear to be key mediators for regulating the expression of *Hox* gene clusters (Chambeyron and Bickmore, 2004; Chambeyron et al., 2005; Eskeland et al., 2010; Noordermeer et al., 2011), however, whether changes in chromatin structure have a direct impact on *Hox* gene expression remains undetermined.

In this study, we have taken advantage of a number of mutants, null in one or several major somatic H1 subtypes, with different levels of reduction in total H1 proteins, to investigate the role of H1, a key component in promoting chromatin compaction, in regulating *Hox* gene clusters in mouse embryos and ESCs. We find that depletion of three H1 subtypes leads to the transcriptional reduction of a group of *Hox* genes in embryos and ESCs, and that the reduced expression levels correlate with dynamic changes in H3K4me3 and H3K27me3 marks. This is in contrast to the deletion of PRC1 or PRC2 repressive chromatin complexes, which causes upregulation of specific *Hox* genes in

embryos (Akasaka et al., 2001; van der Lugt et al., 1996; van Lohuizen, 1998) or ESCs (Boyer et al., 2006; Eskeland et al., 2010; Lee et al., 2006).

We first systematically analyzed the impacts of H1 depletion on expression levels of all 39 *Hox* genes in mouse embryos. Consistent with previous findings (Soshnikova and Duboule, 2009), the posterior genes are not detected by qRT-PCR assays in E8.5 embryos. The 13 affected genes include many paralogous *Hox* gene members (Figure 3.1), suggesting a broad effect of H1 on regulation of *Hox* genes. *Hoxa2*, expressed in hindbrain and crucial for trigeminal system development (Erzurumlu et al., 2010; Oury et al., 2006), is drastically repressed in H1 TKO embryos. The remaining 12 of the 13 *Hox* genes with reduced expression in H1 TKO embryos are located within paralogous genes *Hox*3*–10*, a region important for axial morphology and patterning (Mallo et al., 2010; McIntyre et al., 2007; Vinagre et al., 2010; Wellik, 2007). H1 TKO embryos have significant reduction in total H1 levels and die during midgestation (Fan et al., 2003). H1 depletion *in vivo* causes local reductions in chromatin compaction (Fan et al., 2003; Fan et al., 2005). The finding that all affected *Hox* genes are down-regulated in H1 TKO embryos is surprising because chromatin decompaction and progressive changes in 3D chromatin architecture coincide with activation of *Hox* genes during embryonic development (Chambeyron and Bickmore, 2004; Chambeyron et al., 2005; Eskeland et al., 2010; Morey et al., 2007; Noordermeer et al., 2011) and thus one may expect that H1 depletion would result in up-regulation of certain *Hox* genes. We believe that the down-regulation of *Hox* genes is a direct effect due to H1 depletion, and contributes to, rather than merely reflects, the growth retardation observed in a fraction of H1 TKO embryos at a later stage (Fan et al., 2003). The E8.5 H1 TKO embryos analyzed in this study did not

exhibit obvious phenotypic difference compared with WT littermates. It is noteworthy that H1 depletion in embryos did not lead to changes in expression of any of the *Hox* genes on the entire *Hoxb* cluster, which harbors a large intergenic repeat-rich region with a different 3D chromatin structure compared with other *Hox* clusters (Noordermeer et al., 2011). Furthermore, similar to our findings from analyzing H1 TKO embryos, H1 depletion in ESCs does not lead to increased expression in any of the *Hox* genes, but causes further reduction in the expression of 6 *Hox* genes. The less prominent effects of H1 depletion on ESCs could be due to the following reasons: 1) ESCs have no or minimum expression of most *Hox* genes; 2) embryos consist of a more heterogeneous cell population which are likely to have very different bulk and/or local chromatin structure at *Hox* gene clusters compared with the undifferentiated ESCs. Indeed, embryos at midgestation have a H1/nuc of 0.74 (Fan et al., 2003), suggesting a more compact chromatin than ESCs with a H1/nuc of 0.45 (Fan et al., 2005); and 3) triple-H1 deletion reduces H1/nuc by 0.34 (from 0.74 to 0.40) in embryos, a larger reduction in total H1 levels than the 0.20 (from 0.45 to 0.25) in ESCs (Fan et al., 2003; Fan et al., 2005).

Importantly, we find that the levels of H3K4me3, a chromatin mark catalyzed by TrxG proteins, are decreased at promoters of all affected *Hox* genes, corresponding to the reduction in gene expression levels of these *Hox* genes in H1 TKO ESCs. Likewise, the correlation of changes in H3K4me3 and *Hox* gene expression extends to the single-H1 KO ESCs, suggesting that individual H1 subtypes may also contribute to epigenetic regulation of H3K4me3 at specific *Hox* genes. The effects of triple-H1 deletion on H3K27me3 are more limited, with mild increase at 4 of the 6 affected genes. We speculate that loss of H1 may lead to changes in occupancy of H3K4me3

methyltransferases/demethylases, and/or affect binding of polycomb complex components to the *Hox* genes (Christensen et al., 2007), resulting in alterations in the histone H3K4 and H3K27 trimethyl marks. It is especially interesting to note that JARID proteins contain an AT-rich interacting domain (Cloos et al., 2008; Kortschak et al., 2000) that preferentially binds to AT rich tracts (Huang et al., 1996) and the matrix attachment region (MAR) (Herrscher et al., 1995), a region that is involved in the regulation of *Hox* genes (Dobreva et al., 2006) and has a high affinity for H1 binding (Izaurralde et al., 1989). However, the levels of JARID1A and JARID1B, two H3K4me2/3 demethylases, do not appear to differ significantly in cellular protein amounts or at affected *Hox* genes in H1 TKO ESCs compared with WT (Cao, Zhang and Fan, unpublished observations). Similarly, H3K4 methyltransferase MLL1 (Dou et al., 2006) does not display consistent changes by H1 depletion in ESCs (Cao, Zhang and Fan, unpublished observations). Whether any other H3K4me3 methyltransferase(s)/ demethylase(s) is responsible for H1 regulated H3K4me3 at *Hox* genes in ESCs remains to be determined. We also cannot exclude additional possible regulatory mechanisms mediated through changes in other epigenetic events upon H1 depletion. For instance, nucleosome positioning is thought to impact DNA accessibility and transcription (Bai and Morozov, 2010), and H1 depletion leads to a reduction in nucleosome repeat length of bulk chromatin and at specific loci (Fan et al., 2003; Fan et al., 2005). Nucleosomes are found to be positioned at *Hox* gene clusters, preferentially at 3′ of the expressed *Hox* genes (Kharchenko et al., 2008), thus the expression of *Hox* genes may be impaired by altered nucleosome positioning in H1 TKO embryos and ESCs. Alternatively, DNA methylation may be affected at *Hox* gene clusters by H1 depletion, which has been shown to affect specific DNA methylation

patterns at specific imprinted genes and other loci (Fan et al., 2005; Giambra et al., 2008; Maclean et al., 2011; Zhang et al., 2012). Furthermore, the distance between enhancers or regulatory regions for *Hox* clusters and individual *Hox* genes (Deschamps, 2007; Montavon et al., 2011; Spitz et al., 2003) may be altered by H1 loss, which in turn reduces *Hox* gene expression.

In order to determine if any of the three deleted H1 subtypes is responsible for the reduction of *Hox* genes identified in H1 TKO ESCs, we derived single-H1 KO ESCs that are null for H1c, or H1d, or H1e. Surprisingly, unlike adult tissues of the single-H1 knockout mice (Fan et al., 2001), which display no changes in the total H1 levels, single-H1 KO ESCs established in this study exhibit a moderate reduction in the total H1 levels, and a lack of significant compensation for the deleted H1s by the remaining H1 subtypes. Interestingly, the analysis of the 6 *Hox* genes whose expression levels were significantly reduced in H1 TKO ESCs shows that loss of H1c or H1d has similar effects on *Hoxa1*, *Hoxb8*, and *Hoxc13* as triple-H1 deletions. On the other hand, 5 of these 6 *Hox* genes show no expression change in $H1e^{-/-}$ ESCs (Figure 3.8 C). This differential role of the individual H1 subtypes in activating expression of specific genes is reminiscent of the effects of loss of H1a on the expression of non-variegating transgenes in mice (Alami et al., 2003) and the activation of MMTV promoter by overexpression of $H1^0$ and H1c (Gunjan and Brown, 1999). *Hoxb5, Hoxb13* and *Hoxd13* are not changed in single-H1 null ESCs, suggesting that the expression reduction of these genes in H1 TKO ESCs may be due to additive effects of deficiency of all three H1 subtypes. It is interesting to note that the levels of H3K4me3 are differentially affected at several *Hox* genes, suggesting

potential roles of individual H1 subtypes in contributing to the patterns of this histone mark at specific *Hox* genes.

Taken together, the results in this study establish a novel link between histone H1 and *Hox* gene regulation. Furthermore, the reduction of *Hox* gene expression by marked H1 depletion correlates with dynamic patterns of H3K4me3 and H3K27me3 marks. The single-H1 KO ESCs established in this study should be useful cell resources for studying specificity of the individual H1 subtypes in regulating gene expression and epigenetic events.

3.6 Reference

Akasaka, T., van Lohuizen, M., van der Lugt, N., Mizutani-Koseki, Y., Kanno, M., Taniguchi, M., Vidal, M., Alkema, M., Berns, A., and Koseki, H. (2001). Mice doubly deficient for the Polycomb Group genes Mel18 and Bmi1 reveal synergy and requirement for maintenance but not initiation of Hox gene expression. Development *128*, 1587-1597.

Alami, R., Fan, Y., Pack, S., Sonbuchner, T.M., Besse, A., Lin, Q., Greally, J.M., Skoultchi, A.I., and Bouhassira, E.E. (2003). Mammalian linker-histone subtypes differentially affect gene expression in vivo. Proceedings of the National Academy of Sciences of the United States of America *100*, 5920-5925.

Alexander, T., Nolte, C., and Krumlauf, R. (2009). Hox genes and segmentation of the hindbrain and axial skeleton. Annual review of cell and developmental biology *25*, 431-456.

Azuara, V., Perry, P., Sauer, S., Spivakov, M., Jorgensen, H.F., John, R.M., Gouti, M., Casanova, M., Warnes, G., Merkenschlager, M.*, et al.* (2006). Chromatin signatures of pluripotent cell lines. Nature cell biology *8*, 532-538.

Bai, L., and Morozov, A.V. (2010). Gene regulation by nucleosome positioning. Trends in genetics : TIG *26*, 476-483.

Bednar, J., Horowitz, R.A., Grigoryev, S.A., Carruthers, L.M., Hansen, J.C., Koster, A.J., and Woodcock, C.L. (1998). Nucleosomes, linker DNA, and linker histone form a unique structural motif that directs the higher-order folding and compaction of chromatin. Proceedings of the National Academy of Sciences of the United States of America *95*, 14173-14178.

Bernstein, B.E., Kamal, M., Lindblad-Toh, K., Bekiranov, S., Bailey, D.K., Huebert, D.J., McMahon, S., Karlsson, E.K., Kulbokas, E.J., 3rd, Gingeras, T.R.*, et al.* (2005). Genomic maps and comparative analysis of histone modifications in human and mouse. Cell *120*, 169-181.

Bernstein, B.E., Mikkelsen, T.S., Xie, X., Kamal, M., Huebert, D.J., Cuff, J., Fry, B., Meissner, A., Wernig, M., Plath, K.*, et al.* (2006). A bivalent chromatin structure marks key developmental genes in embryonic stem cells. Cell *125*, 315-326.

Boyer, L.A., Plath, K., Zeitlinger, J., Brambrink, T., Medeiros, L.A., Lee, T.I., Levine, S.S., Wernig, M., Tajonar, A., Ray, M.K., *et al.* (2006). Polycomb complexes repress developmental regulators in murine embryonic stem cells. Nature *441*, 349-353.

Bracken, A.P., Dietrich, N., Pasini, D., Hansen, K.H., and Helin, K. (2006). Genome-wide mapping of Polycomb target genes unravels their roles in cell fate transitions. Genes & development *20*, 1123-1136.

Cao, R., Wang, L., Wang, H., Xia, L., Erdjument-Bromage, H., Tempst, P., Jones, R.S., and Zhang, Y. (2002). Role of histone H3 lysine 27 methylation in Polycomb-group silencing. Science *298*, 1039-1043.

Chamberlain, S.J., Yee, D., and Magnuson, T. (2008). Polycomb repressive complex 2 is dispensable for maintenance of embryonic stem cell pluripotency. Stem cells *26*, 1496-1505.

Chambeyron, S., and Bickmore, W.A. (2004). Chromatin decondensation and nuclear reorganization of the HoxB locus upon induction of transcription. Genes & development *18*, 1119-1130.

Chambeyron, S., Da Silva, N.R., Lawson, K.A., and Bickmore, W.A. (2005). Nuclear re-organisation of the Hoxb complex during mouse embryonic development. Development *132*, 2215-2223.

Christensen, J., Agger, K., Cloos, P.A., Pasini, D., Rose, S., Sennels, L., Rappsilber, J., Hansen, K.H., Salcini, A.E., and Helin, K. (2007). RBP2 belongs to a family of demethylases, specific for tri-and dimethylated lysine 4 on histone 3. Cell *128*, 1063-1076.

Cloos, P.A., Christensen, J., Agger, K., and Helin, K. (2008). Erasing the methyl mark: histone demethylases at the center of cellular differentiation and disease. Genes & development *22*, 1115-1140.

Deschamps, J. (2007). Ancestral and recently recruited global control of the Hox genes in development. Current opinion in genetics & development *17*, 422-427.

Dobreva, G., Chahrour, M., Dautzenberg, M., Chirivella, L., Kanzler, B., Farinas, I., Karsenty, G., and Grosschedl, R. (2006). SATB2 is a multifunctional determinant of craniofacial patterning and osteoblast differentiation. Cell *125*, 971-986.

Dou, Y., Milne, T.A., Ruthenburg, A.J., Lee, S., Lee, J.W., Verdine, G.L., Allis, C.D., and Roeder, R.G. (2006). Regulation of MLL1 H3K4 methyltransferase activity by its core components. Nature structural & molecular biology *13*, 713-719.

Efroni, S., Duttagupta, R., Cheng, J., Dehghani, H., Hoeppner, D.J., Dash, C., Bazett-Jones, D.P., Le Grice, S., McKay, R.D., Buetow, K.H., *et al.* (2008). Global transcription in pluripotent embryonic stem cells. Cell stem cell *2*, 437-447.

Endoh, M., Endo, T.A., Endoh, T., Fujimura, Y., Ohara, O., Toyoda, T., Otte, A.P., Okano, M., Brockdorff, N., Vidal, M., *et al.* (2008). Polycomb group proteins Ring1A/B are functionally linked to the core transcriptional regulatory circuitry to maintain ES cell identity. Development *135*, 1513-1524.

Erzurumlu, R.S., Murakami, Y., and Rijli, F.M. (2010). Mapping the face in the somatosensory brainstem. Nature reviews Neuroscience *11*, 252-263.

Eskeland, R., Leeb, M., Grimes, G.R., Kress, C., Boyle, S., Sproul, D., Gilbert, N., Fan, Y., Skoultchi, A.I., Wutz, A., *et al.* (2010). Ring1B compacts chromatin structure and represses gene expression independent of histone ubiquitination. Molecular cell *38*, 452-464.

Fan, Y., Nikitina, T., Morin-Kensicki, E.M., Zhao, J., Magnuson, T.R., Woodcock, C.L., and Skoultchi, A.I. (2003). H1 linker histones are essential for mouse development and affect nucleosome spacing in vivo. Molecular and cellular biology *23*, 4559-4572.

Fan, Y., Nikitina, T., Zhao, J., Fleury, T.J., Bhattacharyya, R., Bouhassira, E.E., Stein, A., Woodcock, C.L., and Skoultchi, A.I. (2005). Histone H1 depletion in mammals alters global chromatin structure but causes specific changes in gene regulation. Cell *123*, 1199-1212.

Fan, Y., Sirotkin, A., Russell, R.G., Ayala, J., and Skoultchi, A.I. (2001). Individual somatic H1 subtypes are dispensable for mouse development even in mice lacking the H1(0) replacement subtype. Molecular and cellular biology *21*, 7933-7943.

Fan, Y., and Skoultchi, A.I. (2004). Genetic analysis of H1 linker histone subtypes and their functions in mice. Methods in enzymology *377*, 85-107.

Giambra, V., Volpi, S., Emelyanov, A.V., Pflugh, D., Bothwell, A.L., Norio, P., Fan, Y., Ju, Z., Skoultchi, A.I., Hardy, R.R., *et al.* (2008). Pax5 and linker histone H1 coordinate

DNA methylation and histone modifications in the 3' regulatory region of the immunoglobulin heavy chain locus. Molecular and cellular biology *28*, 6123-6133.

Goodman, F.R. (2002). Limb malformations and the human HOX genes. American journal of medical genetics *112*, 256-265.

Gouti, M., and Gavalas, A. (2008). Hoxb1 controls cell fate specification and proliferative capacity of neural stem and progenitor cells. Stem cells *26*, 1985-1997.

Graham, A., Papalopulu, N., and Krumlauf, R. (1989). The murine and Drosophila homeobox gene complexes have common features of organization and expression. Cell *57*, 367-378.

Gunjan, A., and Brown, D.T. (1999). Overproduction of histone H1 variants in vivo increases basal and induced activity of the mouse mammary tumor virus promoter. Nucleic acids research *27*, 3355-3363.

Happel, N., and Doenecke, D. (2009). Histone H1 and its isoforms: contribution to chromatin structure and function. Gene *431*, 1-12.

Herrscher, R.F., Kaplan, M.H., Lelsz, D.L., Das, C., Scheuermann, R., and Tucker, P.W. (1995). The immunoglobulin heavy-chain matrix-associating regions are bound by Bright: a B cell-specific trans-activator that describes a new DNA-binding protein family. Genes & development *9*, 3067-3082.

Huang, T.H., Oka, T., Asai, T., Okada, T., Merrills, B.W., Gertson, P.N., Whitson, R.H., and Itakura, K. (1996). Repression by a differentiation-specific factor of the human cytomegalovirus enhancer. Nucleic acids research *24*, 1695-1701.

Izaurralde, E., Kas, E., and Laemmli, U.K. (1989). Highly preferential nucleation of histone H1 assembly on scaffold-associated regions. Journal of molecular biology *210*, 573-585.

Izpisua-Belmonte, J.C., Falkenstein, H., Dolle, P., Renucci, A., and Duboule, D. (1991). Murine genes related to the Drosophila AbdB homeotic genes are sequentially expressed during development of the posterior part of the body. The EMBO journal *10*, 2279-2289.

Jorgensen, H.F., Giadrossi, S., Casanova, M., Endoh, M., Koseki, H., Brockdorff, N., and Fisher, A.G. (2006). Stem cells primed for action: polycomb repressive complexes

restrain the expression of lineage-specific regulators in embryonic stem cells. Cell cycle *5*, 1411-1414.

Kharchenko, P.V., Woo, C.J., Tolstorukov, M.Y., Kingston, R.E., and Park, P.J. (2008). Nucleosome positioning in human HOX gene clusters. Genome research *18*, 1554-1561.

Kortschak, R.D., Tucker, P.W., and Saint, R. (2000). ARID proteins come in from the desert. Trends in biochemical sciences *25*, 294-299.

Lachner, M., O'Carroll, D., Rea, S., Mechtler, K., and Jenuwein, T. (2001). Methylation of histone H3 lysine 9 creates a binding site for HP1 proteins. Nature *410*, 116-120.

Lee, T.I., Jenner, R.G., Boyer, L.A., Guenther, M.G., Levine, S.S., Kumar, R.M., Chevalier, B., Johnstone, S.E., Cole, M.F., Isono, K.*, et al.* (2006). Control of developmental regulators by Polycomb in human embryonic stem cells. Cell *125*, 301-313.

Leucht, P., Kim, J.B., Amasha, R., James, A.W., Girod, S., and Helms, J.A. (2008). Embryonic origin and Hox status determine progenitor cell fate during adult bone regeneration. Development *135*, 2845-2854.

Maclean, J.A., Bettegowda, A., Kim, B.J., Lou, C.H., Yang, S.M., Bhardwaj, A., Shanker, S., Hu, Z., Fan, Y., Eckardt, S.*, et al.* (2011). The rhox homeobox gene cluster is imprinted and selectively targeted for regulation by histone h1 and DNA methylation. Molecular and cellular biology *31*, 1275-1287.

Mallo, M., Wellik, D.M., and Deschamps, J. (2010). Hox genes and regional patterning of the vertebrate body plan. Developmental biology *344*, 7-15.

McIntyre, D.C., Rakshit, S., Yallowitz, A.R., Loken, L., Jeannotte, L., Capecchi, M.R., and Wellik, D.M. (2007). Hox patterning of the vertebrate rib cage. Development *134*, 2981-2989.

Medrzycki, M., Zhang, Y., Cao, K., and Fan, Y. (2012). Expression analysis of mammalian linker-histone subtypes. Journal of visualized experiments : JoVE.

Mikkelsen, T.S., Ku, M., Jaffe, D.B., Issac, B., Lieberman, E., Giannoukos, G., Alvarez, P., Brockman, W., Kim, T.K., Koche, R.P.*, et al.* (2007). Genome-wide maps of chromatin state in pluripotent and lineage-committed cells. Nature *448*, 553-560.

Montavon, T., Soshnikova, N., Mascrez, B., Joye, E., Thevenet, L., Splinter, E., de Laat, W., Spitz, F., and Duboule, D. (2011). A regulatory archipelago controls Hox genes transcription in digits. Cell *147*, 1132-1145.

Morey, C., Da Silva, N.R., Perry, P., and Bickmore, W.A. (2007). Nuclear reorganisation and chromatin decondensation are conserved, but distinct, mechanisms linked to Hox gene activation. Development *134*, 909-919.

Noordermeer, D., Leleu, M., Splinter, E., Rougemont, J., De Laat, W., and Duboule, D. (2011). The dynamic architecture of Hox gene clusters. Science *334*, 222-225.

Oury, F., Murakami, Y., Renaud, J.S., Pasqualetti, M., Charnay, P., Ren, S.Y., and Rijli, F.M. (2006). Hoxa2- and rhombomere-dependent development of the mouse facial somatosensory map. Science *313*, 1408-1413.

Panyim, S., and Chalkley, R. (1969). A new histone found only in mammalian tissues with little cell division. Biochemical and biophysical research communications *37*, 1042-1049.

Pehrson, J., and Cole, R.D. (1980). Histone H10 accumulates in growth-inhibited cultured cells. Nature *285*, 43-44.

Ringrose, L., and Paro, R. (2004). Epigenetic regulation of cellular memory by the Polycomb and Trithorax group proteins. Annual review of genetics *38*, 413-443.

Rinn, J.L., Kertesz, M., Wang, J.K., Squazzo, S.L., Xu, X., Brugmann, S.A., Goodnough, L.H., Helms, J.A., Farnham, P.J., Segal, E.*, et al.* (2007). Functional demarcation of active and silent chromatin domains in human HOX loci by noncoding RNAs. Cell *129*, 1311-1323.

Ruddle, F.H., Bartels, J.L., Bentley, K.L., Kappen, C., Murtha, M.T., and Pendleton, J.W. (1994). Evolution of Hox genes. Annual review of genetics *28*, 423-442.

Schuettengruber, B., Chourrout, D., Vervoort, M., Leblanc, B., and Cavalli, G. (2007). Genome regulation by polycomb and trithorax proteins. Cell *128*, 735-745.

Shah, N., and Sukumar, S. (2010). The Hox genes and their roles in oncogenesis. Nature reviews Cancer *10*, 361-371.

Soshnikova, N., and Duboule, D. (2009). Epigenetic temporal control of mouse Hox genes in vivo. Science *324*, 1320-1323.

Spitz, F., Gonzalez, F., and Duboule, D. (2003). A global control region defines a chromosomal regulatory landscape containing the HoxD cluster. Cell *113*, 405-417.

Stock, J.K., Giadrossi, S., Casanova, M., Brookes, E., Vidal, M., Koseki, H., Brockdorff, N., Fisher, A.G., and Pombo, A. (2007). Ring1-mediated ubiquitination of H2A restrains poised RNA polymerase II at bivalent genes in mouse ES cells. Nature cell biology *9*, 1428-1435.

Thoma, F., Koller, T., and Klug, A. (1979). Involvement of histone H1 in the organization of the nucleosome and of the salt-dependent superstructures of chromatin. The Journal of cell biology *83*, 403-427.

van der Lugt, N.M., Alkema, M., Berns, A., and Deschamps, J. (1996). The Polycomb-group homolog Bmi-1 is a regulator of murine Hox gene expression. Mechanisms of development *58*, 153-164.

van Lohuizen, M. (1998). Functional analysis of mouse Polycomb group genes. Cellular and molecular life sciences : CMLS *54*, 71-79.

Vinagre, T., Moncaut, N., Carapuco, M., Novoa, A., Bom, J., and Mallo, M. (2010). Evidence for a myotomal Hox/Myf cascade governing nonautonomous control of rib specification within global vertebral domains. Developmental cell *18*, 655-661.

Wagner, G.P., Amemiya, C., and Ruddle, F. (2003). Hox cluster duplications and the opportunity for evolutionary novelties. Proceedings of the National Academy of Sciences of the United States of America *100*, 14603-14606.

Wellik, D.M. (2007). Hox patterning of the vertebrate axial skeleton. Developmental dynamics : an official publication of the American Association of Anatomists *236*, 2454-2463.

Yekta, S., Shih, I.H., and Bartel, D.P. (2004). MicroRNA-directed cleavage of HOXB8 mRNA. Science *304*, 594-596.

Zhang, Y., Cooke, M., Panjwani, S., Cao, K., Krauth, B., Ho, P.Y., Medrzycki, M., Berhe, D.T., Pan, C., McDevitt, T.C., *et al.* (2012). Histone h1 depletion impairs embryonic stem cell differentiation. PLoS genetics *8*, e1002691.

CHAPTER 4

CONCLUSION AND FURTURE STUDIES

This dissertation is focused on the role of linker histone H1 in the regulation of pluripotency genes and *Hox* genes during ESCs differentiation and embryogenesis. The results demonstrate that H1 depletion impairs effective repression of pluripotency genes *Oct4* and *Nanog*, and leads to reduction in *Hox* genes. H1 depletion also affects core histone modifications and DNA methylation at the promoter regions of these genes.

A nearly 50% reduction of total H1 amount by deletion of H1c, H1d and H1e does not affect ESCs self-renewal, but it leads to inefficient repression of pluripotency genes and impairs ESCs spontaneous differentiation, embryoid bodies differentiation, and neural differentiation. The levels of H1 histones elevate in both WT and H1 TKO ESCs during differentiation, however, the level of H1 in TKO EBs is still lower than WT ESCs. Increasing the total H1 level into H1 TKO ESCs by reconstitution of H1d restores the effective repression of *Oct4* and *Nanog* expression during differentiation. We also note that H1c, H1d, H1e and $H1^0$, but not H1a and H1b, contribute to the increase of total H1 level during ESCs differentiation, suggesting that the expression of H1c, H1d, H1e and $H1^0$ are regulated during differentiation. In the future, we can further reduce the total H1 level by knockdown of H1a, H1b and $H1^0$ in ESCs to determine whether minimal level of total H1 is required for ESCs self-renewal and differentiation.

The expression of *Hox* genes is minimal or not present in ESCs but is developmentally activated during embryogenesis. Reduction of total H1 levels causes reduction in *Hox* gene expression in both ESCs and mouse embryos. In ESCs, the

expression of *Hoxb5*, *Hoxb13* and *Hoxd13* are reduced by H1c/H1d/H1e depletion, whereas the expression of *Hoxa1*, *Hoxb8*, and *Hoxc13* is reduced in H1c, or H1d, or H1e single KO ESCs, suggesting these *Hox* genes may be regulated by specific H1 subtypes. The regulations of certain *Hox* genes are biased toward specific H1 subtypes although these H1 subtypes are replaceable during development. This effect is reminiscent of the role of H1c in mouse retina maturation (Popova et al., 2013).

During WT ESCs differentiation, inhibition of *Oct4* transcription is accompanied by elevation of H1 level, the reduction of active histone mark H3K4me3, and the increase of repressive marks, H3K9me3 and H3K27me3, in the in promoter regions. Impaired repression of *Oct4* in H1 TKO ESCs during differentiation is correlated with similar levels of H1 binding and histone modifications in H1 TKO ESCs when compared with TKO EBs. In addition to changes in histone modifications, H1c/H1d/H1e depletion leads to a reduction in DNA methylation at *Oct4* promoter region. Methylation of cytosine nucleotide at CpG sites in the promoters contributes to gene silencing (Farthing et al., 2008). These results provide evidence that H1 contributes to the establishment or maintenance of DNA methylation at *Oct4* promoter during embryogenesis and EB differentiation. These results suggest that H1 may contribute to effective silencing of *Oct4* through its effects on DNA methylation and histone modfications.

H1 depletion also impairs expression repression of another pluripotency gene, *Nanog*, and leads to a decrease in H3K4me3 and an increase of H3K9me3 levels at *Nanog* promoter region. However, DNA methylation at the promoter region was not affect by H1 depletion, suggesting that H1 may participate in the regulation of *Oct4* and *Nanog* through different mechanisms.

Ample evidence suggests that H1 could regulate specific histone modifications through its interaction with histone modifying enzymes. Previous *in vitro* studies show that H1 interacts with HP1α, which can bind to SUV39H, a H3K9 methyltransferase (Daujat et al., 2005; Nielsen et al., 2001). We observed interactions between H1 and components of PRC2 (unpublished observation), which has methylation activity toward H3K27me3. Others show that H1 inhibits H3K4 methylation through interfering the binding of H3K4 histone methyltransferase SET7/9 (Yang et al., 2013). Moreover, we have found that H1 directly interacts with Dnmts in ESCs, which is consistent with recent studies (Yang et al., 2013). Therefore we envision that the mechanism of H1 regulate the repression of *Oct4* during ESC differentiation is as following: H1 level increases which leads to the inhibition of SET7/9 H3K4 methyltransfease binding (a reduction of H3K4me3), recruitment of SUV39H (an increase of H3K9me3), PRC2 (an increase of H3K27me3) and Dnmts (an increase in DNA methylation) at *Oct4* promoter. These changes together inhibit the formation of active epigenetic mark, promote the establishment and /or maintenance of repressive epigenetic modifications, and silence the expression of pluripotency genes.

Induction of pluripotency from somatic cells is a promising tool for clinic use and regenerative medicine. Exogenous expression of *Oct4*, Sox2, *Klf4* and *c-myc* or expression fewer of the four factors combining with small molecules or cocktail of small molecules alone can induce reprogramming (Hou et al., 2013; Li et al., 2011; Takahashi and Yamanaka, 2006). Many chromatin proteins participate in reprogramming processes, indicating the importance of chromatin in induced pluripotency. For example, SWI/SNF (or Brg1/Brm-associated factor [BAF]) complex, a chromatin remodeling complex,

promotes the programming of fibroblasts and liver cell into pluripotent stem cells (iPSCs) (Kleger et al., 2012; Singhal et al., 2010). Ezh2, a core subunit of PRC2, is critical for efficient generation of iPSC, but it is not required for maintaining iPSC state (Ding et al., 2014). Deletion of Mbd3, a component of NuRD (nucleosome remodeling and deacetylation) repressor complex promotes reprogramming (Rais et al., 2013). Notably, mouse histone variants, TH2A and TH2B highly expressed in oocytes, can induce reprogramming with *Oct4* and *Klf4* alone and enhance generation of induced iPSCs (Shinagawa et al., 2014). Depletion of Peptidylarginine deiminases (PADIs) which citrullinate H1, disrupt the binding of H1 and leads to chromatin decondensation, significantly reduces reprogramming efficiency (Christophorou et al., 2014). Although our finding suggest chromatin structure is involved in repression of *Oct4* during differentiation, it would be interesting to investigate the role of H1 and high order chromatin structure in reprogramming, the reverse process of differentiation. The results will fill another half loop of the connection between chromatin structure and pluripotency genes, and may be useful to increase reprogramming efficiency.

We find that H1c, H1d and H1e deletion causes reduced expression of a distinct set of *Hox* genes in mouse embryos and ESCs. As appeared in pluripotency gene regulation, H1 deletion leads to histone modification changes in ESCs, which may also affect the regulation of *Hox* genes. The mechanisms of *Hox* gene regulation have been extensively studied. Local and long distance *cis*-regulator elements (Montavon et al., 2011; Noordermeer et al., 2011; Spitz et al., 2003), DNA methylation (Tsumagari et al., 2013), and core histone modification (Mikkelsen et al., 2007; Noordermeer et al., 2011; Soshnikova and Duboule, 2009) are all associated in the regulation. Notably, activation

and silencing of *Hox* genes are accompanied with visible chromatin decondencation and nuclear reorganization in embryos and ESCs differentiation (Chambeyron and Bickmore, 2004; Chambeyron et al., 2005; Morey et al., 2007; Weicksel et al., 2013; Williamson et al., 2012). Therefore, *Hox* gene cluster is a good system to investigate the functions of H1 in epigenetic regulation of genes. The further study can be focused on the role of H1 in chromatin folding at *Hox* clusters. Whether H1 brings additional regulatory elements at remote sites within close proximity of *Hox* cluster, and whether H1 promotes epigenetic modifications, and what is the role of H1 in orderly dynamic changes of chromatin structure during *Hox* genes regulation are all interesting questions to pursue.

During ESCs differentiation, although the influence of H1 on many developmental genes could be caused by the impaired repression of pluripotency genes, the effects might also be caused by deletion of H1 on lineage specific genes or other developmental genes. In order to explore the functions of H1 in developmental gene regulation and cell fate determination, we can analyze the expression changes of H1 during multipotent stem cells, such as multipotent mesenchymal stromal cells, multipotential hematopoietic progenitor cell, and neuron progenitor cells, *in vivo* or *in vitro* differentiation. Establishing H1 mutant multipotent stem cells will aid in analysis of the role H1 in differentiation of these cells. Given the embryonic lethality of H1 TKO embryos, conditional knockout mouse will be a good strategy to investigate functions of H1 in specific tissues and development time point.

4.2 Reference

Chambeyron, S., and Bickmore, W.A. (2004). Chromatin decondensation and nuclear reorganization of the HoxB locus upon induction of transcription. Genes & development *18*, 1119-1130.

Chambeyron, S., Da Silva, N.R., Lawson, K.A., and Bickmore, W.A. (2005). Nuclear re-organisation of the Hoxb complex during mouse embryonic development. Development *132*, 2215-2223.

Christophorou, M.A., Castelo-Branco, G., Halley-Stott, R.P., Oliveira, C.S., Loos, R., Radzisheuskaya, A., Mowen, K.A., Bertone, P., Silva, J.C., Zernicka-Goetz, M.*, et al.* (2014). Citrullination regulates pluripotency and histone H1 binding to chromatin. Nature *507*, 104-108.

Daujat, S., Zeissler, U., Waldmann, T., Happel, N., and Schneider, R. (2005). HP1 binds specifically to Lys26-methylated histone H1.4, whereas simultaneous Ser27 phosphorylation blocks HP1 binding. The Journal of biological chemistry *280*, 38090-38095.

Ding, X., Wang, X., Sontag, S., Qin, J., Wanek, P., Lin, Q., and Zenke, M. (2014). The Polycomb Protein Ezh2 Impacts on Induced Pluripotent Stem Cell Generation. Stem cells and development.

Farthing, C.R., Ficz, G., Ng, R.K., Chan, C.F., Andrews, S., Dean, W., Hemberger, M., and Reik, W. (2008). Global mapping of DNA methylation in mouse promoters reveals epigenetic reprogramming of pluripotency genes. PLoS genetics *4*, e1000116.

Hou, P., Li, Y., Zhang, X., Liu, C., Guan, J., Li, H., Zhao, T., Ye, J., Yang, W., Liu, K.*, et al.* (2013). Pluripotent stem cells induced from mouse somatic cells by small-molecule compounds. Science *341*, 651-654.

Kleger, A., Mahaddalkar, P.U., Katz, S.F., Lechel, A., Joo, J.Y., Loya, K., Lin, Q., Hartmann, D., Liebau, S., Kraus, J.M.*, et al.* (2012). Increased reprogramming capacity of mouse liver progenitor cells, compared with differentiated liver cells, requires the BAF complex. Gastroenterology *142*, 907-917.

Li, Y., Zhang, Q., Yin, X., Yang, W., Du, Y., Hou, P., Ge, J., Liu, C., Zhang, W., Zhang, X., *et al.* (2011). Generation of iPSCs from mouse fibroblasts with a single gene, Oct4, and small molecules. Cell research *21*, 196-204.

Mikkelsen, T.S., Ku, M., Jaffe, D.B., Issac, B., Lieberman, E., Giannoukos, G., Alvarez, P., Brockman, W., Kim, T.K., Koche, R.P., *et al.* (2007). Genome-wide maps of chromatin state in pluripotent and lineage-committed cells. Nature *448*, 553-560.

Montavon, T., Soshnikova, N., Mascrez, B., Joye, E., Thevenet, L., Splinter, E., de Laat, W., Spitz, F., and Duboule, D. (2011). A regulatory archipelago controls Hox genes transcription in digits. Cell *147*, 1132-1145.

Morey, C., Da Silva, N.R., Perry, P., and Bickmore, W.A. (2007). Nuclear reorganisation and chromatin decondensation are conserved, but distinct, mechanisms linked to Hox gene activation. Development *134*, 909-919.

Nielsen, A.L., Oulad-Abdelghani, M., Ortiz, J.A., Remboutsika, E., Chambon, P., and Losson, R. (2001). Heterochromatin formation in mammalian cells: interaction between histones and HP1 proteins. Molecular cell *7*, 729-739.

Noordermeer, D., Leleu, M., Splinter, E., Rougemont, J., De Laat, W., and Duboule, D. (2011). The dynamic architecture of Hox gene clusters. Science *334*, 222-225.

Popova, E.Y., Grigoryev, S.A., Fan, Y., Skoultchi, A.I., Zhang, S.S., and Barnstable, C.J. (2013). Developmentally regulated linker histone H1c promotes heterochromatin condensation and mediates structural integrity of rod photoreceptors in mouse retina. The Journal of biological chemistry *288*, 17895-17907.

Rais, Y., Zviran, A., Geula, S., Gafni, O., Chomsky, E., Viukov, S., Mansour, A.A., Caspi, I., Krupalnik, V., Zerbib, M., *et al.* (2013). Deterministic direct reprogramming of somatic cells to pluripotency. Nature *502*, 65-70.

Shinagawa, T., Takagi, T., Tsukamoto, D., Tomaru, C., Huynh, L.M., Sivaraman, P., Kumarevel, T., Inoue, K., Nakato, R., Katou, Y., *et al.* (2014). Histone variants enriched in oocytes enhance reprogramming to induced pluripotent stem cells. Cell stem cell *14*, 217-227.

Singhal, N., Graumann, J., Wu, G., Arauzo-Bravo, M.J., Han, D.W., Greber, B., Gentile, L., Mann, M., and Scholer, H.R. (2010). Chromatin-Remodeling Components of the BAF Complex Facilitate Reprogramming. Cell *141*, 943-955.

Soshnikova, N., and Duboule, D. (2009). Epigenetic regulation of vertebrate Hox genes: a dynamic equilibrium. Epigenetics : official journal of the DNA Methylation Society *4*, 537-540.

Spitz, F., Gonzalez, F., and Duboule, D. (2003). A global control region defines a chromosomal regulatory landscape containing the HoxD cluster. Cell *113*, 405-417.

Takahashi, K., and Yamanaka, S. (2006). Induction of pluripotent stem cells from mouse embryonic and adult fibroblast cultures by defined factors. Cell *126*, 663-676.

Tsumagari, K., Baribault, C., Terragni, J., Chandra, S., Renshaw, C., Sun, Z., Song, L., Crawford, G.E., Pradhan, S., Lacey, M.*, et al.* (2013). DNA methylation and differentiation: HOX genes in muscle cells. Epigenetics & chromatin *6*, 25.

Weicksel, S.E., Xu, J., and Sagerstrom, C.G. (2013). Dynamic nucleosome organization at hox promoters during zebrafish embryogenesis. PloS one *8*, e63175.

Williamson, I., Eskeland, R., Lettice, L.A., Hill, A.E., Boyle, S., Grimes, G.R., Hill, R.E., and Bickmore, W.A. (2012). Anterior-posterior differences in HoxD chromatin topology in limb development. Development *139*, 3157-3167.

Yang, S.M., Kim, B.J., Norwood Toro, L., and Skoultchi, A.I. (2013). H1 linker histone promotes epigenetic silencing by regulating both DNA methylation and histone H3 methylation. Proceedings of the National Academy of Sciences of the United States of America *110*, 1708-1713.